Two-Stage Hydrophobic and Hydrophilic Aggregation for the Flotation Separation of Fine and Ultrafine Minerals

by

Daowei Wang

A thesis submitted in partial fulfillment of the requirements for the degree of

Doctor of Philosophy

in

Materials Engineering

Department of Chemical and Materials Engineering

University of Alberta

Abstract

In mineral processing froth flotation is the most important technique to recover and separate different minerals. However, the flotation process deteriorates significantly with low efficiency and selectivity when mineral particles are smaller than 20 μm. Low flotation kinetics of fine hydrophobic particles and high mechanical entrainment of fine gangue hydrophilic particles are two major problems associated with fine and ultrafine mineral flotation.

In view of the two problems, the strategy of a two-stage hydrophobic and hydrophilic aggregation/flocculation process was proposed, aiming to separately aggregate hydrophobic particles and hydrophilic particles with appropriate approaches and ideally develop both hydrophobic and hydrophilic aggregates in the slurry simultaneously or sequentially. The two types of aggregates are then separated using conventional froth flotation procedures. Since the extensive study of hydrophobic particles aggregation in literature, significant efforts in this dissertation were made to investigate the aggregation, dispersion, and flocculation property of ultrafine hydrophilic particles and their entrainment reduction when different polymers were used in flotation.

In this dissertation, hematite and quartz of high purity were used as a model mineral system. Flotation tests were conducted using a Denver D-12 laboratory flotation machine and a custom-built flotation column. Natural polymers including corn starch, corn dextrin, tannic acid and synthetic polymer poly(ethylene oxide) were used as depressants, dispersants, and flocculants for the study.

It was found that the aggregation of hydrophilic particles benefited their entrainment reduction while the dispersion state aggravated their entrainment. In the reverse cationic flotation of quartz from hematite in the mechanical flotation cell, the polymer flocculation of hematite by corn starch and the hydrophobic flocculation of quartz by octadecyalmine acetate could

significantly improve the flotation separation. When the corn starch was replaced by corn dextrin which had a much lower molecular weight, severe hematite entrainment to the froth product was observed. Test work using in-situ particle size analysis by focused beam reflectance measurement, coarse hematite particles, and particle surface hydrophilicity measurement, confirmed that the different separation results were solely caused by the different degrees of aggregation/dispersion of the hematite.

As a typical gangue mineral, flocculation behaviors of ultrafine hydrophilic quartz by poly(ethylene oxide) (PEO, 8M) were investigated with and without tannic acid (TAN). It was found that using PEO alone as a flocculant, the floc size and flocculation effectiveness of quartz decreased in the order of pH 3.1 > pH 6.3 >> pH 9.4. However, the prior addition of tannic acid reversed this trend so that floc size decreased in the order of pH 9.4 > pH 6.3 >> pH 3.1. Tannic acid was also found to change the shear resistance and reversibility properties of quartz flocs formed by PEO in turbulence, depending on the TAN/PEO ratios and medium pH. Measurements including zeta potential, adsorption density, confocal scanning microscope and freeze-drying-SEM imaging indicated that the pathway of the dual polymer flocculation was via the initial formation of TAN-PEO associative complexes in solution and then bridging of quartz by the associative complexes. The TAN-PEO associative complexes showed different structures and configurations at different pH, in line with a change in hydrogen bonding, which in turn affected floc structures and properties under turbulent conditions.

The TAN-PEO dual polymer combination was tested in column flotation to flocculate quartz and reduce its entrainment, with hematite floated directly using n-octyl hydroxamic acid (OHA) as a collector. It was confirmed that flocculating quartz by TAN-PEO polymer system to form hydrophilic flocs was effective to reduce its mechanical entrainment, however, the reduced degree of quartz entrainment was dependent on the agitation intensity applied for slurry conditioning. A linear correlation was established between mean floc size and the reduced

entrainment degree when the average floc size was less than 68 μm. Moreover, dual TAN-PEO polymers enhanced both flotation kinetics and recovery for hematite by OHA, benefiting from a synergistic effect between OHA and PEO. Overall, a dual function of tannic acid was revealed in that it could not only improve the flocculation of quartz and helped to obtain more shear-resistant flocs by PEO but also could weaken the surface activity and foaming stability of PEO, both of which will be beneficial in reducing the entrainment of ultrafine quartz in flotation.

Preface

This thesis is compiled in the manuscript-based format, centering on the concept of two-stage hydrophobic and hydrophilic aggregation/flocculation of fine and ultrafine minerals followed by their separation using conventional froth flotation. Below is a statement of my contributions to co-authored journal papers contained in this thesis.

Chapter 1 and 2, partial content of the two chapters has been published as "D. Wang, Q. Liu, Hydrodynamics of froth flotation and its effects on fine and ultrafine mineral particle flotation: A literature review, *Minerals Engineering*, 173 (2021) 107220." I contributed to organizing the content and writing the original draft. Dr. Q. Liu was the supervisory author and contributed to the writing review/editing and manuscript composition.

Chapter 3 has been published as "D. Wang, Q. Liu, Influence of aggregation/dispersion state of hydrophilic particles on their entrainment in fine mineral particle flotation, *Minerals Engineering*, 166 (2021) 106835." I contributed to designing/performing the experiments, collecting/analyzing data, and writing the original draft. Dr. Q. Liu was the supervisory author and contributed to concept formation, writing review/editing, and manuscript composition.

Chapter 4 has been published as "D. Wang, D. Wang, C. Deng, K. Wang, X. Tan, Q. Liu, Flocculation of quartz by a dual polymer system containing tannic acid and poly (ethylene oxide): Effect of polymer chemistry and hydrodynamic conditions, *Chemical Engineering Journal*, (2022) 137403." I contributed to designing/performing the experiments, collecting/analyzing data, and writing the original draft. Dong Wang contributed to performing X-ray powder diffraction, BET, and scanning electron microscope experiments. C. Deng helped to perform and analyze the flocs structure using confocal scanning microscope. Dr. K. Wang and Dr. X. Tan contributed to discussing and commenting on the manuscript. Dr. Q. Liu was the supervisory author and contributed to data interpretation, writing review/editing, and manuscript composition.

A version of Chapter 5 is under preparation for submission as “Effects of agitation intensity and foaming property on the flocculation flotation of fine and ultrafine minerals using a laboratory-scale flotation column”. I contributed to designing/performing the experiments, collecting/analyzing data, and writing the original draft. Dong Wang and Dr. K. Wang contributed to FBRM investigation and data analysis. Dr. Q. Liu was the supervisory author and contributed to concept formation, writing review/editing, and manuscript composition.

Acknowledgements

Doing a Ph.D. is about exploring unknowns as well as self-discovery. I appreciate my decision four years ago to pursue a doctoral study in Canada. The training I obtained from this precious experience has brought me not only knowledge but also the ability to think critically and address challenges independently. On top of that, I have been learning how to recognize and get along better with myself. Finally, I have got this opportunity to say thank you to the people who have helped me throughout this journey.

First I would like to sincerely thank Dr. Qi Liu who is a very knowledgeable and approachable supervisor and inspired me a lot both academically and morally. During my graduate studies, Dr. Liu could always provide timely feedback and practical guidance with my program, meanwhile, he gave me the freedom to explore subjects of interest. Without his continuous guidance and encouragement, the research work would have not been completed. I also thank Dr. Liu for offering me the opportunity to participate in the oil sands industrial projects, which expands my knowledge on petroleum production and tailings management.

Thank you to my supervisory committee members, Dr. Vinay Prasad and Dr. Rajender Gupta, for their advice on my candidacy report and the work in this dissertation.

I acknowledge the scholarships and financial support from China Scholarship Council, Faculty of Graduate Studies and Research at the University of Alberta, and the Natural Sciences and Engineering Research Council of Canada (NSERC).

I would like to thank Dr. Xiaoli Tan, Lisa Brandt, Brittany Mackinnon, and Ni Yang at the Imperial Institute for Oil Sands Innovation (IOSI) for their assistance and technical support for lab work.

I appreciate the enthusiastic help and meaningful discussion from Dr. Kaipeng Wang for my research. My thanks are also extended to my fellow Ph.D. students Hanyu Zhang, Dong Wang, Xuyang Liu, Menatalla Ahmed and so many friends I met in Canada for creating a pleasant working environment and their friendship. I am thankful to visiting students Xianfeng Sun, Chao Wang, Wei Yao, Chao Deng, and Haoran Sun for sharing their knowledge and experience on froth flotation.

I must express my gratitude to my family for their forever support and understanding, I am sorry that it is not convenient to go back home for years due to the Covid-19 pandemic. The deepest gratitude goes to my dear grandma Ms. Wenying Gao for her love and care along the way of my growth and my uncle Dr. Wujun Gao for his long-time encouragement and suggestions with my studies since primary school.

Lastly, I want to dedicate this dissertation to my girlfriend, JIAN. In such a long-distance relationship you have always been there for me with enduring patience and confidence. Thank you for believing in me and our future.

Table of Contents

List of Tables

List of Figures

CHAPTER 1 Introduction

1.1 Research background

The world economic development and infrastructure improvement has driven the growing demand for mineral commodities globally. Meanwhile, advances in technologies are pushing many countries to launch strategies for rare/critical mineral resources exploration and utilization. This brings about the challenges for mining industry considering the finite and non-renewable nature of mineral reserves on the Earth. In order to meet the metal/minerals supply and cope with the depletion of high-grade and easy-to-process minerals deposits, one essential subject that faces the mining sector is to find effective and economically viable technologies to utilize the low-grade and complex ores. Besides, re-processing tailings and wastes from metallurgical processes are also thought of as potential resources for fulfilling such requirements since these waste streams still contain value minerals/metals [1, 2]. In all cases, one shared problem is to treat a large amount of fine-grained particles to achieve mineral separation. Froth flotation, being the primary technique for mineral separation and recovery, is most effective in some intermediate particle sizes. Although the optimum particle size is not identical for different types of minerals, it is generally considered that froth flotation works best when the mineral particle size is between 20 and 150 μm [3, 4]. Outside of this range, flotation efficiency or/and separation selectivity can be adversely impacted. As a long-standing and unsolved problem, finding effective approaches to improve the flotation of fine and ultrafine minerals has been an important subject for both academia and industry over the past several decades. The improvement of this subject would be significant for the sustainable development of minerals/mining industry.

1.1.1 Technology challenges of fine and ultrafine minerals flotation

Fine and ultrafine mineral particles have the characteristics of small momentum and large specific surface area. When they are present in the pulp, the two features contribute to the main challenges of recovering and separating them by flotation. One problem is the inefficient flotation kinetics/rate of fine hydrophobic minerals, which is largely dependent on particle-bubble collision frequency [5]. Due to the turbulent hydrodynamic conditions and unmatched particle/bubble size ratios in conventional mechanical cells, small-sized hydrophobic particles tend to follow the streamlines rather than collide with and attach to air bubbles as they approach each other, resulting in a low probability of bubble-particle collision and slow/poor recovery of fine hydrophobic particles. Another problem is deteriorated flotation selectivity primarily caused by mechanical entrainment of fine and ultrafine hydrophilic particles into (hydrophobic) flotation concentrate, which lowers the grade of the concentrate [6]. Entrained fine and ultrafine hydrophilic particles in the froth phase usually fail to drain back to the pulp since the small mass cannot guarantee enough inertia. The entrainment problem can become even worse when the particle size decreases to less than 10 μm. Apart from the two major problems, other challenges associated with fine particle flotation include non-specific adsorption, high chemicals consumption, slime coating, rapid surface oxidation and high dissolution, undesired pulp rheology behavior and persistent frothing property [7, 8]. All these issues together make it more complicated for flotation system containing both fine hydrophobic and hydrophilic particles.

1.1.2 Current approaches to improve fine mineral flotation

In view of the challenges, many approaches have been proposed and some of them have been commercially applied on the plant scale. Figure 1.1 presents the main current technical routes to improve the flotation process of fine and ultrafine minerals. These methods or research directions can generally be divided into two categories, i.e., improving variables of hydrodynamic conditions and solution chemistry. Certainly, some approaches consider the factors of both aspects for flotation. Increasing the effective size of fine and ultrafine mineral particles through aggregation is a common way to improve their flotation recovery [9]. The main mechanism of the aggregation is via hydrophobic association between particles and is achieved using methods such as shear flocculation, oil-assisted agglomeration, and carrier flotation. Reducing bubble size is another major line of research to increase the flotation rate of fine minerals. The study of micro and nano bubbles has attracted significant attention in mineral processing due to their remarkable roles in aiding the collection of fine and ultrafine particles. For example, employing hydrodynamic cavitation to generate micro and nano bubbles can greatly accelerate the attachment rate of hydrophobic particles to bubbles [10, 11], and significantly improve the froth flotation of fine and ultrafine particles when coupled with regular mm-sized bubbles [7]. Designing specific flotation cells with the principle of optimized and intensified hydrodynamic conditions is also an important way for fine and ultrafine minerals flotation. Compared with conventional cells, the new flotation equipment, like Jameson cell, flotation column, StackCell^{TM}, Reflux^{TM}, etc., share advantageous hydrodynamic regimes such as high energy dissipation rate, short residence time, high gas holdup, and the capability to generate micron-size bubbles [1, 12]. These factors can contribute to higher particle-bubble collision efficiency. Flotation cells designed using the concept of "reactor-separator" have also gained promising application by decoupling different stages of flotation in spatially separated zones [13]. In addition, developing more efficient flotation reagents (e.g., collectors and regulators) to improve collection efficiency and selectivity of fine minerals has been continuing to attract attention in flotation research. In recent years, researchers have been realizing the critical roles of pulp rheology and frothing propensity in flotation performance, especially in the presence of fine and ultrafine minerals. To minimize the adverse effect, some beneficiation plants may firstly reject the ultrafine fractions (<10 μm) by desliming the flotation feed although the operation can cause significant loss of valuable minerals [14].

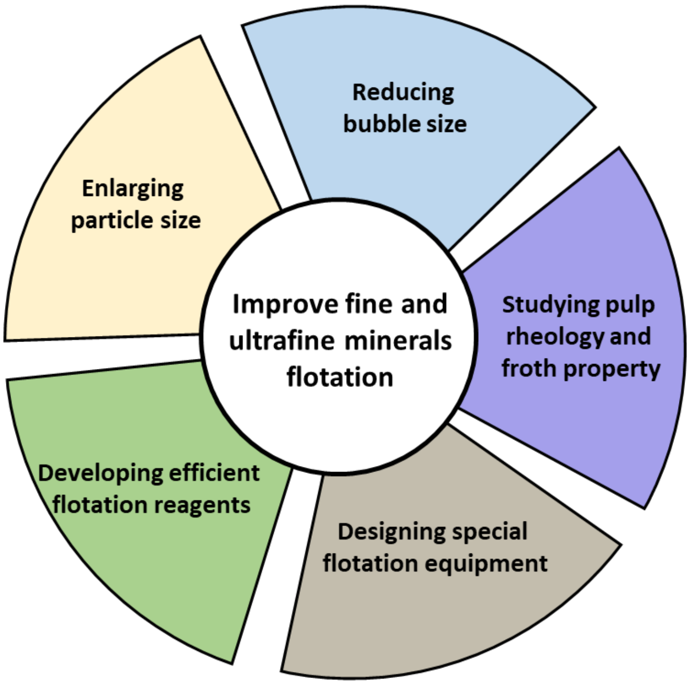

Figure 1.1 Current technical routes to improve fine and ultrafine minerals flotation.

Most of the research work has focused on fine hydrophobic particles, usually the value minerals that need to be recovered. Regardless of whether increasing the particle size, using small bubbles, or optimizing the flotation hydrodynamics, the primary objective is to enhance the collection of hydrophobic particles with air bubbles and thus improve their flotation rate and recovery. In contrast, there is not as much research effort that examines the potential effect of fine hydrophilic particles. When low-grade and finely disseminated ores are being processed by flotation, in the communication stage the mined ores need to be crushed/ground to a sufficiently fine size to liberate the value minerals from the gangue. The operation is unselective and it can indeed generate substantial fine and ultrafine hydrophilic particles as well as hydrophobic ones. As the major solid constituent of flotation pulp, a large proportion of fine hydrophilic particles may pose both hydrodynamic and chemical threats to the whole flotation system. On top of that, fine hydrophilic particles can affect flotation selectivity and concentrate quality by entrainment recovery. A suitable depressant may render gangue minerals hydrophilic, but cannot impede the mechanical entrainment of the hydrophilic gangue particles if their size is sufficiently small [15]. In this context, it is imperative to consider the effects of both the fine and ultrafine hydrophobic particles and the fine and ultrafine hydrophilic particles for the optimized flotation process.

1.2 Research objectives

The target of this research is fine and ultrafine minerals system. The research aims to use a two-stage flocculation flotation strategy to tackle the challenges of fine and ultrafine flotation. The concept is to explore appropriate ways of aggregation to separately aggregate hydrophobic particles and hydrophilic particles, forming hydrophobic aggregates and hydrophilic aggregates at the same time or sequentially. Then the normal flotation procedure can be applied to separate the hydrophobic aggregates from the hydrophilic aggregates. In this research, significant effort will be made to flocculate the ultrafine hydrophilic particles, to study the dispersion/aggregation, selective polymers flocculation, flocs property, and entrainment behaviors in the flotation pulp. The specific objectives are:

(1) Study the influence of dispersion/aggregation state of fine hydrophilic particles on the entrainment behaviors and flotation separation efficiency.

(2) Demonstrate the feasibility of forming both hydrophobic and hydrophilic flocs in a flotation system containing two ultrafine minerals.

(3) Investigate the polymer flocculation of hydrophilic particles with an emphasis on studying the effects of hydrodynamic conditions and polymer chemistry on flocs properties.

(4) Use the polymers in column flotation and examine the potential correlations between agitation intensity, floc size distribution, foaming property, and flotation performance of fine and ultrafine minerals.

1.3 Thesis scope and structure

Chapter 1 introduces the background of the dissertation research. Technology challenges, current approaches/gaps to improve fine and ultrafine minerals flotation, and the objectives of the present study are introduced.

Chapter 2 reviews and analyzes the related topics in the literature including principal variables associated with froth flotation, the effect of particle size on flotation efficiency and selectivity, the entrainment process and techniques to mitigate hydrophilic gangue entrainment, and the particle aggregation by hydrophobic association and selective (hydrophilic) polymer flocculation.

Chapter 3 investigates the influence of dispersion/aggregation state of hydrophilic particles on their entrainment in flotation. The experiment was conducted in a Denver laboratory flotation machine using the quartz-hematite minerals system. Two chemically similar polysaccharides but with different molecular weights, corn starch and corn dextrin, were used as depressants for hematite, and octadecylamine acetate was used as a collector for quartz. The research was carried out from the perspectives of studying particle aggregation size and surface wettability induced by the different depressants, verifying the feasibility of the two-stage aggregation/flocculation flotation route and revealing the necessity of aggregating hydrophilic fine particles to reduce their entrainment.

Chapter 4 investigates the flocculation of ultrafine quartz by a dual polymers system containing poly(ethylene oxide) and tannic acid, with dynamic floc size monitoring by the in-situ focused beam reflectance measurement technique. The study was carried out from the aspects of how the flocculation process and flocs properties are affected by polymer chemistry and hydrodynamic variables. This study helps to understand the improved flocculation, shear resistance and re-flocculation of fine particles induced by dual polymer systems.

Chapter 5 is based on the research work presented in Chapter 4 and further investigates the application of the tannic acid – poly(ethylene oxide) dual polymer system in flotation. The experiments were conducted using a custom-built flotation column with the hematite-quartz minerals system. Different from the work of Chapter 3, a direct flotation route was used by floating hematite particles using an in-house synthesized n-octyl hydroxamic acid as a collector. Work in this chapter was focused on studying the agitation intensity, floc size distribution, foaming property, and the corresponding flotation performance of fine and ultrafine quartz and hematite.

Chapter 6 summarizes the main observations and conclusions of the current dissertation research. The original contributions and recommendations for future work have been presented.

1.4 References

[1] A. Hassanzadeh, M. Safari, D.H. Hoang, H. Khoshdast, B. Albijanic, P.B. Kowalczuk, Technological assessments on recent developments in fine and coarse particle flotation systems, Minerals Engineering 180 (2022) 107509.

[2] M.S. Lutandula, B. Maloba, Recovery of cobalt and copper through reprocessing of tailings from flotation of oxidised ores, Journal of Environmental Chemical Engineering 1 (2013) 1085-1090.

[3] W. Trahar, A rational interpretation of the role of particle size in flotation, International Journal of Mineral Processing 8 (1981) 289-327.

[4] G.J. Jameson, The effect of surface liberation and particle size on flotation rate constants, Minerals Engineering 36 (2012) 132-137.

[5] T. Miettinen, J. Ralston, D. Fornasiero, The limits of fine particle flotation, Minerals Engineering 23 (2010) 420-437.

[6] L. Wang, Y. Peng, K. Runge, D. Bradshaw, A review of entrainment: Mechanisms, contributing factors and modelling in flotation, Minerals Engineering 70 (2015) 77-91.

[7] S. Farrokhpay, L. Filippov, D. Fornasiero, Flotation of fine particles: A review, Mineral Processing and Extractive Metallurgy Review 42 (2021) 473-483.

[8] M. Sajjad, A. Otsuki, Correlation between Flotation and Rheology of Fine Particle Suspensions, Metals 12 (2022) 270.

[9] E. Forbes, Shear, selective and temperature responsive flocculation: A comparison of fine particle flotation techniques, International Journal of Mineral Processing 99 (2011) 1-10.

[10] Z. Zhou, Z. Xu, J. Finch, J. Masliyah, R. Chow, On the role of cavitation in particle collection in flotation–A critical review. II, Minerals Engineering 22 (2009) 419-433.

[11] J.Z. Zhou, H. Li, R.S. Chow, Q. Liu, Z. Xu, J. Masliyah, Role of mineral flotation technology in improving bitumen extraction from mined Athabasca oil sands—II. Flotation hydrodynamics of water ‐ based oil sand extraction, The Canadian Journal of Chemical Engineering 98 (2020) 330-352.

[12] M. Mankosa, J. Kohmuench, L. Christodoulou, E. Yan, Improving fine particle flotation using the StackCell™(raising the tail of the elephant curve), Minerals Engineering 121 (2018) 83-89.

[13] V. Samygin, V. Panin, L. Filippov, N.Y. Stenin, Development of a reactor-separator flotation machine designed by the Moscow Institute of Steel and Alloys, Metallurgist 54 (2010) 394-400.

[14] Y. Yu, L. Ma, M. Cao, Q. Liu, Slime coatings in froth flotation: A review, Minerals Engineering 114 (2017) 26-36.

[15] Q. Liu, D. Wannas, Y. Peng, Exploiting the dual functions of polymer depressants in fine particle flotation, International journal of mineral processing 80 (2006) 244-254.

CHAPTER 2 Literature Review

2.1 Froth flotation and the principal influencing variables

Froth flotation is a physicochemical separation technique that exploits the difference in the surface wettability of mineral particles [1]. From a heterogeneous mixture of mineral solids, hydrophobic particles are made to attach to gas bubbles and subsequently carried to the froth phase and recovered as a froth product (typically the value mineral concentrate), while hydrophilic particles are kept in the pulp phase and discharged as tailings (typically as gangue minerals, unless the process is the so-called "reverse flotation"). Operating in the multiphase slurry (solid-water-air), froth flotation is a complex process consisting of many sub-processes. These include the initial slurry conditioning for particle suspension and surface property modifications, followed by gas dispersion and aeration, particle capture by bubbles via collision and attachment, and finally, the transport of the bubble/particle aggregates through the slurry and froth phases, during which bubble-particle detachment should be minimized until the aggregates reach the concentrate launder. Overall, froth flotation is an integrated engineering system being affected by several components including chemistry component, operation component and hydrodynamics component, as shown in Figure 2.1.

In froth flotation particles are recovered into the froth phase either by true flotation or entrainment as indicated in Figure 2.1. True flotation refers to the process that particles colloid with bubbles and attach to the bubble surface to form bubble-particle aggregates. It is a chemically selective process. Mineral particles with natural surface hydrophobicity or having collector-induced hydrophobicity are mainly recovered by true flotation. On the other hand, entrainment is a physical transfer process by which particles move upward from the pulp phase to the froth phase along with inter-bubble water. Recovering particles by entrainment is independent of their surface properties, which means entrainment is non-selective and it can occur for both hydrophobic and hydrophilic particles. In general, entrainment of hydrophilic gangue particles is undesirable although it can be the dominant mechanism when particle size is less than 10 μm. Entrainment of hydrophobic particles will be beneficial for the increased overall recovery especially in the finest fractions. Therefore, it may be expected for flotation stages to aim to float as much value minerals as possible, such as in rougher and scavenger flotation of fine and ultrafine minerals processing [2].

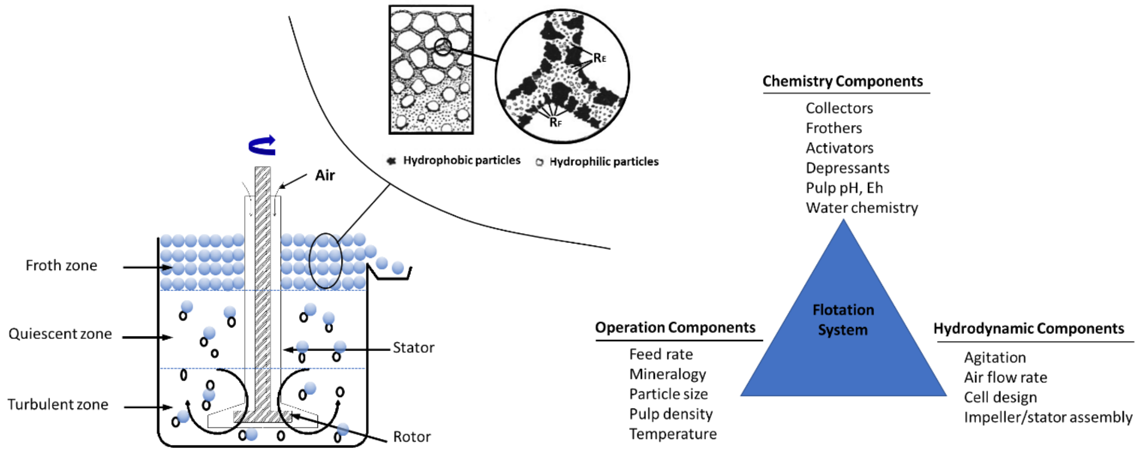

Figure 2.1 Schematic of froth flotation process in conventional flotation cells and the influencing factors. Flotation recovery of hydrophobic and hydrophilic particles by true flotation (R_F) and entrainment (R_E). Reproduced from [2-4].

In flotation of fine and ultrafine particles, finding effective ways to promote true flotation recovery of hydrophobic particles and meanwhile to eliminate or minimize the entrainment of hydrophilic particles has been the long-term goal for a more successful separation. It certainly would not be possible to achieve if we only focused on improvements of single aspects variables considering flotation is such a complicated system. To do a better job, full attention should be paid to all these components associated with the flotation process, from the colloidal and interfacial chemistry of solid-water-air three phases to mineralogy study and operating conditions for flotation, as well as the hydrodynamic regimes of flotation cells. The present research will involve variables from all three aspects, with a focus on aggregation/flocculation of both hydrophobic and hydrophilic particles and an attempt to contribute to improving the efficiency and selectivity of fine and ultrafine minerals flotation.

2.2 Bubble-particle interaction and the effect of particle size

2.2.1 Bubble-particle interaction process

According to the theory proposed by Derjaguin and Dukhin [5], the capture of a mineral particle by bubble surface is a three-stage process during which the particle has to move through three zones surrounding the bubble, namely the hydrodynamic interaction zone, the diffusiophoresis zone, and the surface force zone. Figure 2.2a schematically shows the bubble-particle collision, attachment, and detachment process in flotation. Derjaguin and Dukhin [5] proposed that it is the probabilities or efficiencies of these three sub-processes that determine the overall rate of flotation. Figure 2.2b shows the arrangement of the mentioned three zones and the forces acting on a particle approaching the bubble [6]. These forces can be generally separated into hydrodynamic forces and surface forces, wherein hydrodynamic forces include fluid drag force (F_D), gravitational force (F_g), buoyancy force (F_b), streamline force (F_s) and bubble film thinning force (F_r), and surface forces include van der Waals dispersive force (F_d), electrostatic force (F_e) and hydrophobic force (F_h). In the zone far away from the bubble surface, the hydrodynamic forces act to drive the particle to approach and sweep around the bubble surface, while surface forces begin to dominate when the particle is close to the bubble surface, and they favour particle attachment to the bubble by rupturing the thin wetting intervening water film and forming three-phase contact line between the bubble and the particle [7].

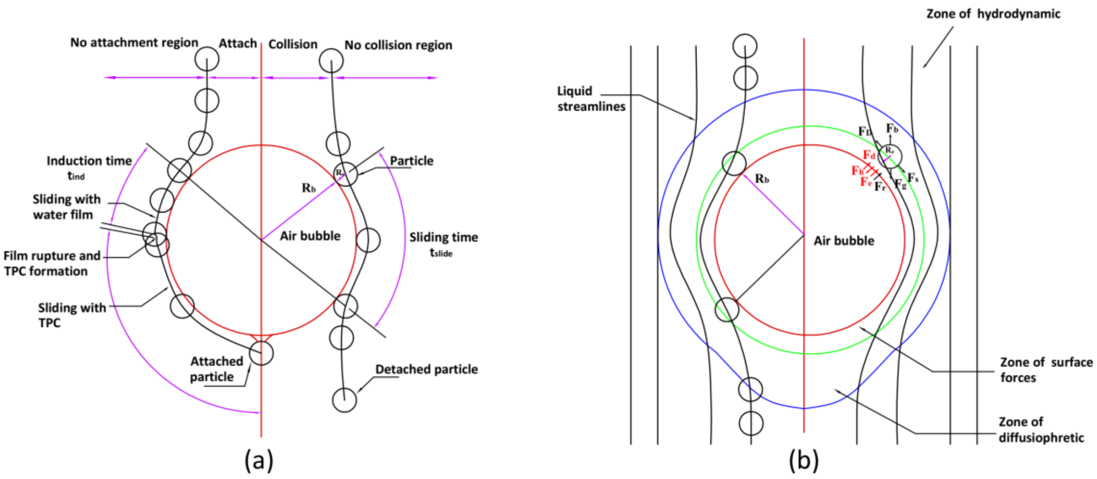

Figure 2.2 (a) Schematic of the bubble-particle collision, attachment, and detachment process in flotation. (b) The arrangement of the three zones for bubble-particle interaction and hydrodynamic and surface forces acting in the process. Reproduced from Derjaguin and Dukhin [5], Nguyen and Schulze [6], and Tao and Sobhy [8].

The probability of bubble-particle collection P_{coll} is a function of the probabilities of bubble-particle collision P_c, attachment P_a, and detachment P_d, which can be defined by

$$P_{coll} = P_c \, P_a \, (1 - P_d) \tag{2.1}$$

2.2.2 Effect of particle size on flotation

Particle size is one of the most important parameters affecting flotation process. It is reflected by the fact that particle size analysis is an essential procedure in mineral processing. It not only can provide useful information to assess grinding quality and evaluate minerals liberation in different size fractions, but also guide the determination of optimum flotation feed size to achieve maximum recovery. In the case of hydrophobic particles, abundant laboratory and plant data have shown that the recovery-particle size curve is usually stable with a characteristic “hill shape”, with the intermediate particles (from 10 μm to 70 μm) having the highest flotation recovery while particles in fine and coarse regions are more difficult to float [9]. From the perspectives of hydrodynamics, fine particles generally have small values of Stokes numbers, which describes the ratio between inertia and drag force and is used to characterize particle trajectories in fluid flow. In turbulent conditions, fine particles are more likely to coincide with the water streamlines and encounter the bubble by interception, which decreases the frequency of the bubble-particle collision as indicated from the following equation.

$$Z_{pb} = 5N_pN_b\left(\frac{d_p + d_b}{2}\right)^2\sqrt{\bar{V}_p^2 + \bar{V}_b^2} \tag{2.2}$$

where Z_{pb} is the number of collisions per unit volume per unit time between bubbles and particles, N_p and N_b are the number densities of particles and bubbles per unit volume, respectively, d_b and d_p are diameters of bubbles and particles, respectively, and $\bar{V}_p$ and $\bar{V}_b$ are the mean relative velocities of particles and bubbles relative to the specific energy dissipation and the pulp viscosity. According to the above equation, flotation kinetics can be extremely slow for fine and ultrafine hydrophobic particles. Even with excellent surface hydrophobicity and prolonged flotation time, it is difficult to obtain satisfactory recovery. In order to increase the flotation rate, the direct way is to enlarge the apparent size of the hydrophobic particles and promote their collision probability (P_c) with bubbles. Other common practices include optimizing hydrodynamic parameters such as using smaller bubbles and/or a high shear rate. The logic of the above measures can be readily inferred based on the following equation theoretically [10, 11].

$$k = \underbrace{2.39\frac{G_{fl}}{d_b\,V_{cell}}}_{mechanical\ term}\underbrace{\left[0.33\frac{\varepsilon^{4/9}\,{d_b}^{7/9}}{\nu^{1/3}}\left(\frac{\Delta\rho_b}{\rho_{fl}}\right)^{2/3}\cdot\frac{1}{v_b}\right]}_{primary\ turbulence\ term}\underbrace{E_c\cdot E_a\cdot E_s}_{elementary\ processes} \tag{2.3}$$

where k is the first-order flotation rate constant, G_{fl} is the gas flow rate, V_{cell} is the volume of flotation cell, ε is the specific energy dissipation, ν is the pulp viscosity and v_b is the bubble velocity.

In a majority of mineral processing operations, gangue minerals constitute the major components of ore feed; the effect of particle size of hydrophilic gangue minerals will certainly have a significant effect on flotation performance. If the gangue particles have a relatively large size, it may not pose severe problems for the flotation system. However, when a large amount of fine and ultrafine gangue mineral particles is present in the pulp, it becomes a challenge to maintain flotation separation efficiency. It has been suggested that a high solid content of fine gangue minerals increases pulp viscosity, which has a marked effect on cell hydrodynamics like gas dispersion. An increase in pulp viscosity with a high proportion of fine solids also reduces the energy dissipation rate and the turbulence intensity in the cell. Schubert [2] reported that dispersion of fines in flotation pulp (thus low apparent viscosity) helps to achieve a substantial reduction of turbulence damping. Therefore, he suggested that the local energy dissipation rate must be much higher than the kinematic viscosity of the flotation pulp to enhance the flotation of fine particle. Research work reported in the literature generally recognized that fine gangue mineral particles can directly or indirectly affect the recovery and grade of concentrate by mechanical entrainment [12], slime coating [13], alteration of froth properties [14], competitive adsorption of chemicals and dissolution of deleterious ions [1].

The current modelling studies of bubble-particle collision process have barely considered the potential effects of gangue particles apart from target (value) mineral particles. Leistner et al. [15] proposed that, in addition to the generally recognized governing factor of target particle/bubble size ratio, the ultrafine hydrophilic gangue particles may hinder the particle-bubble collision efficiency even when present at a low volume fraction. Their hypothesis was based on the test results shown in Figure 2.3. The effect of gangue particle size on the flotation recovery of fine (defined as 10-50 μm in their study and represented by “f”) and ultrafine (<10 μm, represented by “uf”) particles was investigated in a GTK LabCell using magnetite (MAG) as target value mineral and quartz (QRZ) as gangue mineral. The interesting observation is that, of the four combinations, the results of f-uf and uf-f feed systems were somewhat unexpected. The fine MAG had a low recovery in the f-uf feed seems due to the presence of the ultrafine QRZ, but in the uf-f feed system, even the ultrafine MAG had a relatively high recovery (~80%) in the presence of fine QRZ. By comparing the results of the f-uf and uf-f flotation system, it is reasonable to assume that the low recovery of fine MAG particles may be caused by the altered hydrodynamic conditions caused by the ultrafine hydrophilic QRZ gangue particles [15], which represent a large portion of the flotation feed. Without the ultrafine QRZ gangue particles, even the ultrafine MAG could be efficiently recovered using relatively large bubbles [15]. In light of the results, Leistner et al. [15] suggested that the current collision models may need to be re-examined to incorporate the potential effect of ultrafine hydrophilic gangue particles. Indeed, it may be necessary to selectively enlarge the size of those ultrafine gangue particles to minimize their negative effects on the flotation system [9]. In fact, the treatment of ultrafine hydrophilic gangue particles has been gaining more attention. For example, selective aggregation of fine and ultrafine hydrophilic particles including quartz, iron oxide, hydroxyapatite, sphalerite, and kaolinite by inorganic coagulants or high molecular weight polymers has been studied recently to lower their entrainment in flotation [16-20].

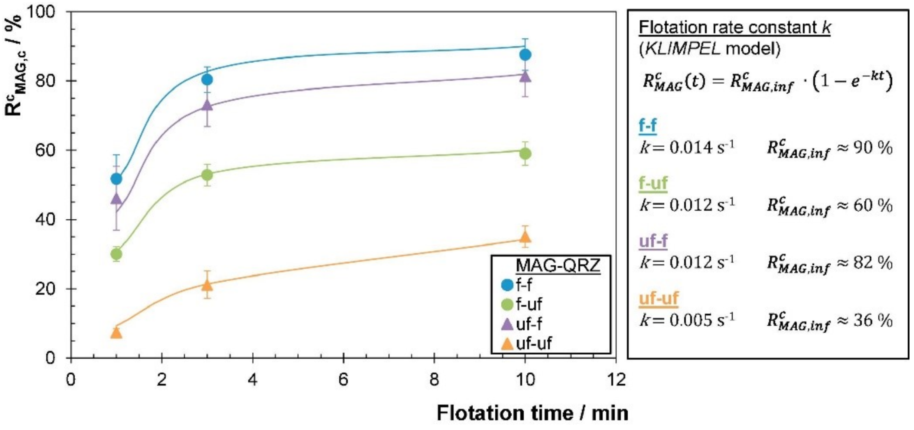

Figure 2.3 Experimental and fitted kinetic models of flotation tests for the four particle feed systems – cumulative recovery of magnetite as a function of flotation time. The flotation rate

constant for each feed system is calculated using the KLIMPEL model. Adapted from Leistner et al. [15].

2.3 Entrainment of hydrophilic particles and current mitigation measures

2.3.1 Entrainment process and water recovery

As the primary mechanism for gangue particle recovery, mechanical entrainment is considered as a two-step process. Suspended fine particles enter the froth from the region just below the pulp-froth interface, and then they are transferred through the froth phase to the concentrate [21]. The bubble swarm theory proposed by Smith and Warren [12] explains the mechanism through which water and entrained particles are transported from the pulp into the froth. Briefly, bubbles rise through the pulp and accumulate in the region below the pulp-froth interface. Due to the restricted paths between crowded bubbles plus the upward push of constantly formed new bubble layers, a part of water and suspended particles have no sufficient time to drain to the pulp before they are carried to the froth by the buoyancy of the bubble swarm. In the froth phase, the re-entry of particles into the pulp occurs due to the continuous drainage of liquid, which results in a decrease in entrainment recovery. As a whole, the recovery of particles by entrainment is a balance between the upward transfer of suspended particles into the froth and the downward drainage of particles through the froth-pulp interface to the pulp [22]

Entrainment phenomenon is closely connected to water recovery. A linear correlation between the entrainment recovery of fine and ultrafine particles and water recovery has been recognized in many studies [21, 23-25]. In the froth structure, the water content is partially related to the liquid lamella thickness, and it is found that a thicker liquid lamella means a greater content of water which increases the entrainment probability of ultrafine particles [26]. Bubbles are the primary carrier of liquid, and gas bubbles are stabilized by intervening water film to form a stable froth layer which is essential for froth flotation. In general, a compact froth structure of small bubbles is favourable for high water and mineral recoveries while a loose froth of large bubbles is good for froth product grades [26]. Given the important role of water in froth structure and particle transportation, the attempt of reducing gangue entrainment by lowering water recovery may not work. Given that entrainment is linearly related to water recovery, the emphasis should be to reduce the proportionality constant (slope) of that linear relationship.

2.3.2 Current directions to reduce the degree of entrainment

Current ways to reduce entrainment have been practiced from a range of methods. In general, these methods have focused on two aspects, one is to minimize the effect in the pulp phase by reducing the transfer of hydrophilic particles to the pulp-froth interface, and another aspect is to promote the drainage behavior of entrained hydrophilic particles within the froth phase.

Entrainment can become severe with a high solid concentration. Therefore one can decrease the solid content of flotation pulp to reduce entrainment. It is particularly useful when reducing the ultrafine fractions in the slurry, as mentioned in the last chapter that many plants choose to deslime the particles that are less than 10 µm prior to flotation. In addition, the region of the pulp-froth interface has attracted increasing attention and shown great importance in the flotation process. For the purpose of entrainment reduction, it is important to recognize that the majority of entrained solids will be rejected from this interface. The motion of particles at the pulp-froth interface depends on a force balance between gravity settling and upward flow drag. The drag force acting on particles changes as a function of flow velocity. As a result, the extent of gangue entrainment partially depends on the intensity of turbulence at this transition zone between the pulp and the froth. Too high an impeller speed in flotation cells can increase the drag force acting on the particles when they reach the pulp-froth interface and promote their entrainment [22], thus is never desirable in achieving a high-grade concentrate. By contrast, it has been increasingly recognized that it is important to keep a relatively quiescent environment at the pulp-froth interface in order to achieve increased concentrate grade by rejecting more entrained gangue particles [2, 27-29]. To achieve this, attempts have been made in modifying the turbulence generating systems such as impeller-stator assembly, redesigning cell geometry or using flow-modifying draft tubes to regulate the local turbulence distribution within the flotation cell [28, 29]. Schubert [30] compared the flotation cells with different impeller-stator-baffle systems and found that using the double-finger impellers combined with a stator having relatively high blades yields the least entrainment of fine quartz. This reduction of quartz entrainment could be attributed to a more optimized hydrodynamic condition, because such an impeller-stator system not only induces a high energy dissipation rate in the impeller stream but also creates a less turbulent flow in the upper cell zone, thus a relatively stable froth-pulp interface. In a different study by Morrison [28], he installed a horizontal mesh in the pulp below the pulp-froth interface and found that with optimal mesh design (aperture size, thickness, and position) both the recovery and grade of concentrates could be improved. This may be explained by the effect that the inserted mesh could isolate the turbulent impeller zone and the pulp-froth interface, creating a more quiescent zone between them and resulting in a greater separation of gangue particles from value particles [28].

In the froth phase, the motion of entrained materials relies on the balance between liquid velocity profile, hindered settling and particle dispersion [24]. Water and the particles unattached to bubbles are drained along the Plateau border, a structure formed with the junction of three lamellae of bubbles at a 120° angle, or by bubble coalescence and shear activity [31]. Therefore, the degree of gangue entrainment is related to the froth structure and its stability. To promote froth dewatering, one important consideration is the froth height and thus the residence time for the froth to flow from the base of the froth phase to the external concentrate launder. It has been demonstrated that a deeper froth contributes to the improved grade of the final concentrate, which is due to a longer residence time allowing the drainage of water and entrained gangue particles. Moreover, the volumetric gas flow rate is also an important variable affecting froth behaviour. In particular, the increase of airflow rates drives the froth to move more quickly, which reduces the residence time of bubbles in the froth phase and at the same time causes increased recovery of water [21]. Another opinion is held by Wang et al. [32] who argue that a higher net liquid velocity flows through the Plateau borders at the interface with increasing airflow rates, which increases the drag force acting on solid particles relative to the gravitational force and resulting in a lower degree of drainage of solids in the froth. Based on the above analysis, the mineral recovery improves at high airflow rates, but generally at the cost of a decline in concentrate grade.

Rheology property of froth may also influence the drainage process and thus gangue entrainment due to its effect on froth mobility and stability. As a key rheological term, viscosity, however, is difficult to measure in the solid-liquid-gas three-phase flotation froth. Generally, it is believed that froth viscosity affects the drainage process by influencing the residence time. Shi and Zheng [33], for example, have indicated that the froth residence time was prolonged in a viscous froth, which decreased the water content in the froth and promoted the drainage of entrained quartz. But if the froth is excessively sticky or viscous, it becomes too stable and difficult to handle. Such a stabilized froth helps to recover a greater amount of value minerals but also brings more gangue particles into concentrate by entrainment [34]. Water spraying is commonly used to accelerate the drainage process in the froth phase and reduce entrainment especially in column flotation, but if too many ultrafine hydrophilic gangue particles are present in the froth, the so-called “positive bias” brought by washing water can be reversed and lose its efficiency due to the highly viscous and stable froth layer.

2.4 Hydrophobic aggregation and selective polymer flocculation

For different purposes, increasing the effective size of fine and ultrafine mineral particles through aggregation would be beneficial for the flotation process in improving flotation recovery or selectivity [35]. Based on different interaction mechanisms by which fine particles are aggregated, these technologies generally can be divided into two categories: one is hydrophobic aggregation techniques induced by hydrophobic association [36], such as shear flocculation, oil agglomeration, and carrier flotation, and the other is selective flocculation through the bridging or charge neutralization of polymers with sufficient molecular weights [37].

2.4.1 Hydrophobic aggregation technique

Initially coined by Warren [38] when he studied the aggregation of ultrafine scheelite suspended in sodium oleate solution within a baffled beaker, shear-flocculation has become a potential way of upgrading fine-grained mineral particles. To initiate shear flocculation, apart from the surfactant induced surface hydrophobicity, a minimum shear force is needed to overcome the energy barrier caused by repulsive electrostatic forces, making particles approach a closer separation distance where hydrophobic interactions begin to dominate [37]. Due to the existence of energy barriers, the collision would not necessarily cause particle aggregation to occur. In the flotation system, the energy barrier is generally overcome by high-intensity stirring. Numerous studies are published in the literature to investigate the effect of stirring on the formation of hydrophobic flocs, among which stirring speed (rpm) and stirring time are two hydrodynamic variables that draw the most attention. It seems that hydrophobic aggregation process depends upon a balance between particle collision and flocs disruption under different hydrodynamic shear conditions [35]. The general recognition is that a critical shear force exists below which no particle aggregation occurs, while the formed flocs begin to breakdown dramatically if the shear rate is sufficiently high to exceed a certain limit [39]. This point is important for floc flotation, as it is found that the prior formation of large sized hydrophobic flocs can result in a marked improvement in recovery than directly float dispersed fine particles. On the other hand, the breakage of flocs is unwanted in floc flotation. This means that a delicate control of stirring and turbulence intensity is essential during the practical operation. In this context, the hydrodynamics requirement for shear flocculation of fine hydrophobic particles is not different from that of bubble generation (requiring high shear) and stability of bubble-particle aggregates (low shear). Therefore, mechanical flotation machines should also be suitable for shear-flocculation, either separately (in conditioning tanks and flotation tanks) or concurrently (in flotation tanks). However, it is difficult to quantitatively determine the exact value of shear strength to induce flocs formation and the subsequent breakage. This is because hydrophobic aggregation is affected by many parameters other than stirring speed alone, such as surfactant type and concentration, particle size and charge, and geometry of the conditioning tank. Koh et al. [40] presented a stirred-tank compartmentalized model to predict the particle flocculation rate by incorporating stirring speed and geometries of the tank and the impeller, and found that as the shear rate varies from 100 to 1000 s^{-1} the flocculation efficiency increased accordingly and no flocs breakage was observed in this range. In another study of processing fine gold particles using carrier floatation [41], a technique of collecting fine particles with the aid of coarse carrier particles, the aggregation behaviour varied as a function of energy consumption in the pulp. It was reported that hydrophobic aggregates of fine-coarse particles formed at an energy input levels of 0.5-2 kWh per m^3 pulp, whereas a further increase of energy input to 2-4 kWh per m^3 pulp could detach the fines from the surface of coarse carrier and the fine particles began to aggregate themselves. No aggregation was observed when the energy input surpassed 4 kWh per m^3 pulp.

In hydrophobic aggregation process the relationship between the steady floc size distribution and applied shear force is mostly empirical. In general, the maximum floc size is determined by the relative magnitude of aggregate strength and disruption stress of turbulent flow [39]. In a high shear field, large flocs can be broken by either erosion or fragmentation mechanism, highly dependent upon the relative size of eddies and flocs [42]. In a turbulent flow, the dimension of energy-dissipation eddies can be described by the Kolmogorov length scale, which is defined as

$$\eta = \left(\frac{\nu^3}{\varepsilon}\right)^{1/4} \tag{2.4}$$

where η is the Kolmogorov microscale (in length) of turbulence, ν is the kinematic viscosity and ε is the average energy dissipation rate. It is suggested that flocs tend to be ruptured by surface erosion when their size is smaller than the Kolmogorov microscale in the viscosity subrange, whilst flocs are broken by fragmentation when their size is larger than the Kolmogorov microscale in the inertia subrange [43]. The latter is often the case for flocs breakage in shear-flocculation when subjected to sufficiently high shear rates. Also, it has been shown that the breakage of flocs could be minimized with non-polar oil addition [39].

The investigation of shear regimes and the associated effects on the hydrophobic aggregation process have been carried out on the laboratory scale, and not much industrial data are available currently. In fact, shear-flocculation has rarely found application in commercial plants, therefore, it remains a question whether the shear-flocculation of particles occurs in the practical flotation process. To address this gap, more research efforts on both laboratory scale and industrial scale are needed. Such research is expected to provide insight on the effects of hydrodynamic conditions on fine and ultrafine particle shear-flocculation and bubble-particle collision/aggregation, the two processes that share some common features and requirements of hydrodynamic conditions.

2.4.2 Selective polymer flocculation

As a potential way to reduce entrainment selective polymer flocculation has not been well studied in the background of flotation. This is mainly due to the complicated mineral components of flotation slurry and the necessity of selectivity in the flotation process [35]. Whereas most polymers can adsorb unselectively onto particle surface and form hetero-aggregation of both hydrophobic and hydrophilic particles, contradicting the purpose of flotation separation.

In mineral processing the commonly used polymers can be divided into two categories according to their different origins. One is natural polymers that are extracted from plants, soil, or living organisms, such as polysaccharides [44], humate substances [45], tannins [46], chitosan [47], and so on. The other is synthetic polymers that are derived from petroleum products with the representatives such as polyacrylamides [48], nylon, polyethylene [49], etc. In terms of different purposes and functions, these polymers can be used as depressants, dispersants, and flocculants for different unit operations of mineral processing.

Selective adsorption of polymers onto mineral surface is important in froth flotation. In general, the adsorption behaviors are largely dependent on both mineral surface properties and polymer characteristics, as well as the chemistry of suspending medium. The adsorption of polymers on the mineral surface can be physisorption or chemisorption depending on the interaction forces [49]. Figure 2.4 shows the main forces involved in the adsorption reaction between polymer molecules and active sites of mineral surfaces. They are generally classified as either physical forces or chemical forces and are particularly important since these forces determine the adsorption mechanism and are thus related to flotation selectivity. Physical adsorption is reversible and relatively weak. It occurs at a high rate and usually forms monolayers first and then multilayers. For example, polyelectrolytes bear many electrolyte groups, the dissociation of which enables the polymers to be charged in water, and they can adsorb on mineral particles of opposite surface charges without selectivity. In contrast, chemical adsorption is usually selective and irreversible. It is stronger than physical adsorption with more energy changes. Chemical adsorption is limited to monolayer and occurs with the formation of chemical bonds such as covalent bonds between adsorbate and interacting surface species. It should be noted that the distinction between physical adsorption and chemical adsorption is not clear cut in some cases and they may happen at the same time.

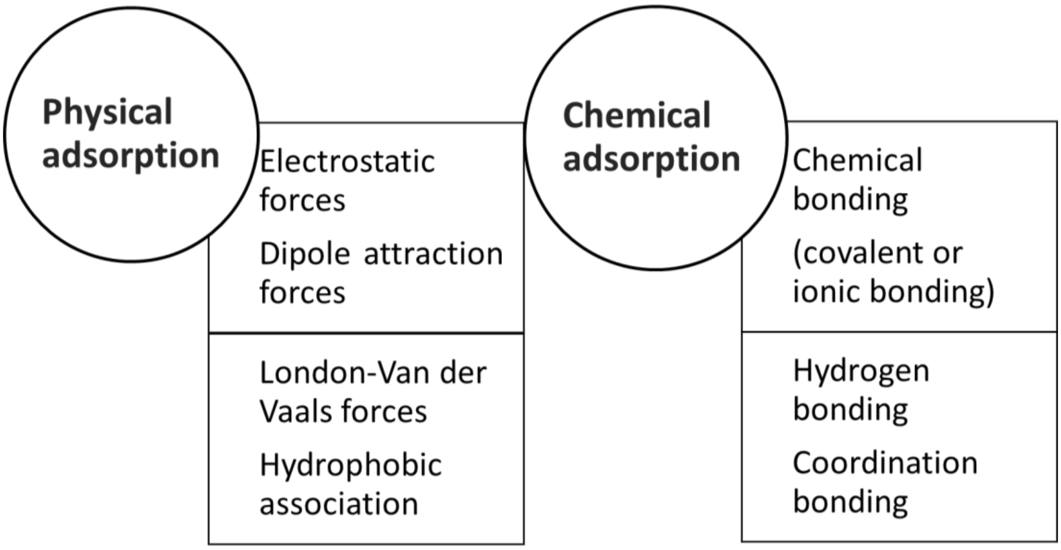

Figure 2.4 Forces involved in the adsorption of polymers onto the mineral surface. Reproduced from [37].

The flocculation process involving the use of polymers will be closely related to their adsorption behaviour. Factors that influence the adsorption also affect flocculation. From the perspective of polymer chemistry, flocculation can be affected by many variables, including functional groups, charge type and density, molecular weight, polymer concentration, water solubility, and the configuration of polymer chains in solutions. Besides, a polymer can work synergistically with another polymer to form crosslinked networks for flocculation, therefore, applying dual polymer systems is sometimes used to improve flocculation efficiency [50, 51].

Polymer flocculation is also affected by solution chemistry such as solution pH, ionic strength, temperature, and the presence of metal ions.

Selective flocculation is used to aggregate fine hydrophilic particles and form hydrophilic flocs. It differs from hydrophobic aggregation in that the formed flocs are not usually recovered by attachment to air bubbles, although exceptions exist. Liu et al. [20] proposed that for the purpose of entrainment reduction using polymers, it may have general requirements of the size of hydrophilic flocs. They may not need to be very large as those formed for thickening purposes where aggregate size should be large to ascertain fast settling rates. In fact, excessively large polymer flocs are detrimental to the selectivity of flotation as they tend to trap hydrophobic particles [52]. But the authors did not indicate the optimum floc size or structure to avoid entrainment and only suggested that it is closely related to hydrodynamic shear and polymer properties, which needs further investigation.

Flocculation process of hydrophilic particles and the property of formed flocs are also subjected to hydrodynamic forces. It is particularly important to be considered in flotation cells, where turbulent environment prevails. Like the case of hydrophobic aggregation, hydrodynamic shear forces not only affect the dispersion of polymer molecules and polymer adsorption, but also affect the formation, growth, breakup, and re-flocculation process of hydrophilic flocs. A recent study showed that cycled shear can influence quartz flocs evolution generated by a non-ionic polymer polyacrylamide [53]. One important effect of hydrodynamic shear on selective polymer flocculation is that the process of breakage and re-flocculation may be controlled by manipulating the shear strength, thereby preventing the occurrence of physical entrapment. Ding and Laskowski [52] studied the role of intense conditioning in the coal reverse flotation using polyacrylamide as a flocculant and depressant for coal, and they found that the coal grade improved under intense agitation by breaking up the bulk larger flocs and releasing entrapped ash mineral particles which could then be floated with collectors. Li et al. [49] also confirmed in their recent work that by exerting appropriate stirring, the flotation selectivity of -20 μm molybdenite from quartz was improved in the presence of poly(ethylene oxide), and it was achieved by disrupting the bulk flocs structure with stirring. Given the studies, the quantitative correlation between shear rate and floc structure as well as the entrapment reduction is not yet available for selective flocculation process [35]. The current description mostly stays in the empirical realm and lacks quantitative data.

Floc property (e.g., floc size distribution and shear resistance) of hydrophilic particles formed by polymers would be important for the flotation process. As mentioned earlier, too large flocs may not benefit flotation selectivity while too small flocs may be ineffective to attain the purpose of entrainment reduction. In addition, flocs should be able to withstand a certain shear so that they can survive the turbulent conditions of flotation cells. It was reported that the floc size distribution and the rupture process were determined by a balance between hydrodynamic forces and surface forces (e.g., Van der Waals force, electrostatic force, hydrophobic force etc.) [42]. Also, the re-flocculation of broken flocs can occur if the intensity of hydrodynamic shear changes. Not all broken flocs can be re-flocculated and it is dependent on the interaction mechanism of polymer flocculation [54]. For example, it was found that flocs re-growth can even be fully reversible when the flocculation was predominant by charge neutralization, such as flocculation by polyelectrolytes [55]. Although many investigations have studied the flocculation process in turbulent conditions, it is still rare to conduct such studies in the background of mineral flotation likely due to the complicated environment of flotation system. It is assumed that selective flocculation of hydrophilic particles by polymers will alter the role they play in the flotation pulp, for example, they may have stronger surface hydrophilicity and a larger size that can decrease the possibility for them to transfer from the pulp phase to the pulp-froth interface and then the froth phase. In this process, it lacks the experimental data to reveal the potential correlation between floc properties, entrainment degree, and flotation selectivity. Therefore, the main task in this dissertation is to study the flocculation property of hydrophilic particles using high molecular weight polymers and polymer combination, and to establish the possible relationship between flocs characteristics and flotation performance.

Starch and dextrin are two natural polysaccharides that have found widespread application in mineral processing. The two polymers have the same chemical composition except that dextrin has a much smaller molecular weight and more branched chains. In mineral flotation, it is mainly used as a depressant/dispersant. A series of systematic investigations have revealed that the adsorption of amylopectin/dextrin was through the interaction with metal-hydroxylated species on mineral surfaces [56-58]. An acid/base interaction was proposed since the fact that surface metal hydroxyl groups with a lower acidity exhibit stronger interaction [59]. According to the intensity of acid/base interaction, hydrogen bonds or chemical complexation will take effect [59]. Despite those similarities, starch has been demonstrated to have the flocculating capability for fine minerals (e.g., iron oxides) arising from its high molecular weights [19, 60, 61], while dextrin does not have flocculation capability. Given so, it would be logical for a contract study to investigate how the aggregation/dispersion state of hydrophilic particles would affect flotation entrainment using the two polysaccharides.

Poly(ethylene) oxide (PEO) is a non-ionic synthetic polymer. The application of PEO in minerals industry has been more frequently reported in recent years. It was used as a flocculant even though it also possesses the characteristic of surfactants. In some cases, PEO was used as collector/frother for hydrophobic minerals flotation [62, 63]. In aqueous solutions, two main mechanisms have been confirmed for the adsorption of PEO molecules on particle surface, namely hydrogen bonding and hydrophobic interaction [64, 65]. The flocculation behavior by PEO can vary widely based on the different surface properties of mineral particles. Research reported in the literature has reported the flocculation of oxide minerals (e.g., quartz) by PEO but the results were not consistent [17, 64-66]. In addition, it was observed that the flocculation efficiency of PEO can be improved when introducing a cofactor, a type of polymers having phenolic hydroxyls in their structures (e.g., tannic acid) [67, 68]. The improved flocculation of PEO by the cofactors was attributed to a different flocculation mechanism, namely the complex bridging [67], which is different from the traditional bridging mechanism by a single polymer. The combination of PEO-cofactors has been widely used in the papermaking industry, mainly being used for the retention of ultrafine fillers in the paper sheet [69, 70]. However, there is no such report on the application of dual polymers of PEO-cofactor in mineral flotation. It is hypothesized that using a dual polymer system containing PEO and cofactor would be effective to promote the flocculation of ultrafine hydrophilic particles in flotation. It would be interesting to study the flocculation process, flocs property, and the corresponding flotation entrainment and flotation selectivity when such a polymer combination is used for the flotation process.

2.5 References

[1] B.A. Wills, J.A. Finch, Froth flotation, Wills' Mineral Processing Technology 7 (2016).

[2] H. Schubert, On the optimization of hydrodynamics in fine particle flotation, Minerals Engineering 21 (2008) 930-936.

[3] B. Gorain, J. Franzidis, E. Manlapig, Flotation cell design: application of fundamental principles, Julius Kruttschnitt Mineral Research Centre. Indooroopilly. Queensland. Australia (2000).

[4] A. Haxhiaj, B. Haxhiaj, The Management of Lead Concentrate Acquisition in "Trepca", TMS Annual Meeting & Exhibition, Springer, 2018, pp. 185-198.

[5] B. Derjaguin, S. Dukhin, Theory of flotation of small and medium-size particles, Progress in Surface Science 43 (1993) 241-266.

[6] A. Nguyen, H.J. Schulze, Colloidal science of flotation, CRC Press2003.

[7] A. Nguyen, H. Schulze, J. Ralston, Elementary steps in particle—bubble attachment, International Journal of Mineral Processing 51 (1997) 183-195.

[8] D. Tao, A. Sobhy, Nanobubble effects on hydrodynamic interactions between particles and bubbles, Powder technology 346 (2019) 385-395.

[9] W. Trahar, A rational interpretation of the role of particle size in flotation, International Journal of Mineral Processing 8 (1981) 289-327.

[10] J. Duan, D. Fornasiero, J. Ralston, Calculation of the flotation rate constant of chalcopyrite particles in an ore, International Journal of Mineral Processing 72 (2003) 227-237.

[11] C.M. Phan, A.V. Nguyen, J.D. Miller, G.M. Evans, G.J. Jameson, Investigations of bubble–particle interactions, International Journal of Mineral Processing 72 (2003) 239-254.

[12] P. Smith, L. Warren, Entrainment of particles into flotation froths, Mineral Procesing and Extractive Metallurgy Review 5 (1989) 123-145.

[13] Y. Yu, L. Ma, M. Cao, Q. Liu, Slime coatings in froth flotation: A review, Minerals Engineering 114 (2017) 26-36.

[14] I. Achaye, Effect of particle properties on froth stability, (2017).

[15] T. Leistner, U.A. Peuker, M. Rudolph, How gangue particle size can affect the recovery of ultrafine and fine particles during froth flotation, Minerals Engineering 109 (2017) 1-9.

[16] M. Cao, Q. Liu, Reexamining the functions of zinc sulfate as a selective depressant in differential sulfide flotation—The role of coagulation, Journal of colloid and interface science 301 (2006) 523-531.

[17] J. Gong, Y. Peng, A. Bouajila, M. Ourriban, A. Yeung, Q. Liu, Reducing quartz gangue entrainment in sulphide ore flotation by high molecular weight polyethylene oxide, International Journal of Mineral Processing 97 (2010) 44-51.

[18] D. Liu, Y. Peng, Reducing the entrainment of clay minerals in flotation using tap and saline water, Powder Technology 253 (2014) 216-222.

[19] Q. Liu, D. Wannas, Y. Peng, Exploiting the dual functions of polymer depressants in fine particle flotation, International journal of mineral processing 80 (2006) 244-254.

[20] Q. Liu, Selective aggregation of hydrophilic gangue minerals in froth flotation, MRS Online Proceedings Library (OPL) 1380 (2012).

[21] X. Zheng, N. Johnson, J.-P. Franzidis, Modelling of entrainment in industrial flotation cells: Water recovery and degree of entrainment, Minerals Engineering 19 (2006) 1191-1203.

[22] L. WAng, Y. Peng, K. Runge, D. Bradshaw, A review of entrainment: Mechanisms, contributing factors and modelling in flotation, Minerals Engineering 70 (2015) 77-91.

[23] Z. Konopacka, J. Drzymala, Types of particles recovery—water recovery entrainment plots useful in flotation research, Adsorption 16 (2010) 313-320.

[24] S. Neethling, J. Cilliers, The entrainment of gangue into a flotation froth, International Journal of Mineral Processing 64 (2002) 123-134.

[25] L.J. Warren, Determination of the contributions of true flotation and entrainment in batch flotation tests, International Journal of Mineral Processing 14 (1985) 33-44.

[26] T. Subrahmanyam, E. Forssberg, Froth stability, particle entrainment and drainage in flotation—a review, International Journal of Mineral Processing 23 (1988) 33-53.

[27] D. Mesa, A.J. Morrison, P.R. Brito-Parada, The effect of impeller-stator design on bubble size: Implications for froth stability and flotation performance, Minerals Engineering 157 (2020) 106533.

[28] A.J. Morrison, Tank design modifications for the improved performance of froth flotation equipment, Imperial College London, 2017.

[29] E. Tabosa, K. Runge, P. Holtham, The effect of cell hydrodynamics on flotation performance, International Journal of Mineral Processing 156 (2016) 99-107.

[30] H. Schubert, On the turbulence-controlled microprocesses in flotation machines, International journal of mineral processing 56 (1999) 257-276.

[31] G. Cutting, Effect of froth structure and mobility on plant performance, Mineral Procesing and Extractive Metallurgy Review 5 (1989) 169-201.

[32] L. Wang, Y. Xing, J. Wang, Mechanism of the combined effects of air rate and froth depth on entrainment factor in copper flotation, Physicochemical Problems of Mineral Processing 56 (2020).

[33] F. Shi, X. Zheng, The rheology of flotation froths, International Journal of Mineral Processing 69 (2003) 115-128.

[34] S. Farrokhpay, The significance of froth stability in mineral flotation—A review, Advances in colloid and interface science 166 (2011) 1-7.

[35] E. Forbes, Shear, selective and temperature responsive flocculation: A comparison of fine particle flotation techniques, International Journal of Mineral Processing 99 (2011) 1-10.

[36] T. Subrahmanyam, K.E. Forssberg, Fine particles processing: shear-flocculation and carrier flotation—a review, International Journal of Mineral Processing 30 (1990) 265-286.

[37] J.S. Laskowski, J. Ralston, Colloid chemistry in mineral processing, Elsevier2015.

[38] L.J. Warren, Shear-flocculation of ultrafine scheelite in sodium oleate solutions, Journal of Colloid and Interface Science 50 (1975) 307-318.

[39] S. Lu, Y. Ding, J. Guo, Kinetics of fine particle aggregation in turbulence, Advances in Colloid and Interface Science 78 (1998) 197-235.

[40] P. Koh, J.R. Andrews, P. Uhlherr, Flocculation in stired tanks, Chemical engineering science 39 (1984) 975-985.

[41] L. Valderrama, J. Rubio, High intensity conditioning and the carrier flotation of gold fine particles, International Journal of Mineral Processing 52 (1998) 273-285.

[42] P. Jarvis, B. Jefferson, J. Gregory, S.A. Parsons, A review of floc strength and breakage, Water research 39 (2005) 3121-3137.

[43] D. Thomas, S. Judd, N. Fawcett, Flocculation modelling: a review, Water research 33 (1999) 1579-1592.

[44] Q. Liu, J.S. Laskowski, Polysaccharide application in mineral processing, Encyclopaedia of surface and colloid science. Marcel & Dekker, New York (2006) 5035-5055.

[45] D. Wang, F. Jiao, W. Qin, X. Wang, Effect of surface oxidation on the flotation separation of chalcopyrite and galena using sodium humate as depressant, Separation Science and Technology 53 (2018) 961-972.

[46] J. Rutledge, C.G. Anderson, Tannins in mineral processing and extractive metallurgy, Metals 5 (2015) 1520-1542.

[47] P. Huang, M. Cao, Q. Liu, Using chitosan as a selective depressant in the differential flotation of Cu–Pb sulfides, International Journal of Mineral Processing 106 (2012) 8-15.

[48] P. Huang, L. Wang, Q. Liu, Depressant function of high molecular weight polyacrylamide in the xanthate flotation of chalcopyrite and galena, International Journal of Mineral Processing 128 (2014) 6-15.

[49] S. Li, L. Gao, J. Wang, H. Zhou, Y. Liao, Y. Xing, X. Gui, Y. Cao, Polyethylene oxide assisted separation of molybdenite from quartz by flotation, Minerals Engineering 162 (2021) 106765.

[50] M. Lapointe, B. Barbeau, Dual starch–polyacrylamide polymer system for improved flocculation, Water research 124 (2017) 202-209.

[51] J. Gregory, S. Barany, Adsorption and flocculation by polymers and polymer mixtures, Advances in colloid and interface science 169 (2011) 1-12.

[52] K. Ding, J. Laskowski, Effect of conditioning on selective flocculation with polyacrylamide in the coal reverse flotation, Mineral Processing and Extractive Metallurgy 116 (2007) 108-114.

[53] C. Wang, C. Sun, Q. Liu, Formation, breakage, and re-growth of quartz flocs generated by non-ionic high molecular weight polyacrylamide, Minerals Engineering 157 (2020) 106546.

[54] W. Yu, G. Li, Y. Xu, X. Yang, Breakage and re-growth of flocs formed by alum and PACl, Powder Technology 189 (2009) 439-443.

[55] W. Yu, J. Gregory, L.C. Campos, Breakage and re-growth of flocs formed by charge neutralization using alum and polyDADMAC, Water research 44 (2010) 3959-3965.

[56] Q. Liu, J. Laskowski, The role of metal hydroxides at mineral surfaces in dextrin adsorption, II. Chalcopyrite-galena separations in the presence of dextrin, International Journal of Mineral Processing 27 (1989) 147-155.

[57] J. Laskowski, Q. Liu, N. Bolin, Polysaccharides in flotation of sulphides. Part I. Adsorption of polysaccharides onto mineral surfaces, International journal of mineral processing 33 (1991) 223-234.

[58] Q. Liu, J. Laskowski, The role of metal hydroxides at mineral surfaces in dextrin adsorption, I. Studies on modified quartz samples, International Journal of Mineral Processing 26 (1989) 297-316.

[59] Q. Liu, Y. Zhang, J. Laskowski, The adsorption of polysaccharides onto mineral surfaces: an acid/base interaction, International Journal of Mineral Processing 60 (2000) 229-245.

[60] H. Hao, L. Li, P. Somasundaran, Z. Yuan, Adsorption of pregelatinized starch for selective flocculation and flotation of fine siderite, Langmuir 35 (2019) 6878-6887.

[61] K. Shrimali, V. Atluri, Y. Wang, S. Bacchuwar, X. Wang, J.D. Miller, The nature of hematite depression with corn starch in the reverse flotation of iron ore, Journal of Colloid and Interface Science 524 (2018) 337-349.

[62] E. Manev, R. Pugh, Frother/collector interactions in thin froth films and flotation, Colloids and Surfaces A: Physicochemical and Engineering Aspects 70 (1993) 289-295.

[63] R. Pugh, Non-ionic polyethylene oxide frothers in graphite flotation, Minerals Engineering 13 (2000) 151-162.

[64] J. Rubio, J. Kitchener, The mechanism of adsorption of poly (ethylene oxide) flocculant on silica, Journal of Colloid and Interface Science 57 (1976) 132-142.

[65] S. Mathur, B.M. Moudgil, Adsorption mechanism (s) of poly (ethylene oxide) on oxide surfaces, Journal of colloid and interface science 196 (1997) 92-98.

[66] E. Koksal, R. Ramachandran, P. Somasundaran, C. Maltesh, Flocculation of oxides using polyethylene oxide, Powder technology 62 (1990) 253-259.

[67] T.G. van de Ven, Association-induced polymer bridging by poly (ethylene oxide)–cofactor flocculation systems, Advances in colloid and interface science 114 (2005) 147-157.

[68] T. Lindström, G. Glad-Nordmark, Flocculation of latex and cellulose dispersions by means of transient polymer networks, Colloids and surfaces 8 (1984) 337-351.

[69] M.R. Wu, J. Paris, T.G. van de Ven, Flocculation of papermaking fines by poly (ethylene oxide) and various cofactors: Effects of PEO entanglement, salt and fines properties, Colloids and Surfaces A: Physicochemical and Engineering Aspects 303 (2007) 211-218.

[70] M. Cadotte, M.E. Tellier, A. Blanco, E. Fuente, T.G. Van De Ven, J. Paris, Flocculation, retention and drainage in papermaking: a comparative study of polymeric additives, The Canadian Journal of Chemical Engineering 85 (2007) 240-248.

CHAPTER 3 Influence of Aggregation/Dispersion State of Hydrophilic Particles on Their Entrainment in Fine Minerals Flotation

3.1 Introduction

In froth flotation, mineral particles are collected into froth product either by true flotation or mechanical entrainment. True flotation involves the collision and attachment of hydrophobic particles to gas bubbles to form mineralized bubbles. The mineralized bubbles rise to the top of pulp phase to form a froth layer which are scraped off as the froth product. It is a selective process. Unlike true flotation, entrainment is a physical process by which mineral particles are carried upwards with the inter-bubble water from pulp to froth product [1, 2]. Entrainment is unselective and therefore undesirable.

Entrainment is affected by many factors including particle properties such as particle size and density [3, 4] pulp and froth conditions such as solid content, slurry viscosity, froth depth and structure [5-7] and operating parameters such as impeller speed, air flow rate, flotation time and wash water [8, 9]. Particle size and water recovery are the two most important factors [10, 11]. Entrainment increases as particle sizes decrease [12]. Fine hydrophilic particles smaller than about 20 µm usually do not have enough inertia to drain back to the pulp once they are pushed to the froth phase, and their entrainment can become the predominant mechanism for recovery into the froth product. Water recovery also plays a critical role in entrainment. Research work reported in literature has indicated a linear correlation between the degree of entrainment and water recovery in a given flotation time [11, 13-15].

Several methods have been proposed to distinguish entrainment from true flotation. The method of Trahar [16] determines true flotation by the gaps of mineral recoveries in two groups of batch flotation, with one group using only frother and the other using both frother and collector. However, the froth structure which dictates entrainment tends to be different in the two situations, therefore this method does not give an accurate analysis. Another method was proposed by Warren based on the effect of water recovery [12, 15]. According to Warren's model, the recoveries of floatable and non-floatable particles are summarized by equations (3.1) and (3.2) below:

$$R_M = F_M + e_M \cdot W_{water} \tag{3.1}$$

$$R_G = e_G \cdot W_{water} \tag{3.2}$$

where F_M is the intercept of the extrapolated line on the mineral recovery axis in the mineral recovery versus water weight plot, representing the recovery by true flotation; e_M and e_G are entrainment factors for floatable and non-floatable minerals, respectively; and $W_{water}$is the weight of water recovered in a given time.

In addition to the Warren model, the method developed by Mhonde et al. [17] assumes that the amount of gangue particles reported to concentrate is solely due to entrainment when a high dosage of depressant (>500 g/t) is used.

Reducing the entrainment of fine gangue particles is necessary especially under the current state of the mining industry where more low-grade and complex ores are being explored. To fully liberate value minerals from gangue, ultrafine milling by Tower mill, Verti mill and Isamill is replacing traditional ball mills, particularly in the rougher concentrate regrinding stage [18]. As a result, a large amount of fine and ultrafine particles is generated in the feed for flotation. Several approaches have been used to reduce entrainment: desliming so that only the sand fraction is floated; maintaining a deep froth layer in flotation columns coupled with wash water; flotation at a low pulp density and moderate agitation and aeration rate. However, these all have their undesirable shortcomings.

Selective polymer flocculation is reported as a potential technique to reduce entrainment. Polymers with sufficient molecular weights can aggregate ultrafine gangue particles and form large hydrophilic flocs, which is beneficial to lower entrainment. For example, it was shown that a small dosage of high molecular weight PEO could reduce quartz or kaolinite entrainment [19, 20].

In iron ore flotation, starch has been used as an effective depressant for iron oxide while the associated quartz gangue is floated directly by a cationic collector, or by an anionic collector after calcium activation (e.g., [21, 22]). Cooke et al. [23] reported the flocculation of iron oxide minerals by different starches. It followed that Frommer & Colombo [24] and Colombo [25] reported that starch was used in the desliming of iron ores as a selective flocculant to lower the losses of fine iron oxide to the slime product. The deslimed iron ore was then floated by a cationic collector while more starch was introduced to depress iron oxide. Clearly, in Frommer and Colombo's reports, the starch acted as both a depressant that rendered the iron oxide hydrophilic, and a flocculant that flocculated the fine iron oxide to form larger sized flocs. Therefore, starch performed the dual functions of depressant/flocculant in the iron ore flotation.

A variation of starch, called dextrin, is obtained as a degradation product of starch through pyrolysis in an acidic environment [26]. Dextrin typically has a branched structure but with much smaller molecular weights than starch. Interestingly, dextrin has rarely been used in iron ore flotation. Chang et al. [27] tested several starch and starch derivatives including dextrin as iron oxide depressants and noted that dextrin performed the worst but did not explain why. On the other hand, dextrin has been used as a selective depressant for molybdenite [28], coal [29], lead sulfide [30-32], nickel sulfide [33], iron sulfide [34, 35]. An interesting and also important question is whether starch and dextrin, derived from the same sources, can be used interchangeably for the reported applications? In some cases researchers did use both starch and dextrin in their applications and observed different behaviors but did not elucidate the reasons for the differences.

Starch and dextrin contain the same chemical moieties, and their adsorption mechanisms have been shown to be similar. IR spectra and X-ray photoelectron spectroscopy have indicated that a chemical complex (chemisorption) can be formed between the iron atoms of hematite surface and starch [36-38]. Dextrin is also shown to interact with the metal hydroxides at mineral surfaces [31, 32, 39].

Being of a low molecular weight, dextrin is typically considered as a dispersant, while starch a flocculant. Since the chemical entity of starch and dextrin is the same, and the only perceived difference is the molecular weight, it becomes an interesting prospect to examine their effects in a froth flotation system. This would help answer an important question in fine and ultrafine particle flotation, i.e., to improve fine and ultrafine flotation efficiency, should the fine/ultrafine hydrophilic particles be kept highly dispersed or flocculated?

This study would be particularly useful as in the past several decades, the majority of the effort in fine/ultrafine particle flotation has been focused on enlarging the particle size of the hydrophobic minerals by hydrophobic (shear) flocculation or oil agglomeration while keeping the fine/ultrafine hydrophilic particles highly dispersed. If polymer flocculation of hydrophilic minerals is beneficial to froth flotation, then is it possible to combine the hydrophobic flocculation or oil agglomeration with polymer flocculation to achieve the so-called dual-flocculation flotation? That is, to form homogenous hydrophobic flocs and homogenous hydrophilic flocs, and then using froth flotation to separate them?

The purpose of the present work is to study the influence of aggregation/dispersion state of a hydrophilic mineral on its degree of entrainment for a feed system containing both fine value and fine gangue minerals in a mechanical flotation machine. Quartz and hematite were selected as model minerals. The reverse cationic flotation route was chosen using octadecylamine acetate (ODA) as a collector for quartz. The relatively long carbon chain in ODA makes it possible to cause aggregation of fine quartz particles through hydrophobic association when the ODA is adsorbed on quartz surface. Corn starch and corn dextrin were used as depressants for hematite. As indicated earlier, due to the molecular weight difference, corn starch and corn dextrin may induce either polymer flocculation or dispersion of fine hematite and thus different flotation results. Focused beam reflectance measurement (FBRM) particle size analysis was used to perform in-situ measurement of particle/floc size evolution in a simulated system resembling the batch flotation environment to monitor both the hydrophobic flocculation and polymer flocculation.

3.2 Materials and methods

3.2.1 Mineral samples and reagents

A hematite sample with purity greater than 90% was obtained from a spiral concentrate stream of an iron ore mine in eastern Canada. X-ray diffraction analysis showed that the sample consisted of a small amount of quartz and pyrolusite besides hematite. In the study, two size fractions of the hematite sample were prepared and used in batch flotation. The spiral concentrate was wet ground in a laboratory ball mill and the -20 μm fraction was obtained by wet sieving on a 635-mesh sieve (aperture 20 μm). A -75+20 μm size fraction of hematite was obtained by wet sieving the +20 μm product on a 200-mesh sieve (aperture 75 μm). The sieved fractions were collected, dried and homogenized. High purity quartz (Min-U-Sil 15) used in the present study was purchased from U.S. SILICA. The vendor-specified particle size was less than 15 μm. The chemical analyses of the -20 μm hematite and the -15 μm quartz samples are shown in Table 3.1. The particle size distributions of hematite and quartz samples were determined by a Malvern Mastersizer 3000 particle size analyzer and the results were shown in Figure 3.1. Additionally, the granulometric parameters such as D_{10}, D_{50} and D_{90}, Sauter mean diameter D_{32} and de Brouckere mean diameter D_{43} were also given as listed in the inset table of Figure 3.1. As can be seen, the particle size distributions of quartz and fine hematite samples were quite close with a mode around 6-7 μm, and more than 80% of the particles were less than 10 μm. In contrast, the particle size of coarse hematite sample was relatively larger with a mode about 30-35 μm. It should be noted that part of fine fractions (<10 μm) existed in the coarse hematite sample, accounting for 18% approximately.

Table 3.1 Chemical analysis of pure mineral samples by whole rock analysis.

Components	SiO_2	Al_2O_3	Fe_2O_3	MgO	CaO	Na_2O	K_2O	TiO_2	P_2O_3	MnO
Hematite (%)	4.44	0.11	90.94	<0.01	0.01	<0.01	0.03	0.02	<0.01	3.65
Quartz (%)	98.5	1.00	0.03	0.01	0.03	0.01	0.01	0.01	-	-

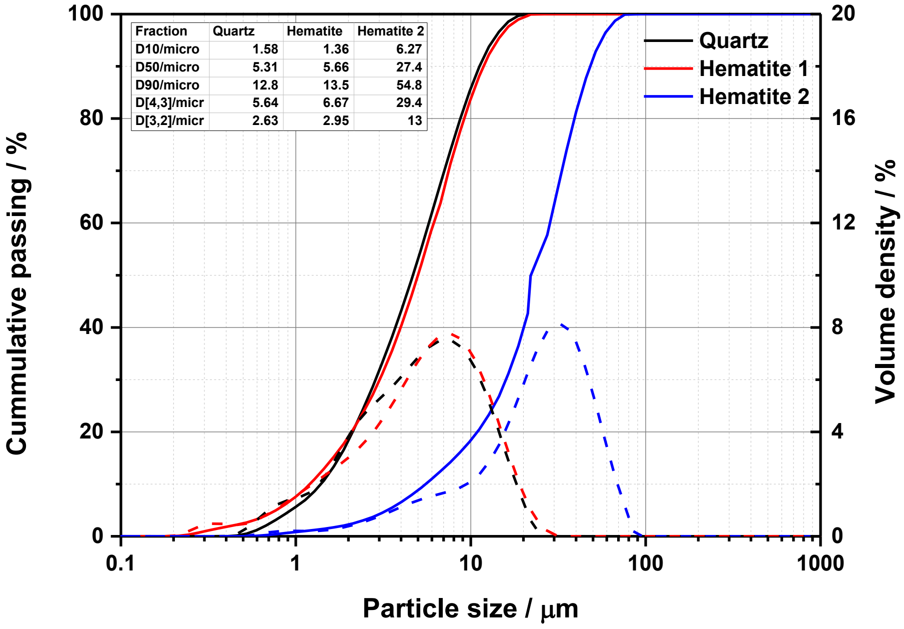

Figure 3.1 Particle size distribution of mineral samples.

Flotation chemicals included starch from corn (corn starch) and dextrin from corn, type 1 (corn dextrin), and they were purchased from Sigma-Aldrich. The 0.5 wt% corn starch stock solution was prepared by alkali gelatinization using 1 M sodium hydroxide. The 0.5 wt% dextrin solution was prepared by dispersing dextrin powder in distilled water followed by heating in a water bath until the dextrin was completely dissolved. The collector used was octadecylamine acetate (ODA, $C_{18}H_{39}N.C_2H_4O_2$) acquired from Tokyo Chemical Industry Co., Ltd. The ODA purity provided by the supplier was >60% analyzed by gas chromatograph. Due to the frothing property of amine-based reagent, the ODA also served as a frother in flotation. At room temperature, the solution of ODA was a milky viscous colloidal liquid, and it became clear as the solution temperature was raised above 75°C. Therefore, the ODA stock solution was heated in a water bath each time it was used. Hexane was purchased from Fisher Scientific and used as extracting agent in the water/hexane partition tests. Sodium hydroxide (NaOH) and hydrochloric acid (HCl) of analytical grade were purchased from Fisher Scientific and used as pH modifiers. Distilled water was used in all experiments to eliminate the effect of calcium and magnesium ions and other impurities in the Edmonton tap water on flotation.

3.2.2 Batch flotation test

Batch flotation was carried out using a laboratory Denver D-12 flotation machine with a 1.5-liter stainless steel cell. As high amounts of fine particles were contained in the feed, a relatively low solid content of ~10 wt% was selected for all the tests to minimize the effect of slurry viscosity on flotation process. In each flotation test, a total mass of 100 g mixed minerals (at a mass ratio of hematite and quartz of 1:1) was dispersed in 900 mL distilled water. The pulp pH was adjusted to ~10.5 to ensure that both minerals were negatively charged and the initial heterocoagulation was minimized by electrostatic repulsion. The pulp was conditioned with 125 g/t sodium silicate as a dispersant for 2 min, then with varying dosages of corn starch or corn dextrin for 5 min, followed by 1000 g/t ODA as a collector and frother for 2 min. The concentration of ODA was confirmed by the specific surface area of quartz (2.8 m^2/g) and related research work. At this dosage, the starting concentration of ODA in the flotation pulp was about 1×10^{-4} mol/L. A total flotation time of 12 min was conducted due to the low flotation rate of the fine minerals. Three concentrates (i.e., quartz concentrates) were collected at 1 min, 4 min and 12 min. The concentrates were weighed wet and dry to determine the water recovery. The Fe and SiO_2 contents in the three concentrates and the tailings were determined using a CTX 810 Benchtop XRF Analyzer (Bruker). During flotation, the pulp level in the cell was kept constant by added water. The rotor speed (1000 rpm) and air flowrate (4 L/min) were kept constant for all the experiments to ensure the similar hydrodynamic conditions.

3.2.3 Micro-flotation test

Micro-flotation flotation tests were carried out in a custom-made glass flotation tube as depicted in Figure 3.2. A sintered glass frit (7) with a pore size of 1.6 μm was fitted in the base of the tube, on which a magnetic stirring bar (6) was placed and used to stir the pulp. The top of the tube was modified after Siwek et al. [40]. In the ideal case when no frother was added, each time only one gas bubble could pass through the narrow throat (4) that connects the tube to the collection bulb, and only the particles attached to the bubble could be collected. Therefore, the tube was designed to minimize the amount of water recovered into the froth phase and thus the degree of entrainment. For a typical experiment, 1.5 g -20 μm mineral particles were mixed with 150 mL distilled water and agitated in a 250-mL beaker. The pulp pH was adjusted to ~10.5 using NaOH, followed by conditioning with corn starch or corn dextrin for 5 min and ODA for another 2 min. The conditioned pulp was then transferred to the flotation tube and floated for 7 min with high purity nitrogen at a flow rate of 15 mL/min. Afterwards, the froth product and the tailing were filtered, dried and weighed to calculate the flotation recovery, which was taken as the floatability of the mineral sample under the tested conditions.

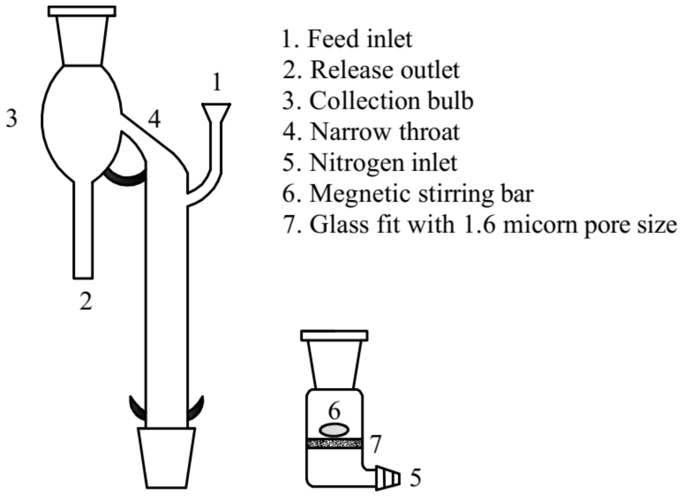

Figure 3.2 Flotation tube for micro-flotation.

3.2.4 Surface wettability characterization

A solvent extraction method was used to assess the surface wettability of fine hematite treated with corn starch or corn dextrin. This method was based on the principle of oil agglomeration flotation that hydrophobic particles tend to be oil-wet and are floatable with the assistance of oil [41-43]. A 200 mL hematite suspension containing 0.5 wt% fine hematite was prepared in a 250-mL beaker under moderate magnetic stirring. The pH of the suspension was adjusted to ~10.5 using NaOH. For each test, 20 mL hematite suspension was firstly pipetted to a glass bottle with a volume of approximately 40 mL, followed by the addition of corn starch or corn dextrin and ODA of desired concentrations. Afterwards, 10 mL hexane was added to the glass bottle as extracting solvent, and a clear oil phase could be observed on the upper level of the bottle due to the lower density of hexanes (660.6 kg/m^3). The water-hematite-hexane mixture was then hand-shaken for 30 seconds and subsequently left to stand overnight for phase separation. It was found that hydrophobic particles can stay in the oil phase (hexane) or the oil-water interface, while the hydrophilic particles settled down in the aqueous phase. The particles in hexane and on the hexane/water interface were siphoned out and separated from the particles in the bottom of the bottle. The particles were dried and weighed using an analytical balance.

The weight percentage of the solids in the oil phase (hexane) and oil-water interface was calculated. Each experiment with the same condition was repeated three times and the average result was reported.

3.2.5 Viscosity measurement using an Ostwald viscometer

The intrinsic viscosity is a reflection of the molecular weight of polymer solution. The Mark-Houwink equation gives the relationship between molecular weight and viscosity as shown below [44]:

$$[\eta] = KM^{\alpha} \tag{3.3}$$

where $[\eta]$ is the intrinsic viscosity, M is the molecular weight and K and α are constants for a given polymer-solvent system. Typically, the polymer with a high molecular weight has the higher viscosity of its solution. The Ostwald viscometer is a simple laboratory device for determining the viscosity of the liquid with a certain density as shown in Figure 3.3. It measures the time it takes for a known volume liquid (the volume between the upper mark A and lower mark B) to flow through the capillary tube under the influence of gravity. The viscosities of corn starch and corn dextrin solution (0.5 wt%) were measured at room temperature using the Ostwald viscometer. Distilled water with standard viscosity and density was used as reference liquid. Before the test, the viscometer was fixed in a vertical position by a holder. For each test, 3.0 mL liquid sample was pipetted and added into the large bulb on the left. The liquid was then pulled into the higher bulb on the right by suction until the upper level of the liquid was above the Upper mark A. A stopwatch was used to read the time that liquid flowed from mark A to mark B. The average time was calculated from three repeated runs. The viscosity of test sample was expressed as

$$\eta_2 = \eta_1 . \frac{\rho_2 t_2}{\rho_1 t_1} \tag{3.4}$$

where η_1 and η_2 are viscosities of distilled water and test sample, and ρ_1 and ρ_2 are densities of water and test sample, respectively. t_1 is the average time it takes for water to flow from mark A to mark B, and t_2 is the average time of flow of test sample from mark A to mark B. At room temperature, the density of water ρ_1 is 1000 kg/m^3, and the viscosity of water η_1 is 0.001 Pa·s. The density of the test sample solution was determined using pycnometer method in the laboratory.

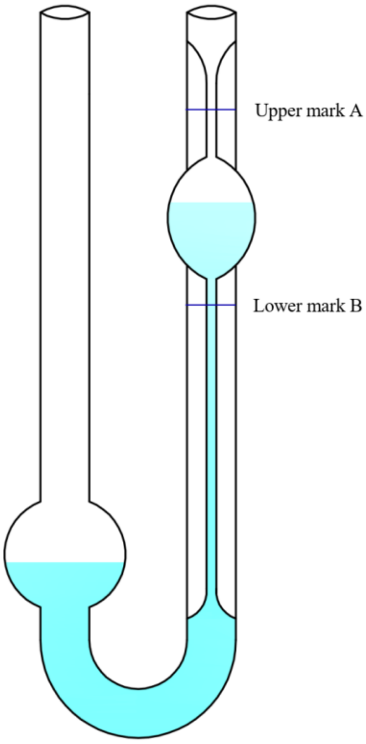

Figure 3.3 A laboratory U-shaped Ostwald viscometer.

3.2.6 In-situ particle size distribution measurement

To investigate the particle aggregation/dispersion behaviors in flotation process, a FBRM measurement system was set up to simulate flotation conditions as shown in Figure 3.4. The FBRM probe (Particle Track G400, Mettler Toledo) was placed directly in the slurry and monitored particle size and count evolution continuously with flotation reagents addition. As FBRM technique is applicable for direct in-process measurement at full concentrations without sampling, it is more likely to provide the real-time picture of particle size distribution in complex flotation system compared with other particle characterization methods. The working principle of FBRM is based on laser backscattering [45, 46]. A highly focused beam spot is formed through a set of optics at the sapphire widow, and it rotates at a fixed velocity (2 m/s). As the focused beam scans across the slurry, the particles that flow past the window can backscatter the laser light to the detector. The duration of each backscattered light pulse multiplied by the scan speed gives the distance of the particle which is defined as chord length [45, 47]. Typically, thousands of chord length data can be measured during each measurement resulting in a sensitive chord length distribution (CLD) reported. The dispersion or the aggregation status of particle suspension can be reflected by FBRM chord length data. The measurement range is from 0.5 to 1000 μm. The primary mode which better detects the dispersed fine particles was used. Both the "no weighted" and "squared weighted" statistical methods were applied on chord length distribution, representing the raw and volumetric chord length of particles, respectively.

For each measurement, the slurry was prepared in a 600-mL beaker by mixing 40 g mineral solid (single hematite or quartz or the mixture of hematite and quartz at 1:1 mass ratio) with 360 mL distilled water. The beaker was placed on the FBRM stand and stirred by an upper side assembled stirrer with a four-blade turbine impeller. A high agitation intensity (650 rpm) was used to simulate the turbulent environment as closely as in a flotation cell. The slurry pH was adjusted to ~10.5 using NaOH solution. Each measurement ran 15 min. The 100 mg/L corn starch or corn dextrin and 100 mg/L ODA were added into slurry at 4 and 9 min, respectively. The changes of particle count and chord length were monitored throughout the process.

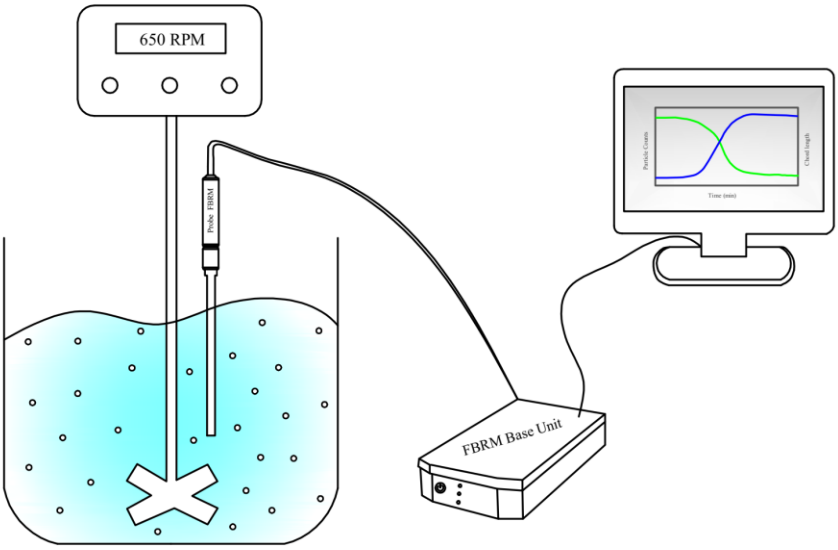

Figure 3.4 FBRM system for in-situ particle size distribution measurement.

3.2.7 Microscope observation

An optical microscope (Zeiss, Axiovert 200M, USA) equipped with a high-resolution CCD camera was used to directly examine the aggregation/dispersion of mineral particles. As the transparency of quartz is higher than that of hematite, the quartz is shown as brighter spots under a microscope while hematite is opaque black. The samples were prepared following the same procedure described in FBRM test, and the slurry was diluted 20 times using distilled water. After pH adjustment and the addition of reagents, a small amount of suspension (two or three drops) was deposited on a sample cell and observed under the microscope using the objective lens with 20× magnification.

3.3 Results

3.3.1 Batch flotation

3.3.1.1 Batch flotation of mixtures of fine hematite and quartz

Batch flotation was carried out using synthetic mixtures of fine hematite and quartz. A total solid content of ~10 wt% slurry was prepared by blending 50 g fine hematite (-20 µm) and 50 g quartz (-15 μm) with 900 mL distilled water in a 1.5 L flotation cell. Firstly, each test was conducted for three times to achieve repeatable results, and standard deviations were calculated as indicated by error bars. Figure 3.5a shows the cumulative Fe recoveries into the froth as a function of water recovery using corn starch or corn dextrin at varying dosages. As can be seen, regardless of the depressants used, a nearly linear relationship existed between Fe recovery and water recovery. It was therefore inferred that the primary mechanism for Fe recovered into froth was entrainment. When corn dextrin was used, a relatively higher Fe recovery and water recovery were observed under the same dosage conditions than when corn starch was used. For example, up to ~30% of Fe was recovered into froth product at 500 g/t corn dextrin compared with approximately 12% of Fe when 500 g/t corn starch was used. An increased dosage of corn dextrin to 1000 g/t caused the Fe recovery to drop to approximately 20%, however, the further increase of corn dextrin dosage to 2000 g/t had only slight influence on Fe recovery. In contrast, the corn starch induced smaller amount of Fe into the froth at a lower dosage. It was anticipated that two possible reasons might explain the difference in Fe recoveries by using the two depressants. One was that the corn starch imparted much stronger surface hydrophilicity of hematite than corn dextrin, and the other was that corn starch could better reduce the recovery of fine hematite through entrainment. The result in Figure 3.5b showed the cumulative recovery of quartz as a function of flotation time. It can be seen that quartz recovery was slightly reduced in the presence of high dosage of corn starch.

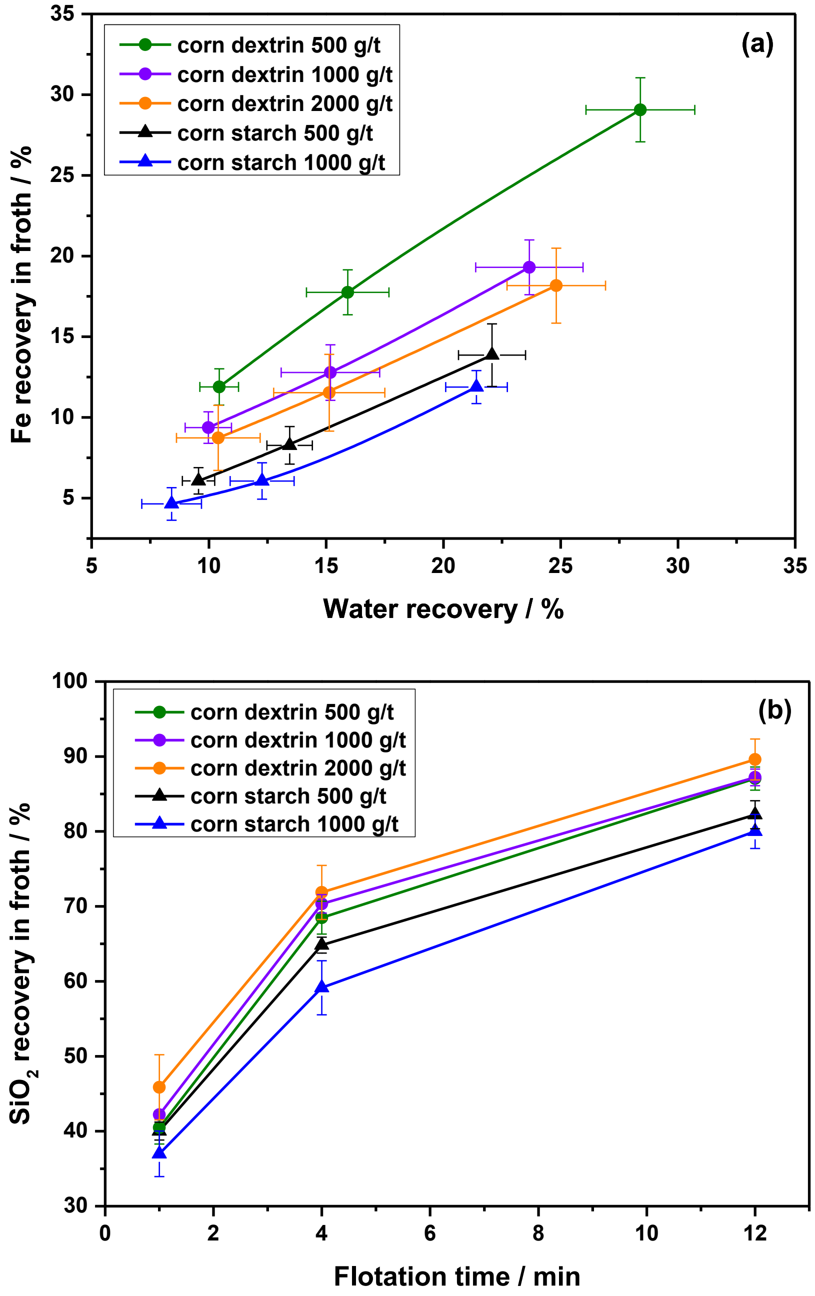

Figure 3.5 Cumulative Fe recovery in froth as a function of water recovery (a) and cumulative quartz recovery as a function of flotation time (b) in the presence of corn starch or corn dextrin for fine hematite-quartz mixtures at pH 10.5. The hematite was -20 µm and the quartz was -15 µm.

3.3.1.2 Batch flotation of mixtures of coarse hematite and quartz

The flotation procedure was the same as that for the mixture of fine hematite and quartz except that the fine hematite (-20 µm) was replaced by 50 g coarse hematite (-75+20 µm) in the feed.

The results are presented in Figure 3.6a and 3.6b. As can be seen, almost the same degree of cumulative Fe recovery in the froth was achieved with 500 g/t corn starch and corn dextrin. Comparing the results of Figure 3.5 and Figure 3.6, it can be concluded that relatively high cumulative Fe recoveries in froth were achieved for the fine hematite-quartz mixture feed system, which may be due to the more severe entrainment. It is worth noting that using corn dextrin in the coarse hematite-quartz feed system resulted in a better performance (less Fe recovery in froth) than when it was used in the fine hematite-quartz system. This indicated that the fine particle size of hematite was the reason leading to its poor flotation behaviour in fine hematite-quartz system for corn dextrin.

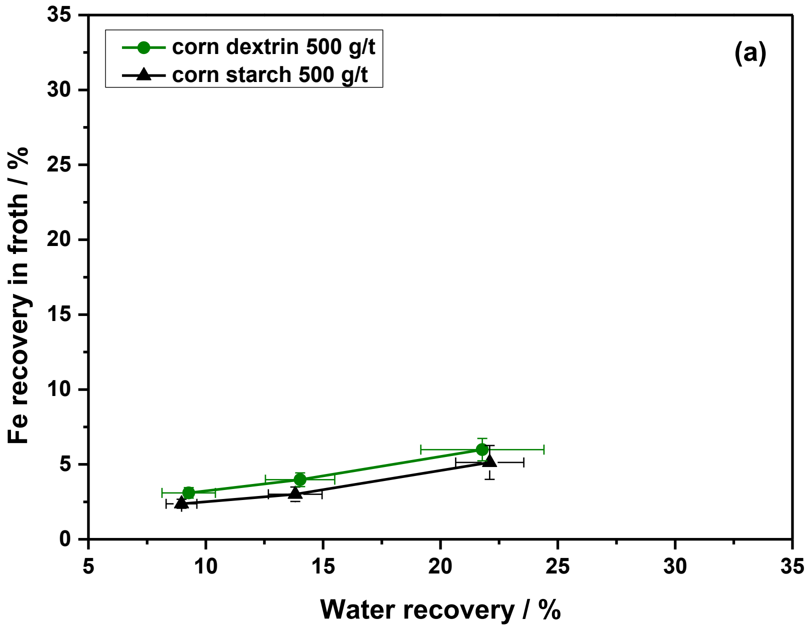

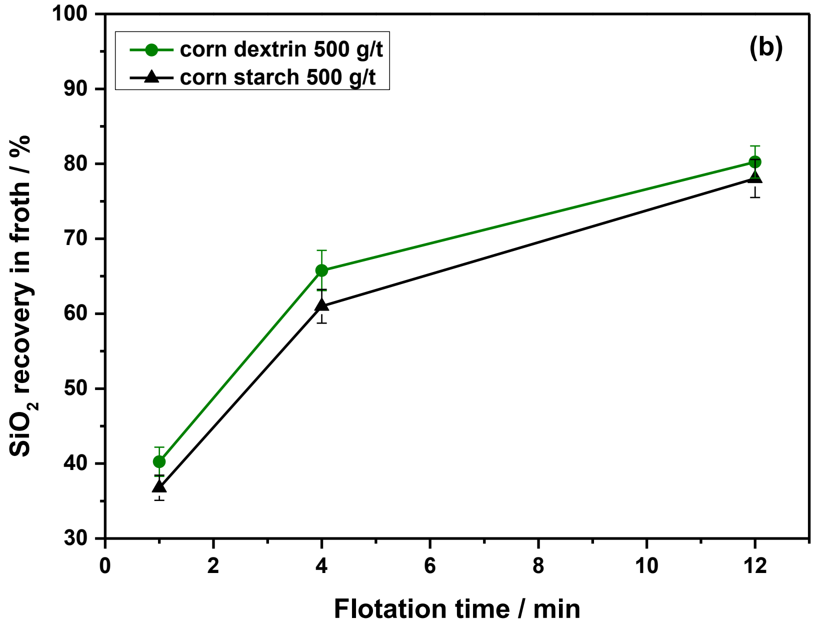

Figure 3.6 Cumulative Fe recovery in froth as a function of water recovery (a) and cumulative quartz recovery as a function of flotation time (b) in the presence of 500 g/t corn starch or corn dextrin for coarse hematite-quartz mixtures at pH 10.5. The hematite was -75+20 µm and the quartz was -15 µm.

3.3.1.3 Effect of mass ratio between fine and coarse hematite on mixture batch flotation

The effect of mass ratio between fine and coarse hematite in the feed on the cumulative Fe recovery into froth was investigated. The fine hematite with mass proportions of 20%, 50% and 80% was used in feed systems (the total weight of fine and coarse hematite was kept at 50 g, which was mixed with 50 g -15 µm quartz). From the results shown in Figure 3.7, it can be seen that the amount of Fe recovered into froth was positively correlated with the increasing proportion of fine hematite in the feed. This is more obvious in the cases where corn dextrin was used as a depressant. Furthermore, the difference of Fe recoveries between the two depressants was the least in the presence of 20% fine hematite, and the gap was enlarged at higher fine hematite content. This indicated again that particle size was the reason that limited the application of corn dextrin. The results in Figure 3.7 also indicated that when the fine hematite content was low (20%), increasing corn dextrin dosage to 1000 g/t could help lower the Fe recovery to froth to the same degree as when starch was used at a lower dosage of 500 g/t. This observation may be useful in iron ore mines where the fine iron oxide content was relatively low. In this case, corn dextrin may be used instead of corn starch. Despite the higher dosage required, corn dextrin tended to allow more quartz to be floated (Figure 3.5b) and would thus benefit iron ore concentrate grade.

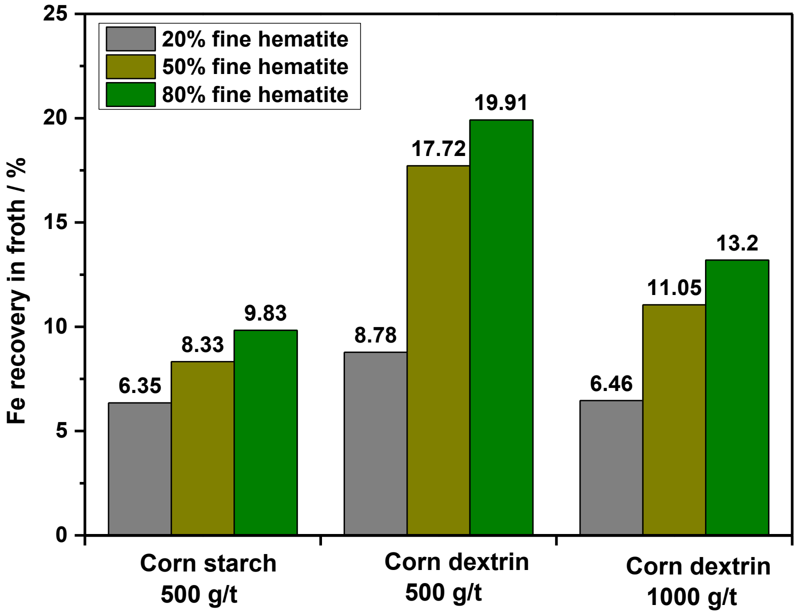

Figure 3.7 The effect of weight ratio between fine and coarse hematite in the feed on Fe recovery in froth using corn starch or corn dextrin at pH 10.5.

3.3.2 Analysis of batch flotation results using Warren's model

Warren proposed a method to distinguish the contributions of true flotation and entrainment for fine particles in batch flotation as discussed in the introduction. The studies in literature indicated that hematite could be made hydrophobic by amine collectors' adsorption or due to the failure of depressant [48], which was also proved in the present research by micro-flotation. Therefore, even with the use of a depressant, it was possible that hematite was recovered by both true flotation and entrainment. To determine the contributions of true flotation or entrainment that hematite was recovered into froth, the data collected in batch flotation were fitted to Warren's model.

Regression analysis of the cumulative Fe recovery into froth as a function of the weight of water recovered in batch flotation was conducted using equation (3.1) and equation (3.2), respectively. The fitting results are shown in Figures 3.8 and 3.9, respectively, and Table 3.2 gives the regression and correlation coefficients. Equation (3.1) was used with the assumptions that hematite particles were recovered by both true flotation and entrainment. However, the fitting result in Figure 3.8 showed that the intercept value F_{Fe} which represented true flotation was quite small in the presence of the depressants. This suggested that the true flotation of hematite was negligible in the presence of dextrin or starch as a depressant, and it was recovered primarily through entrainment.

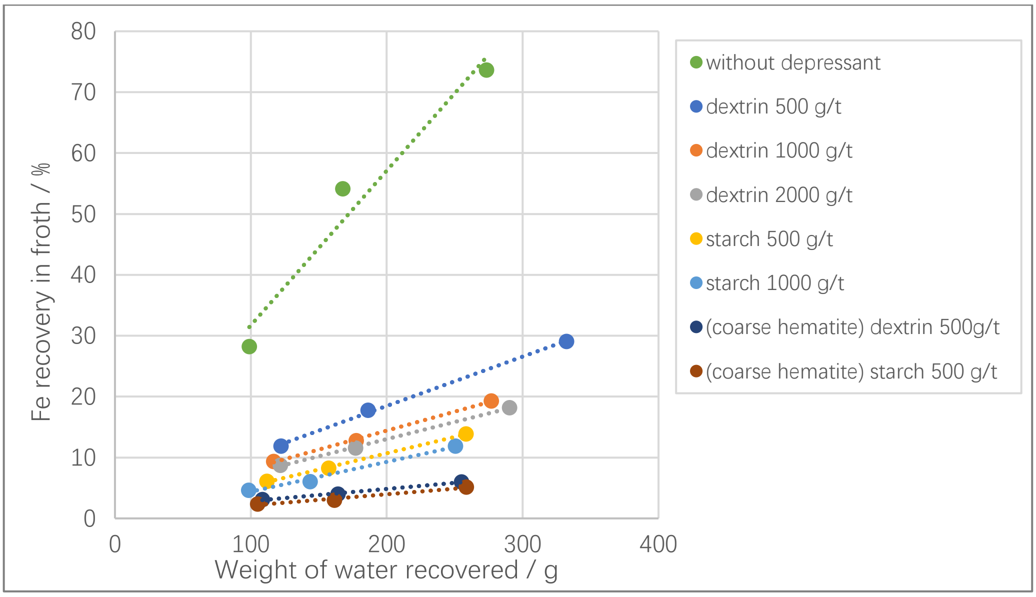

Figure 3.8 Fitted experimental plots (cumulative Fe recovery in froth as a function of weight of water recovered) based on equation (3.1) of Warren's entrainment model.

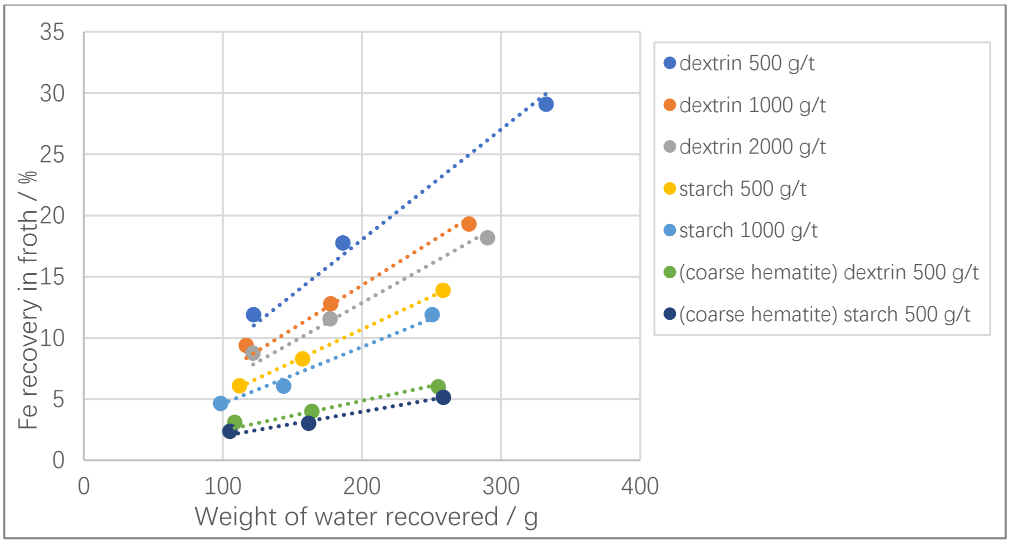

Figure 3.9 Fitted experimental plots (cumulative Fe recovery in froth as a function of weight of water recovered) based on equation (3.2) of Warren's entrainment model.

Table 3.2 Regression and correlation coefficients of the fitted lines.

Equation (3.1) $R_{Fe} = F_{Fe} + e_{Fe} \cdot W_{water}$

	e_{Fe}	F_{Fe}	R^2
without depressant	0.254	6.308	0.959
dextrin 500 g/t	0.081	2.274	0.998
dextrin 1000 g/t	0.062	1.943	0.998
dextrin 2000 g/t	0.056	1.741	0.999
starch 500 g/t	0.053	-0.018	0.999
starch 1000 g/t	0.049	-0.489	0.987
(coarse hematite) dextrin 500 g/t	0.02	0.847	0.993
(coarse hematite) starch 500 g/t	0.018	0.284	0.977

Equation (3.2) $R_{Fe} = e_{Fe} \cdot W_{water}$

	e_{Fe}	R^2
dextrin 500 g/t	0.09	0.998

dextrin 1000 g/t	0.072	0.998
dextrin 2000 g/t	0.064	0.998
starch 500 g/t	0.054	0.999
starch 1000 g/t	0.046	0.998
(coarse hematite) dextrin 500 g/t	0.024	0.996
(coarse hematite) starch 500 g/t	0.02	0.997

The result was also in agreement with the study of Mhonde et al. [17] who assumed that the amount of fine gangue particles reporting to concentrate was only due to the entrainment with a high dosage of depressant (> 500 g/t). Equation (3.2) was used assuming that hematite was non-floatable, therefore, entrainment was the only mechanism that hematite was recovered. Regardless of the equations used, it was found that the fitting lines using corn starch always had smaller regression coefficients than that of corn dextrin, indicating corn starch could better reduce the entrainment of fine hematite. On the other hand, the regression coefficients of coarse hematite were much smaller than that of fine hematite, indicating a lower degree of entrainment of coarse hematite, and it could well explain the similar performance of corn dextrin and corn starch in coarse hematite-quartz batch flotation.

3.3.3 Micro-flotation

Figure 3.10 shows the effect of ODA concentration on quartz recovery at pH 10.5. It can be seen that the initial increase in the concentration of ODA up to 3×10^{-4} mol/L led to a significant increase in quartz recovery from 27% to 57%, after which the further increase in ODA concentration caused a slight decrease in quartz recovery. Overall, quartz had a relatively low recovery (below 60%) from the micro-flotation test. This may be due to the low collision possibility between fine quartz and bubble. However, we noticed that the quartz recovery in hematite-quartz mixture batch flotation could reach 80% or above. The higher quartz recovery in batch flotation may be partly attributed to the entrainment recovery, and partly to shear flocculation of fine quartz in the presence of octadecylamine under the more intensive shear conditions in the batch flotation machine. It is well known that the entrainment of hydrophobic particles would benefit their flotation recovery [15], while the degree of entrainment was low in the in-house made micro-flotation tube. Figure 3.11 shows the flotation recovery of quartz and fine hematite (less than 20 μm) with addition of different depressants. As can be seen, the quartz recovery was not influenced by corn dextrin, and was slightly depressed by corn starch at higher concentration which was consistent with the results in batch flotation. In the absence of depressants, the hematite recovery was approximately 52% using ODA as collector. Both the addition of corn starch and corn dextrin could reduce the hematite recovery. At 100 mg/L depressant concentration, the recovery of hematite decreased to approximately 10.5% and 13%, respectively, for corn starch and corn dextrin. Comparing the curves of hematite recovery, they showed a similar trend and not much difference in micro-flotation experiments whether corn starch or corn dextrin was used, and it indicated that the two depressants resulted in the same level of hydrophilicity of hematite surface.

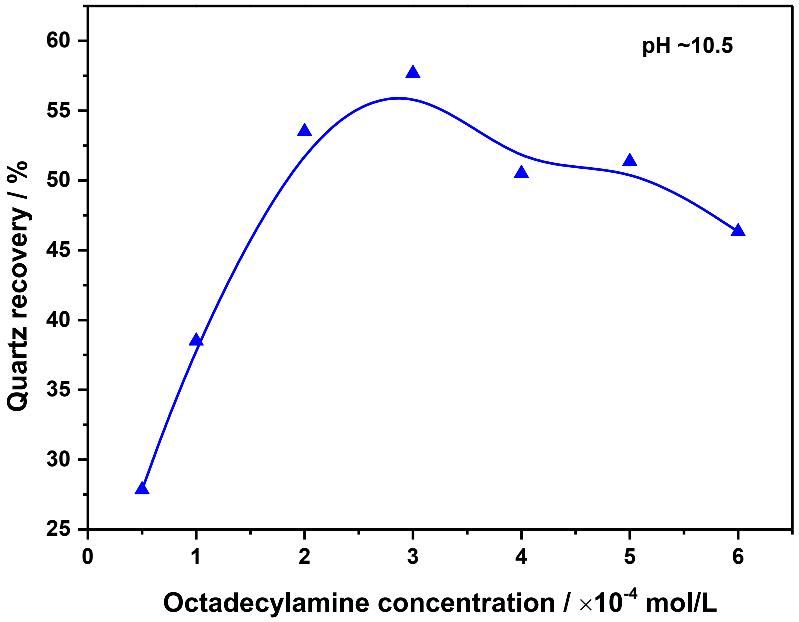

Figure 3.10 Micro-flotation recovery of quartz as a function of ODA concentration at pH 10.5.

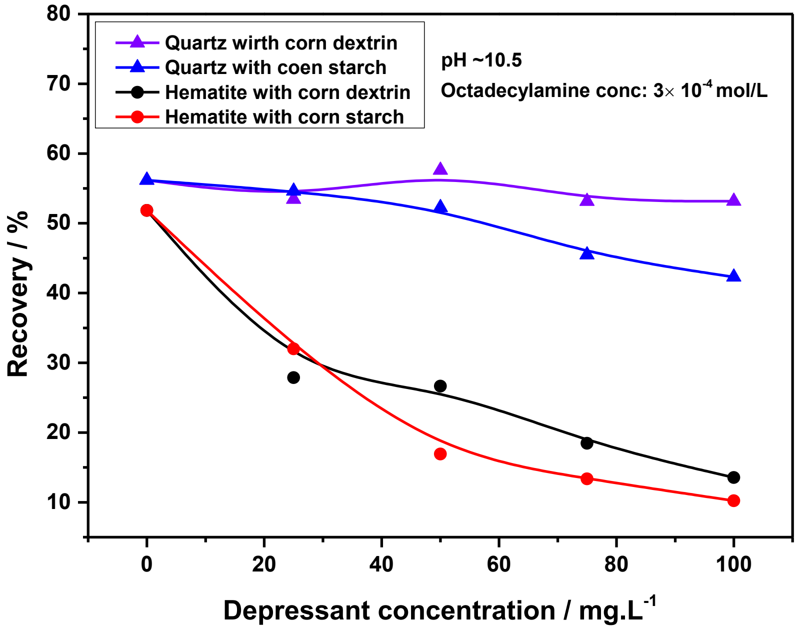

Figure 3.11 Micro-flotation recoveries of quartz and fine hematite as a function of corn starch or corn dextrin concentration at pH 10.5.

3.3.4 Surface wettability characterization

The surface wettability of hematite was further studied using a simple characterization method of solvent extraction. The weight percentage of hematite in the oil phase and at the oil/water interface was measured as a function of varying corn starch or corn dextrin concentrations as shown in Figure 3.12. Images of the test bottles corresponding to each condition were presented above the bars as shown in the figure. As can be seen, approximately 69% of hematite stayed in the oil phase in the presence of only ODA, indicating the high hydrophobicity of hematite surface. When 50 mg/L corn starch or corn dextrin was added, the hematite in the oil phase was reduced to lower than 30%, and it was further reduced to below 20% at 100 mg/L corn starch or corn dextrin. The results indicated that both corn starch and corn dextrin induced similar degree of hydrophilicity of hematite surface when used at the same concentration. The results were consistent with the micro-flotation results.

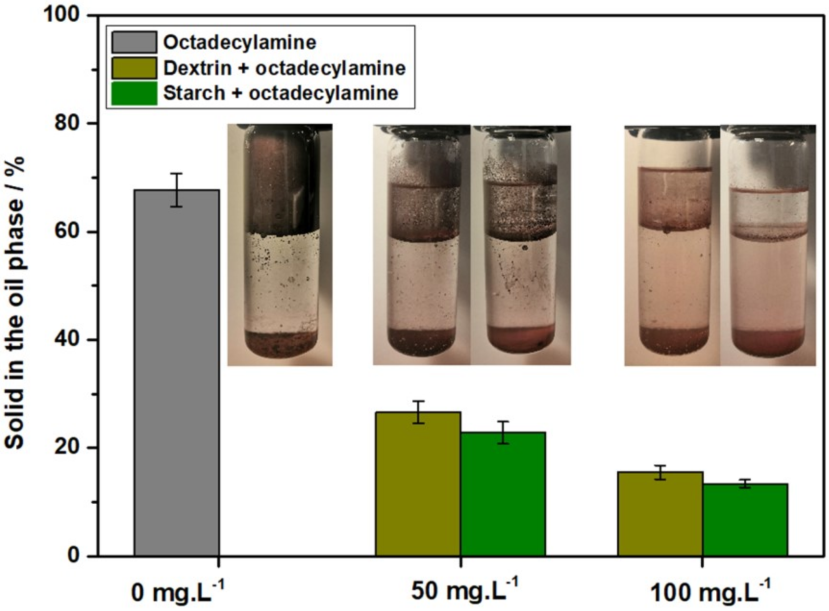

Figure 3.12 The weight percentage of hematite in the oil phase as a function of corn starch or corn dextrin concentrations.

3.3.5 Viscosity measurement

Table 3.3 shows the viscosity of corn starch and corn dextrin solution (0.5 wt%) measured with a U-shaped Ostwald viscometer at room temperature. Distilled water of known density and viscosity was used as a reference liquid. It can be seen from Table 3.3 that the mean time was 99.59 s for distilled water to flow from mark A to mark B, and the mean times that took for corn starch and corn dextrin were 182.66 and 101.38 s, respectively. The densities of corn starch and corn dextrin were measured to be 1004 and 998.3 kg/m^3, respectively, as determined by the pycnometer method. Based on equation (3.4), the viscosities of the 0.5 wt% corn starch and corn dextrin solutions were calculated to be 1.841×10^{-3} Pa·s and 1.016×10^{-3} Pa·s, respectively. The results showed that the solution of corn starch had a higher viscosity than that of corn dextrin, indicating a high molecular weight of corn starch. This is in agreement with the conclusion reported in literature that starch typically has large molecular sizes with MWs up to several million whereas dextrin is a smaller molecule [49, 50].

Table 3.3 Viscosities of corn starch/dextrin solution measured with an Ostwald viscometer.

Sample	Time of flow (sec)			Mean time	Density	Viscosity
	1	2	3	(sec)	(kg/m^3)	(×10^{-3} Pa·s)
Distilled water	99.9	99.53	99.33	99.59	1000	1
Starch solution	182.04	183.95	181.99	182.66	1004	1.841
Dextrin solution	101.39	101.04	101.71	101.38	998.3	1.016

3.3.6 FBRM measurement

As indicated in batch flotation, the addition of corn starch could reduce the entrainment of fine hematite compared to corn dextrin. However, corn dextrin could indeed induce the same level of hydrophilicity of fine hematite and resulted in the similar flotation results in coarse hematite-quartz mixtures flotation as corn starch. Therefore, the aggregation/dispersion behavior of fine hematite in the presence of the two reagents may be the reason for the inconsistence. A series of FBRM measurements were performed under the batch flotation test conditions.

3.3.6.1 FBRM measurement of single minerals

The suspension of pure quartz or fine hematite was prepared at 10 wt% and was agitated at 650 rpm. Figures 3.13A and 3.13B (top panel) show the real-time evolution of particle counts (unweighted) and mean chord length (square weighted) for pure quartz in the presence of corn starch and corn dextrin over time, respectively, and Figures. 3.13a and 3.13b (bottom panel) show the corresponding chord length distributions (both unweighted and square weighted) of quartz suspension at 3, 8 and 13 min. The suspension was initially stirred for 4 min before adding reagents. It can be seen that the -20 μm particle counts were predominant in quartz suspension. After the addition of corn starch or corn dextrin at 4 min, no changes in particle counts or chord length were observed, and chord length distribution curves also overlapped at

3 and 8 min, indicating that corn starch and corn dextrin did not aggregate quartz particles. Notably, a sharp increase of square weighted mean chord length was observed after the addition of ODA at 9 min for both cases, followed by a gradual decrease in the mean chord length with further stirring, although the chord length remained at 50-70 μm at the end of the measurement period of 15 min. In addition, the decrease of fine particle counts (-20 μm) and the shift of peaks to larger chord length at 13 min both indicated that ODA could aggregate the fine quartz in the presence of corn starch or corn dextrin.

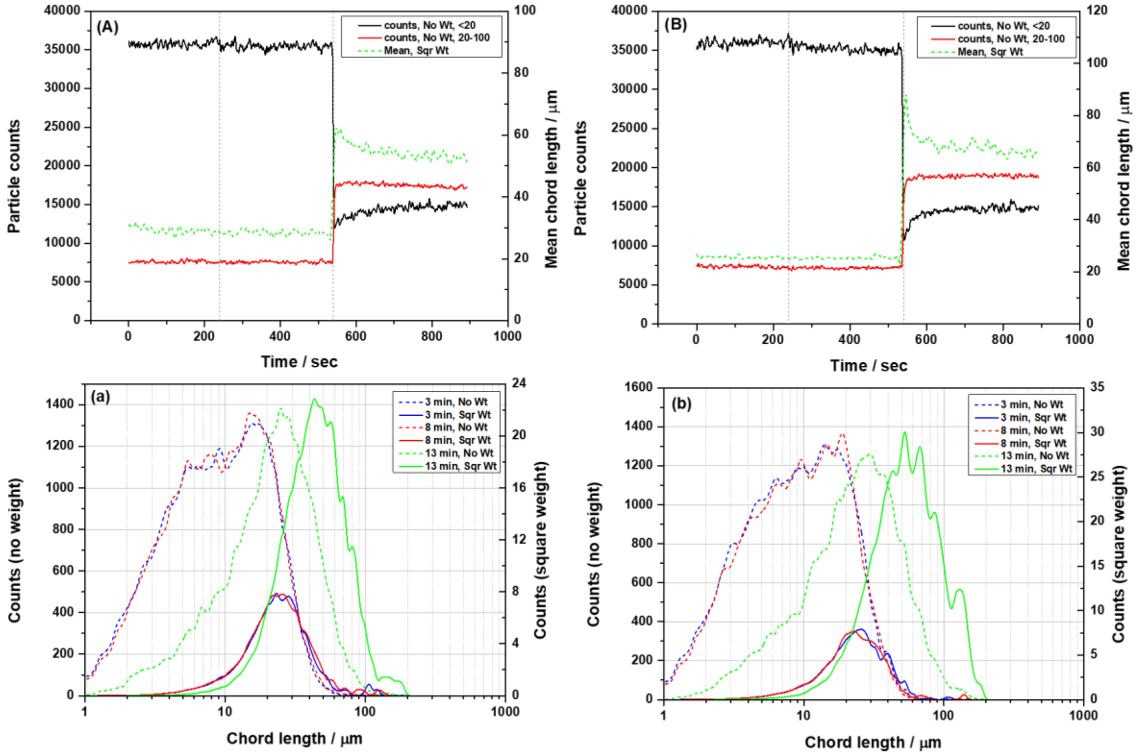

Figure 3.13 Particle counts and mean chord length (dash line) evolution in pure quartz system over time in the presence of corn starch (A) or corn dextrin (B). The corresponding chord length distribution (unweighted in dash lines and square weighted in solid lines) at 3, 8 and 13 min are shown in (a) and (b). Corn starch or corn dextrin was added at 4 min and ODA was added at 9 min.

Figure 3.14 shows the FBRM measurement of suspension of pure fine hematite. As can be seen from Figure 3.14A, the mean square weighted chord length increased at 4 min, indicating the aggregation of fine hematite caused by the addition of corn starch. Accordingly, the higher and larger chord length peaks were observed at 8 min as shown in Figure 3.14a. At 9 min, after the addition of ODA, the mean chord length (squared weighted) increased immediately to the maximum value of 80 μm, followed by the quick decline until it resumed the same level when ODA was not added. The sharp increase at 9 min may be due to the instant electrostatic interaction between the cationic amine collector and hematite that adsorbed starch, leading to aggregation. But the pre-adsorbed corn starch could hinder the adsorption of amine collector on the surface of hematite, and therefore the amine adsorption on starch-coated hematite was not sufficiently strong to resist the shear, resulting in the quick breakage of the aggregates. The chord length distribution curves at 8 and 13 min in Figure 3.14a proved that ODA did not further aggregate the hematite in the presence of corn starch. In contrast, the addition of corn dextrin at 4 min did not cause the aggregation of fine hematite which remained dispersed in the suspension as indicated from the mean chord length in Figure 3.14B. While the addition of ODA at 9 min caused the slight increase of mean square weighted chord length, and the chord length distribution at 13 min shifted slightly to higher values than that at 3 and 8 min. This indicated that ODA could cause slight aggregation of fine hematite treated by corn dextrin.

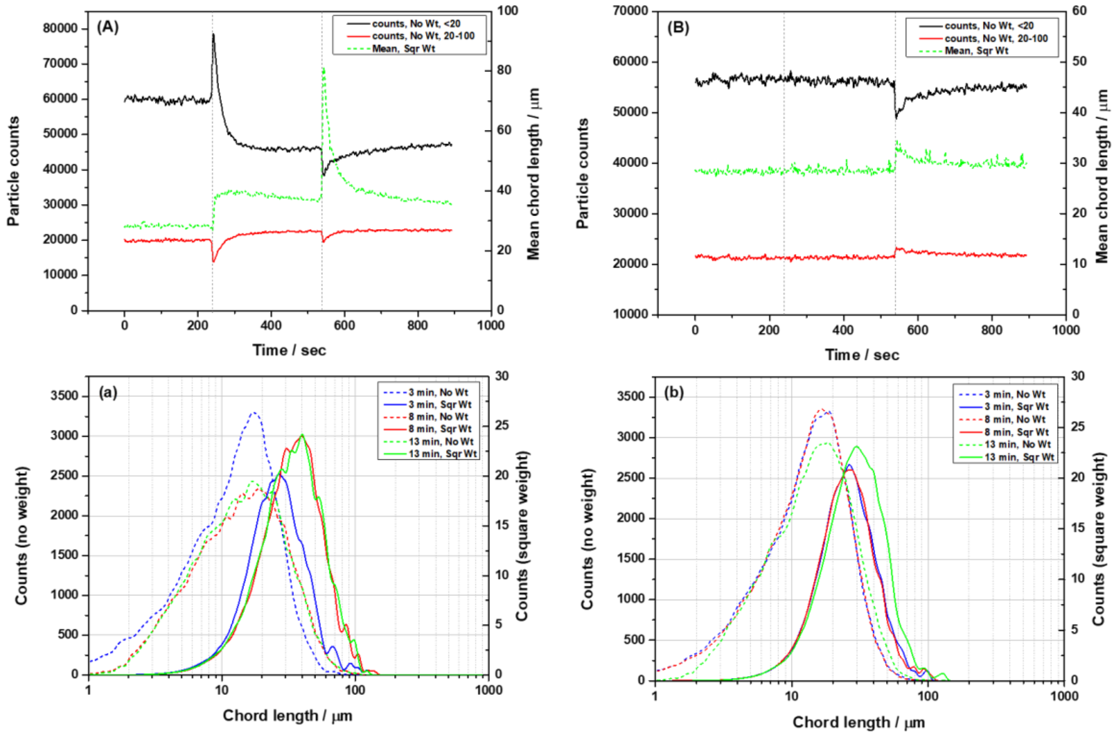

Figure 3.14 Particle counts and mean chord length (dash line) evolution in pure fine hematite system over time in the presence of corn starch (A) and corn dextrin (B). The corresponding chord length distributions (unweighted in dash lines and square weighted in solid lines) at 3, 8 and 13 min are shown in (a) and (b). Corn starch or corn dextrin was added at 4 min and ODA was added at 9 min.

3.3.6.2 FBRM measurement of fine hematite-quartz mixtures

The FBRM measurement of suspensions of fine hematite and quartz mixtures (50 wt% -20 µm hematite and 50 wt% -15 µm quartz) was performed at 10 wt% solid content. The test procedure was the same as single mineral system. Examination of the mean square weighted chord length (green dash line) in Figure 3.15A shows that a two-stage aggregation process occurred judging from the growth trends of curve at 4 min and 9 min. As single mineral test showed that the corn starch did not aggregate quartz, therefore, the first stage increase between 4 min and 9 min was attributed to the aggregation of hematite by corn starch. It was noticeable that the aggregation size was larger than that formed in the pure hematite suspension at this stage, and this might be because a part of fine quartz particles were trapped in the hematite aggregates and led to a relatively larger and loose floc structure. The significant decrease in fine particle counts (-20 μm) in the mixture suspension over the single hematite suspension can also support the above speculation. The second aggregation stage happened after the addition of ODA at 9 min. Pure hematite measurement showed the ODA did not aggregate hematite in the presence of corn starch, it was therefore considered that the second stage particle size increase was resulted from the quartz aggregation by ODA after 9 min. In addition, at the moment that ODA was added, a small drop of mean chord length and an increase of fine particle counts were observed, and it was probably caused by the disruption of the starch-hematite aggregates by ODA because the latter could interact strongly with the fine trapped quartz. This was followed by the formation of quartz aggregation in suspension caused by ODA. The weighted chord length distributions over time also proved that the two-stage aggregation phenomenon as shown in Figure 3.15a. In the case of corn dextrin, it can be seen from Figure 3.15B that both the hematite and quartz were kept dispersed in suspension after the addition of corn dextrin at 4 min, which was consistent with the foregoing results in single mineral system. The aggregation of quartz induced by ODA was observed at 9 min, followed by the gradual breakage of quartz aggregates which was the same as in the pure quartz system.

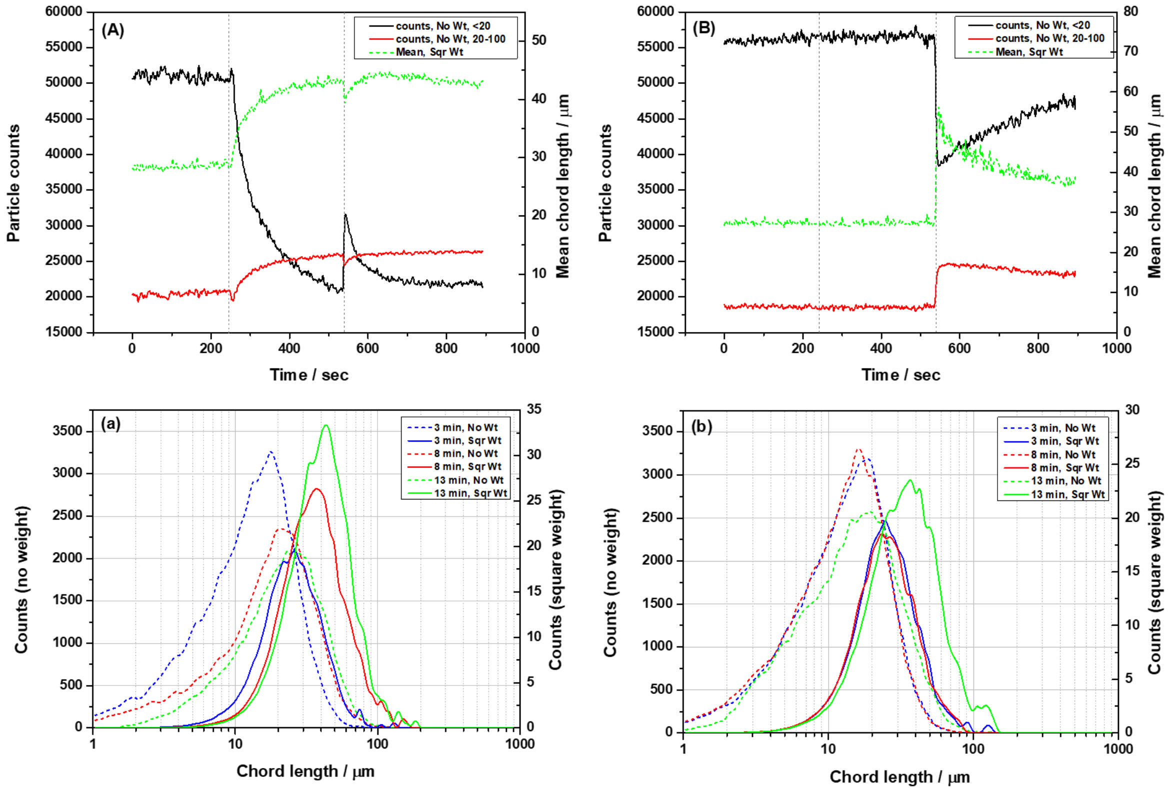

Figure 3.15 Particle counts and mean chord length (dash line) evolution in fine hematite-quartz mixture system (50 wt% fine hematite and 50 wt% quartz) over time in the presence of corn starch (A) and corn dextrin (B). The corresponding chord length distributions (unweighted in dash lines and square weighted in solid lines) at 3, 8 and 13 min are shown in (a) and (b). Corn starch or corn dextrin was added at 4 min and ODA was added at 9 min.

3.3.7 Microscope observation

Microscope imaging was conducted as a supplement of FBRM test because it could provide direct aggregation/dispersion observation of mineral particles in suspension. The result was shown in Figure 3.16. Comparing the images of Figures. 3.16a, 3.16b and 3.16c, it can be concluded that corn starch caused the aggregation of fine hematite while corn dextrin made it dispersed. Figure 3.16e shows that quartz can be aggregated by the addition of ODA. The mixture suspension of fine hematite and quartz was indicated in Figure 3.16f, which showed no obvious hereto-aggregation of hematite and quartz at pH 10.5. After the addition of corn starch, the hematite was selectively aggregated, and a small amount of fine quartz was observed to be trapped in the hematite flocs as shown in Figure 3.16g. When both corn starch and ODA were added in the mixture suspension, it can be seen from Figure 3.16h that two kinds of flocs were formed which may correspond to the two-stage aggregation process observed in FBRM measurement.

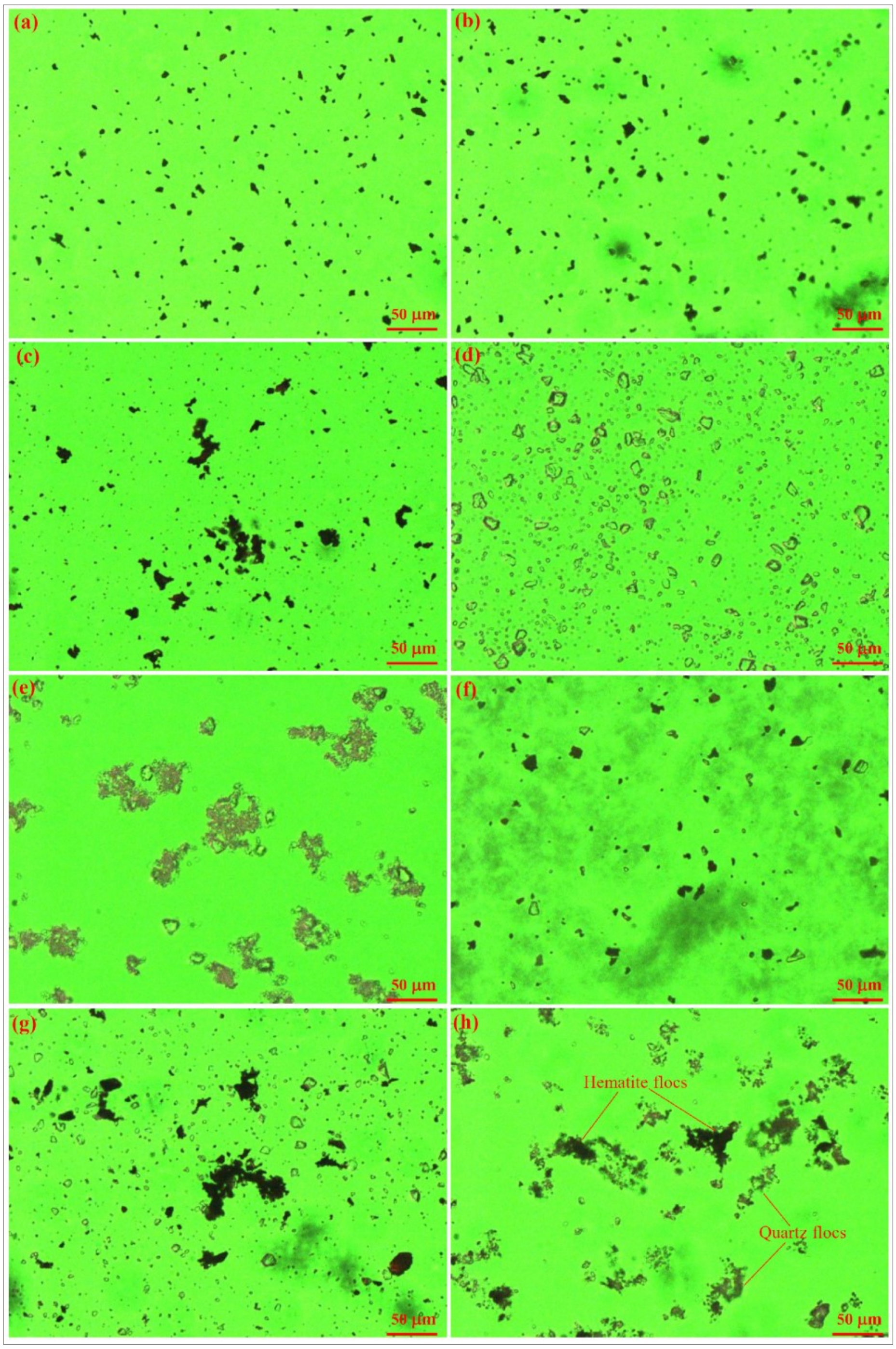

Figure 3.16 Microscope images of mineral particle suspensions. (a) Pure fine hematite; (b) Pure fine hematite treated with corn dextrin; (c) Pure fine hematite treated with corn starch; (d) Pure quartz; (e) Pure quartz treated with ODA; (f) Mixtures of fine hematite and quartz (mass ratio1:1); (g) Mixtures of fine hematite and quartz treated with corn starch; (h) Mixtures of fine hematite and quartz treated with both corn starch and ODA. pH 10.5.

3.4 Discussion

Focus beam reflectance measurement (FBRM) is a powerful tool for real-time particle size characterization and is widely used in the process such as crystallization [51] and flocculation [52, 53]. In the present study, FBRM was used to monitor the aggregation/dispersion behavior of mineral mixtures at a high solid concentration (10 wt%) that was used in the batch flotation. A high agitation speed was used to simulate the hydrodynamic conditions in the flotation cell. Consequently, it is envisaged that the aggregation and dispersion behaviors observed in FBRM measurements would occur in the batch flotation cell.

As indicated in the present study, it was found that the degree of entrainment was largely dependent on the aggregation/dispersion state of the fine hydrophilic particles in suspension. Although corn dextrin induced the same degree of hydrophilicity of hematite as corn starch, FBRM test showed that it failed to aggregate the fine hematite particles due to its lower molecular weight than starch, as reflected from the viscosity measurements of their 0.5 wt% solutions. As a consequence, the fine hematite remained dispersed in slurry and they were more likely to be entrained in the plateau borders between bubbles after air injection in batch flotation, thus more hematite was recovered in the froth via entrainment. On the other hand, corn starch caused the aggregation of fine hematite in the suspension as indicated by FBRM, and the relatively larger hematite floc size reduced their possibility of being entrained into froth. Based on the results, a schematic diagram was drawn to clearly reveal the situations under the two cases as shown in Figure 3.17.

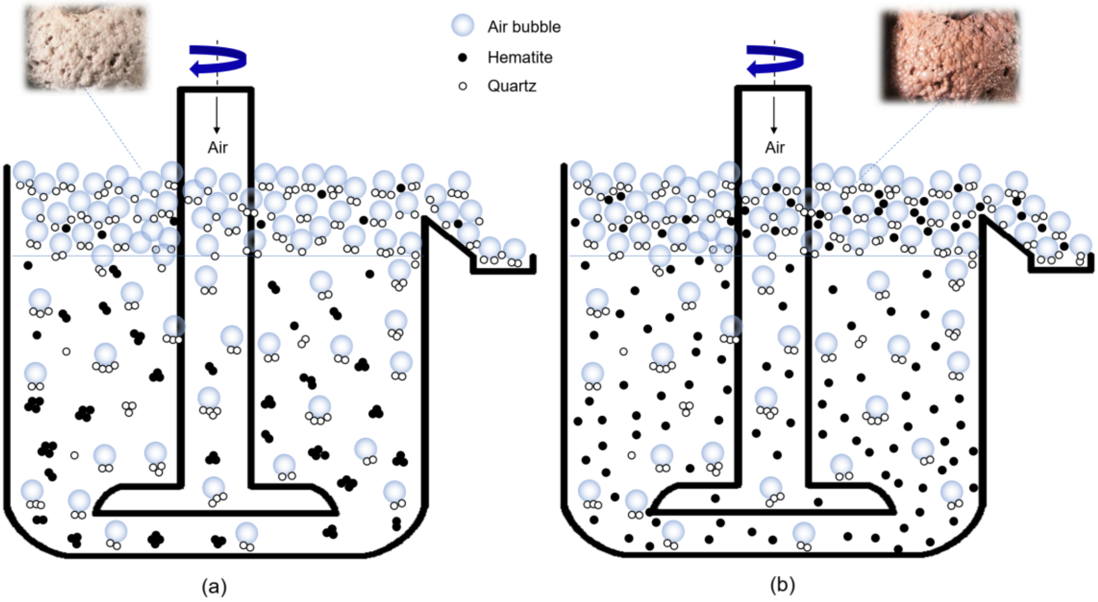

Figure 3.17 Schematic of batch flotation of fine hematite-quartz mixtures in the presence of corn starch (a) and corn dextrin (b).

Corn starch is a higher molecular weight polymer than dextrin, and the flocculation of hematite by corn starch has been reported in literature (e.g., [38, 54]). The superior performance of corn starch over corn dextrin in this study inspired that both the hydrophilicity-inducing and flocculation capability of polymers should be considered for flotation with fine gangue minerals, which was reported in our previous work [55, 56].

Both the fine quartz and fine hematite were included in the feed of batch flotation in this study, and such a feed system is more frequently encountered nowadays when exploiting low-grade and complex ore bodies in mineral industry since both the value and gangue minerals need to be ground very fine to achieve required degree of liberation. In fact, two important problems need to be considered to achieve the efficient flotation separation of minerals for such a feed system. One is the low flotation rate of fine hydrophobic mineral which is primarily caused by the low particle-bubble collision efficiency, and the other is the entrainment of fine hydrophilic minerals which affects the flotation selectivity. The results of this study confirm a two-stage aggregation flotation strategy to solve both problems. As indicated from the FBRM measurement of fine hematite-quartz mixtures, the hydrophobic quartz floc could be formed by shear flocculation using long carbon chain ODA as a collector, and the hydrophilic hematite flocs could be formed by selective polymer flocculation using corn starch. The two flocs could subsequently be separated by conventional froth flotation method. Overall, the hydrophobic (shear) flocculation improves the flotation efficiency of fine hydrophobic mineral and the selective polymer flocculation can reduce the entrainment of fine hydrophilic mineral. The application of this concept may extend to many other flotation systems containing both the fine and ultrafine value and gangue minerals. In this process, the selectivity of polymers, the correlation between the floc structure and entrainment and the influence of hydrodynamic conditions on floc formation are all relevant subjects that are necessary to be studied in future work.

3.5 Conclusions

In this study, the influence of aggregation/dispersion state of hydrophilic particles on entrainment in batch flotation was investigated using hematite and quartz as model minerals. Two structurally similar polysaccharides, corn starch and corn dextrin, were used as depressants for hematite, and octadecylamine acetate (ODA) was used as collector for quartz. Batch flotation of 1:1 fine hematite-quartz mixtures (-20 µm hematite and -15 µm quartz) indicated that less hematite was reported into froth using corn starch than using corn dextrin, while approximately equal Fe recovery in froth was observed in coarse hematite-quartz mixtures using the two depressants (-75+20 µm hematite and -15 µm quartz). It was confirmed that the Fe recovery in froth was positively correlated with the proportion of fine hematite in the feed when corn dextrin was used as a depressant. Warren's model proved that the hematite recovery in froth in this study was primarily through entrainment rather than true flotation in the presence of a high dosage of depressant (> 500 g/t corn starch or corn dextrin), and relatively smaller regression coefficients for corn starch represented a lower degree of entrainment. The micro-flotation and solvent extraction tests showed that surface hydrophilicity of hematite induced by the two depressants (corn starch or corn dextrin) in the presence of ODA was in an identical range. The viscosity measurement using Ostwald viscometer showed that corn starch solution possessed a higher viscosity than corn dextrin solution at room temperature, indicating a higher molecular weight. FBRM measurements were carried out in a system that simulated the batch flotation environment. The results showed that fine hematite particles could be aggregated by corn starch while they were dispersed in slurry with corn dextrin. It explained the different batch flotation responses of the two depressants. In general, the aggregation of hydrophilic particles would reduce entrainment while the dispersion of hydrophilic particles would aggravate their entrainment. FBRM tests also indicated that the addition of ODA could disrupt the hematite aggregates induced by corn starch, thus releasing the trapped quartz, followed by the aggregation of the fine quartz by ODA. Furthermore, a two-stage aggregation process occurred in FBRM measurement regarding this system, and correspondingly two types of flocs were observed in optical microscope imaging. This provides evidence for the feasibility of the proposed two-stage aggregation/flocculation flotation concept for fine and ultrafine mineral particles, the application of which may significantly improve the flotation efficiency of fine hydrophobic minerals by hydrophobic (shear) flocculation as well as reducing the entrainment of fine hydrophilic minerals by selective polymer flocculation. The potential application of this two-stage aggregation flotation concept may extend to many other mineral systems containing both fine and ultrafine value and gangue minerals for improving flotation separation efficiency.

3.6 References

[1] S. Ata, Phenomena in the froth phase of flotation—A review, International Journal of Mineral Processing 102 (2012) 1-12.

[2] L. WAng, Y. Peng, K. Runge, D. Bradshaw, A review of entrainment: Mechanisms, contributing factors and modelling in flotation, Minerals Engineering 70 (2015) 77-91.

[3] J. Drzymala, Characterization of materials by Hallimond tube flotation. Part 1: maximum size of entrained particles, International Journal of Mineral Processing 42 (1994) 139-152.

[4] S. Neethling, J. Cilliers, The entrainment factor in froth flotation: Model for particle size and other operating parameter effects, International Journal of Mineral Processing 93 (2009) 141-148.

[5] T. Leistner, U.A. Peuker, M. Rudolph, How gangue particle size can affect the recovery of ultrafine and fine particles during froth flotation, Minerals Engineering 109 (2017) 1-9.

[6] T. Subrahmanyam, E. Forssberg, Froth stability, particle entrainment and drainage in flotation—a review, International Journal of Mineral Processing 23 (1988) 33-53.

[7] X. Zheng, J.-P. Franzidis, N. Johnson, E. Manlapig, Modelling of entrainment in industrial flotation cells: the effect of solids suspension, Minerals Engineering 18 (2005) 51-58.

[8] E. Cilek, B. Yılmazer, Effects of hydrodynamic parameters on entrainment and flotation performance, Minerals Engineering 16 (2003) 745-756.

[9] E.C. Cilek, The effect of hydrodynamic conditions on true flotation and entrainment in flotation of a complex sulphide ore, International Journal of Mineral Processing 90 (2009) 35-44.

[10] V. Kirjavainen, Review and analysis of factors controlling the mechanical flotation of gangue minerals, International journal of mineral processing 46 (1996) 21-34.

[11] X. Zheng, N. Johnson, J.-P. Franzidis, Modelling of entrainment in industrial flotation cells: Water recovery and degree of entrainment, Minerals Engineering 19 (2006) 1191-1203.

[12] P. Smith, L. Warren, Entrainment of particles into flotation froths, Mineral Procesing and Extractive Metallurgy Review 5 (1989) 123-145.

[13] O.Y. Gulsoy, A simple model for the calculation of entrainment in flotation, Korean Journal of Chemical Engineering 22 (2005) 628-634.

[14] Z. Konopacka, J. Drzymala, Types of particles recovery—water recovery entrainment plots useful in flotation research, Adsorption 16 (2010) 313-320.

[15] L.J. Warren, Determination of the contributions of true flotation and entrainment in batch flotation tests, International Journal of Mineral Processing 14 (1985) 33-44.

[16] W. Trahar, A rational interpretation of the role of particle size in flotation, International Journal of Mineral Processing 8 (1981) 289-327.

[17] N. Mhonde, J. Wiese, B. McFadzean, Comparison of collector performance for a South African and a Brazilian iron ore considering mineralogical characteristics, Minerals Engineering 113 (2017) 55-67.

[18] M. Gao, M. Young, P. Allum, IsaMill fine grinding technology and its industrial applications at Mount Isa Mines, 34th Annual Meeting Of The Canadian Mineral Processors, 2002.

[19] J. Gong, Y. Peng, A. Bouajila, M. Ourriban, A. Yeung, Q. Liu, Reducing quartz gangue entrainment in sulphide ore flotation by high molecular weight polyethylene oxide, International Journal of Mineral Processing 97 (2010) 44-51.

[20] D. Liu, Y. Peng, Reducing the entrainment of clay minerals in flotation using tap and saline water, Powder Technology 253 (2014) 216-222.

[21] V.F.D. De, Cationic froth flotation of iron ore, Google Patents, 1949.

[22] A.F. Colombo, Effect of tapioca flour on the anionic flotation of gangue from iron ores, US Department of Interior, Bureau of Mines1972.

[23] S. Cooke, N. Schulz, E. Lindroos, The effect of certain starches on quartz and hematite suspensions, TRANSACTIONS OF THE AMERICAN INSTITUTE OF MINING AND METALLURGICAL ENGINEERS 193 (1952) 697-698.

[24] D.W. Frommer, A.F. Colombo, Process for improved flotation treatment of iron ores by selective flocculation, Google Patents, 1966.

[25] A. Colombo, Beneficiation of fine-grained iron-bearing materials, Beneficiation of Mineral Fines-Problems and Research Needs. AIME, USA (1979) 237-252.

[26] D. HORTON, Pyrolysis of starch. in Starch, Chemistry and Technology (1965) 428-429.

[27] C. Chang, S. Cooke, R. Huch, Starches and starch products as depressants in amine flotation of iron ore, Trans. AIME 196 (1953) 1282-1286.

[28] J.M. Wie, D. Fuerstenau, The effect of dextrin on surface properties and the flotation of molybdenite, International journal of mineral processing 1 (1974) 17-32.

[29] J. Miller, C. Lin, S. Chang, Coadsorption phenomena in the separation of pyrite from coal by reserve flotation, Coal Perparation 1 (1984) 21-38.

[30] J. Schnarr, Brunswick mining and smelting corporation, Milling Practice in Canada, CIM Special Volume, Brunswick Mining and Smelting Corporation1978, pp. 158-161.

[31] Q. Liu, J. Laskowski, The role of metal hydroxides at mineral surfaces in dextrin adsorption, I. Studies on modified quartz samples, International Journal of Mineral Processing 26 (1989) 297-316.

[32] Q. Liu, J. Laskowski, The role of metal hydroxides at mineral surfaces in dextrin adsorption, II. Chalcopyrite-galena separations in the presence of dextrin, International Journal of Mineral Processing 27 (1989) 147-155.

[33] G. Nyamekye, The differential flotation of INCO matte with the use of polysaccharides, Copper 91(Cobre 91) (1991).

[34] K. Kydros, G. Gallios, K. Matis, Modification of pyrite and sphalerite flotation by dextrin, Separation science and technology 29 (1994) 2263-2275.

[35] A.L. Valdivieso, T.C. Cervantes, S. Song, A.R. Cabrera, J. Laskowski, Dextrin as a non-toxic depressant for pyrite in flotation with xanthates as collector, Minerals engineering 17 (2004) 1001-1006.

[36] G.F. Moreira, E.R. Peçanha, M.B. Monte, L.S. Leal Filho, F. Stavale, XPS study on the mechanism of starch-hematite surface chemical complexation, Minerals Engineering 110 (2017) 96-103.

[37] S. Pavlovic, P.R.G. Brandão, Adsorption of starch, amylose, amylopectin and glucose monomer and their effect on the flotation of hematite and quartz, Minerals Engineering 16 (2003) 1117-1122.

[38] P. Weisseborn, L. Warren, J. Dunn, Selective flocculation of ultrafine iron ore. 1. Mechanism of adsorption of starch onto hematite, Colloids and Surfaces A: Physicochemical and Engineering Aspects 99 (1995) 11-27.

[39] Q. Liu, Y. Zhang, J. Laskowski, The adsorption of polysaccharides onto mineral surfaces: an acid/base interaction, International Journal of Mineral Processing 60 (2000) 229-245.

[40] B. Siwek, M. Zembala, A. Pomianowski, A method for determination of fine-particle flotability, International Journal of Mineral Processing 8 (1981) 85-88.

[41] J. Laskowski, Oil assisted fine particle processing, Developments in mineral processing, Elsevier1992, pp. 361-394.

[42] J.S. Laskowski, Z. Yu, Oil agglomeration and its effect on beneficiation and filtration of low-rank/oxidized coals, International Journal of Mineral Processing 58 (2000) 237-252.

[43] A. Ozkan, S. Aydogan, M. Yekeler, Critical solution surface tension for oil agglomeration, International Journal of Mineral Processing 76 (2005) 83-91.

[44] D. Gómez-Díaz, J.M. Navaza, L. Quintáns-Riveiro, Intrinsic viscosity and flow behaviour of Arabic gum aqueous solutions, International Journal of Food Properties 11 (2008) 773-780.

[45] A. Senaputra, F. Jones, P.D. Fawell, P.G. Smith, Focused beam reflectance measurement for monitoring the extent and efficiency of flocculation in mineral systems, AIChE Journal 60 (2014) 251-265.

[46] R.G. Sparks, C.L. Dobbs, The use of laser backscatter instrumentation for the on‐line measurement of the particle size distribution of emulsions, Particle & particle systems characterization 10 (1993) 279-289.

[47] Y. Kyoda, A. Costine, P. Fawell, J. Bellwood, G. Das, Using focused beam reflectance measurement (FBRM) to monitor aggregate structures formed in flocculated clay suspensions, Minerals Engineering 138 (2019) 148-160.

[48] N.P. Lima, G.E. Valadão, A.E. Peres, Effect of amine and starch dosages on the reverse cationic flotation of an iron ore, Minerals Engineering 45 (2013) 180-184.

[49] G. Caesar, N. Gruenhut, M. Cushing, Molecular weight and intrinsic viscosity of nitric triesters of corn starches and dextrins, Journal of the American Chemical Society 69 (1947) 617-621.

[50] G.B. Raju, A. Holmgren, W. Forsling, Adsorption of dextrin at mineral/water interface, Journal of colloid and interface science 193 (1997) 215-222.

[51] J.W. Chew, P.S. Chow, R.B. Tan, Automated in-line technique using FBRM to achieve consistent product quality in cooling crystallization, Crystal growth & design 7 (2007) 1416-1422.

[52] X. Sun, L. Ma, X. Tan, K. Wang, Q. Liu, Effect of particle size on the flocculation of sub-micron titanium dioxide by polyacrylic acid, Minerals Engineering 149 (2020) 106253.

[53] H. Li, M. Liu, Q. Liu, The effect of non-polar oil on fine hematite flocculation and flotation using sodium oleate or hydroxamic acids as a collector, Minerals Engineering 119 (2018) 105-115.

[54] R. Pascoe, B. Wills, Selective aggregation of ultrafine hematite and quartz under high shear conditions with conventional flotation collectors, Minerals Engineering 7 (1994) 647-656.

[55] M. Cao, Q. Liu, Reexamining the functions of zinc sulfate as a selective depressant in differential sulfide flotation—The role of coagulation, Journal of colloid and interface science 301 (2006) 523-531.

[56] Q. Liu, D. Wannas, Y. Peng, Exploiting the dual functions of polymer depressants in fine particle flotation, International journal of mineral processing 80 (2006) 244-254.

CHAPTER 4 Flocculation of Quartz by a Dual Polymer System Containing Tannic Acid and Poly(ethylene oxide): Effect of Polymer Chemistry and Hydrodynamic Conditions

4.1 Introduction

Depletion of high-grade ore deposits has driven the exploration of low-grade finely disseminated mineral resources in the mineral processing industry globally. When processing these low-grade resources, the industry is faced with challenges to efficiently separate fine and ultrafine mineral particles and effectively dewater the generated ultrafine tailings for reclamation. Froth flotation, a physiochemical separation technique, is used for the separation of different mineral particles and thickening and filtration are used for solid-liquid separation in mineral processing. Studies have shown that employing polymeric flocculants to induce large aggregate size of fine and ultrafine particles can benefit both mineral separation in froth flotation and dewatering processes, such as improved bubble-mineral particle collision probability [1], decreased gangue mineral particle entrainment [2-4], and accelerated thickening/filtration rates [5]. However, the specific floc properties (e.g., floc size, shear resistance, and porosity) that might affect the mineral flotation and filtration performance are not well understood. Thus, it is necessary to investigate the flocculation properties of fine and ultrafine minerals when polymers are used in mineral processing.

As a water-soluble polymer, poly(ethylene oxide) (PEO) of high molecular weight has been used as a flocculant in the papermaking industry [6, 7], wastewater treatment [8], and more recently in mineral processing [9, 10]. Due to its non-ionic nature, PEO is generally considered to adsorb at the solid/liquid interface through hydrogen bonding [11]. Meanwhile, PEO behaves with certain hydrophobic characters resulting from the ethylene groups in the structure and hydrophobic association is proposed as another mechanism by which PEO interacts with particles [12, 13].

PEO in aqueous solution shows complex behavior and its flocculation efficiency is affected by many variables such as molecular weight, shearing intensity, polymer ageing, temperature, etc. [11, 14]. For example, freshly dissolved PEO shows better polymer bridging for flocculation; however, it can disentangle and form individual PEO coils when subjected to intense shear, long storage time, or dilution, all of which result in deteriorated flocculation efficiency [14]. Besides, PEO-induced flocculation is also affected by pH, ionic strength, and hydration state of the particle surface especially for oxide minerals [12, 15]. Consequently, flocculation by PEO is difficult to manage and the flocculation results may vary widely in a seemingly random fashion.

Using dual polymer system is regarded as a more effective strategy to enhance flocculation and achieve robust floc structures. Typically, polyelectrolytes carrying opposite charges are popular combinations to be used. In the case of PEO, synergistic effects for more efficient flocculation have been shown by prior addition of cofactors [7]. These cofactors include compounds containing phenolic groups such as phenolic formaldehyde resin [16, 17], tannins [18], and lignin [19], as well as compounds that do not have a phenolic structure, such as polypeptide [20], polystyrene sulfonate [14], and polyacrylic acid [21]. Cofactors are thought to be associated with PEO and form associative complexes that cause efficient flocculation of fines through the so-called complex bridging [14]. However, the interaction between the cofactor and PEO is complicated and not fully understood. Many studies attribute it to the hydrogen bonding formed between the ether oxygens of PEO and phenolic hydroxyls of cofactors [6, 7, 14, 21, 22]. But there are also studies debating the existence of hydrogen bonding. The formation of cofactor-PEO associative complex depends on many variables including PEO molecular weight (MW), cofactor type, cofactor/PEO ratio as well as the dissolution state of PEO [14]. Salt was also reported to be essential to induce complexation and flocculation [23]. The properties of the polymer complex may affect the structure of the formed flocs and flocculation efficiency. For example, the stickiness of polymer complex has been reported to be more critical for flocculation than the size of the formed complex [20]. When exposed to turbulent conditions, the floc size distribution, fractal dimension, shear resistance, and regrowth trend may also vary based on different cofactor-PEO complex properties. But this is not clear and needs more investigation to gain a better understanding.

Quartz is abundant in the Earth's crust, and it is one of the major constituent gangue minerals in mineral processing. Flocculation of quartz by PEO has been investigated in several studies but the results reported were not consistent. Rubio and Kitchener [12] identified the isolated silanol groups on silica surfaces as the main adsorption sites of PEO (MW > 5 million) and revealed the marked influence of pH for PEO adsorption on silica. Ageing of the silica caused the silanol groups to connect with each other thus losing the adsorptive capacity to PEO. Also, precipitated silica was not flocculated by PEO at alkaline solutions (pH >7). Koksal et al. [15] indicated that quartz could be flocculated by PEO (MW = 5 million) only at pH <3. On the other hand, Mathur and Moudgil [24] showed that PEO (MW = 8 million) could strongly adsorb onto silica surface and cause flocculation at pH 9.5. Likewise, Gong et al. [2] found that PEO (MW = 1 million and 8 million) was able to flocculate quartz and reduce its mechanical entrainment in chalcopyrite-quartz flotation separation at pH 9. Given the controversies, the effect of pH on quartz flocculation by PEO is worth being re-examined. This is particularly important to industrial flotation as it is typically carried out at an alkaline pH rather than very acidic condition such as pH < 3. Moreover, flocs require certain strength to survive the mechanical shear in a turbulent fluid field, but few studies have been reported on quartz flocculation in the presence of both cofactor and PEO under different turbulence intensities. The flocs properties induced by cofactor-PEO are assumed to behave differently from those formed by PEO alone when subjected to turbulence, and floc properties such as strength and shear resistance have indicated important effects on papermaking [25] and fibre-cement production [26]. However, these effects are currently poorly understood in mineral processing.

Tannic acid (TAN) is a natural polyphenolic compound comprising numerous phenolic hydroxyls and shows the capability to complex with polymers such as PEO and PAM [18, 22]. The hydroxyl groups have a low ionization constant and thus remain intact in neutral or even slightly alkaline solutions [27]. As an extract from plants, tannic acid exhibits unique advantageous properties such as biodegradability and eco-friendliness, and it has been frequently used in mineral flotation either as a depressant or a dispersant, or both [28, 29].

In this work, the flocculation of quartz by a dual TAN-PEO polymers system has been investigated. Dynamic floc size was monitored using an in-situ particle size measurement technique, namely focused beam reflectance measurement (FBRM), under turbulent conditions. Attention was paid to variables affecting quartz flocculation properties from both physicochemical and hydrodynamic aspects, including solution pH, TAN/PEO ratio, and shear intensity. The flocculation mechanism was investigated by zeta potential and adsorption density measurements. Floc structure formed by TAN-PEO dual polymers system and the PEO single polymer system was studied employing confocal scanning microscopy and freeze-drying-SEM imaging techniques. An attempt has been made to correlate the flocs properties with the structure of TAN-PEO associative complexes formed under different experimental conditions, enabling a better understanding of the flocculation process of fine and ultrafine particles when dual polymers are used.

4.2 Materials and Methods

4.2.1 Materials

Fine quartz powder used in this study was purchased from U.S. Silica with the vendor-specified designation of Min-U-Sil 15. As illustrated by the X-ray diffraction (XRD) pattern (Figure 4.1a) the quartz was highly crystalline with a high purity. Chemical analysis showed that the SiO_2 content of the quartz sample was 98.5% with minor impurities of Al_2O_3 (1.0%), CaO (0.03%), MgO (0.01%), Fe_2O_3 (0.03%), Na_2O (0.01%), K_2O (0.01%) and TiO_2 (0.01%). The particle size distribution, measured using a Malvern Mastersizer 3000, is shown in Figure 4.1b, and the D_{50} and D_{90} were 5.3 μm and 12.8 μm, respectively. The specific surface area of the quartz was 2.8 m^2/g as determined by BET N_2 adsorption analysis. Tannic acid (TAN, $C_{76}H_{52}O_{46}$, MW 1.7 kDa) was purchased from Fisher Scientific and used as received. Poly(ethylene oxide) (PEO, MW 8 MDa) was obtained from Polysciences Inc. The main functional groups of TAN and PEO were characterized by diffuse reflectance infrared Fourier transform spectroscopy (DRIFTS) and their FT-IR spectra and chemical structures are shown in Figs. 1c-1f. Absorption peaks at 1202 cm^{-1} and 1450 cm^{-1} in the FT-IR spectrum of TAN are assigned to the stretching vibrations of C-O and aromatic C-C bonds, respectively, and a broad band at 3392 cm^{-1} indicates the presence of phenolic hydroxyls [30, 31]. In the FT-IR spectrum of PEO, the featured peak at 1107 cm^{-1} represents the asymmetric stretching of the ether group [32]. In the present work, TAN solutions (1 g/L) were prepared by dissolving 0.1 g TAN in 100 mL deionized water, followed by stirring until the TAN was completely dissolved. Recognizing that the PEO efficacy is sensitive to the applied agitation scheme when preparing its stock solution, 0.1 g dry PEO powder was dispersed into 100 mL deionized water with mild stirring (400 rpm on a magnetic stirrer) at room temperature (~20°C), and the stirring was stopped after 1 hour. Our experience indicated that this scheme could keep the PEO solution in a viscous state and avoid degradation by excess shear. Afterwards, the PEO solution was allowed to stand overnight at room temperature before use. To minimize the ageing and shearing on the efficacy of PEO, its solutions were freshly prepared before each experiment and the same procedure was strictly followed. Potassium chloride (KCl, ACS reagent grade, Fisher Scientific) with a concentration of 10^{-3} mol/L was used to maintain a constant ionic strength in electrophoresis measurement. The pH of solution was adjusted by either sodium hydroxide (NaOH, ACS reagent grade, Fisher Scientific) or hydrochloric acid (HCl, ACS reagent grade, Fisher Scientific). All the experiments were carried out using deionized water (Millipore water purification system) having a resistivity of 18.2 mΩ·cm at room temperature.

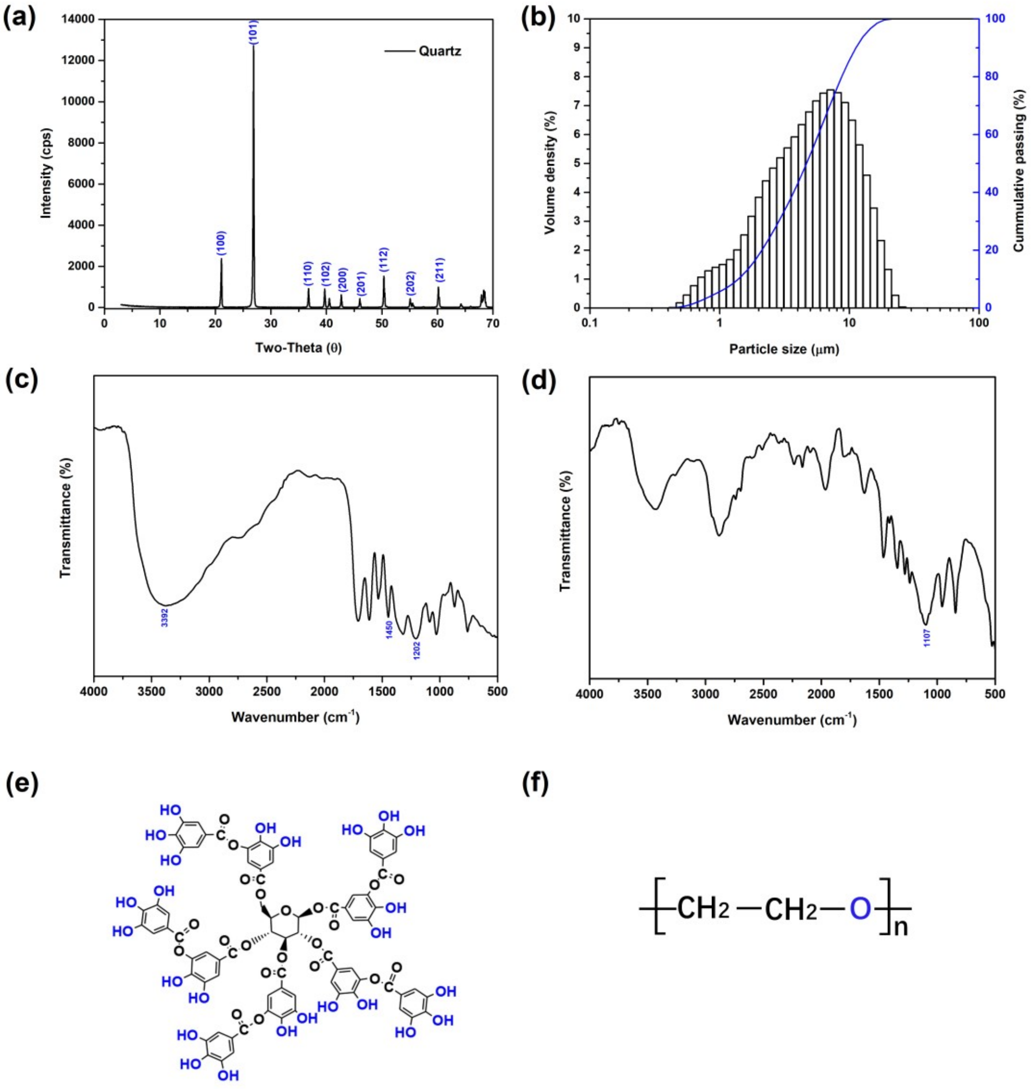

Figure 4.1 XRD pattern of quartz (a) and particle size distribution (b); diffuse reflectance Fourier transform infrared spectra and chemical structure of tannic acid (c) (e) and poly(ethylene oxide) (d) (f).

4.2.2 Methods

4.2.2.1 Flocculation test monitored by in-situ focused beam reflectance measurement

Flocculation process was monitored by FBRM G400 (Mettler Toledo, Switzerland), an in-situ technique to perform real-time particle size analysis. It is a probe-based tool using a highly focused laser beam and can detect the particle counts variation as well as the particle size distribution (chord length) over the range from 0.5 to 1000 μm. The principle of FBRM has been introduced elsewhere in the literature [33-35]. In this study, data collection of FBRM was set at 2 s intervals for flocculation tests. The setup of the flocculation experiment is shown in Figure 4.2. As illustrated, ~1 wt% suspension was prepared by dispersing 3 g quartz powder in 300 mL deionized water in a 500-mL beaker. For each test, the suspension was conditioned for 5 mins using a magnetic mixer, during which suspension pH was adjusted to the desired value. Afterwards, the suspension was transferred to a lab jack stand to perform flocculation tests. For all the flocculation tests, PEO concentration was fixed at 0.1 mg PEO per g of quartz (100 g/t). The TAN was added 1 minute prior to PEO for tests using dual polymers. The dosage of TAN was varied to achieve the desired TAN/PEO ratio.

The flocculation mixing system included an overhead mechanical stirrer (Caframo, Canada) with torque readout and a pitch blade impeller (4 blades, 45° pitch) having a diameter of 5 cm. Different hydrodynamic conditions were generated by adjusting the rotation speed of the impeller. Under a certain agitation speed, the average shear rate (G, s^{-1}), which is closely related to the specific energy dissipation rate, was calculated as follows [36]:

$$G = \left(\frac{1}{\mu}\frac{P}{V}\right)^{\frac{1}{2}} \tag{4.1}$$

where μ is the viscosity of the fluid ($\mathrm{Pa \cdot s}$), P is the power input (W) and V is the volume of the fluid ($\mathrm{m^3}$). The power input was obtained by torque reading multiplied by rotation speed using the following equation,

$$P = 2\pi \cdot M \cdot N \tag{4.2}$$

where M is the torque ($\mathrm{N \cdot m}$) and N is the agitation speed (rev per second). A relatively low shear rate of $G = 476\ s^{-1}$ (400 rpm) was used when investigating the effects of pH and TAN/PEO ratio on flocculation efficiency. A cycled shear schedule of $G = 476 \rightarrow 1103 \rightarrow 476\ s^{-1}$ (400→700→400 rpm) was applied to study the effect of turbulence on floc properties, i.e., the flocculation, de-flocculation and re-flocculation behaviors of flocs when exposed to different shear intensities.

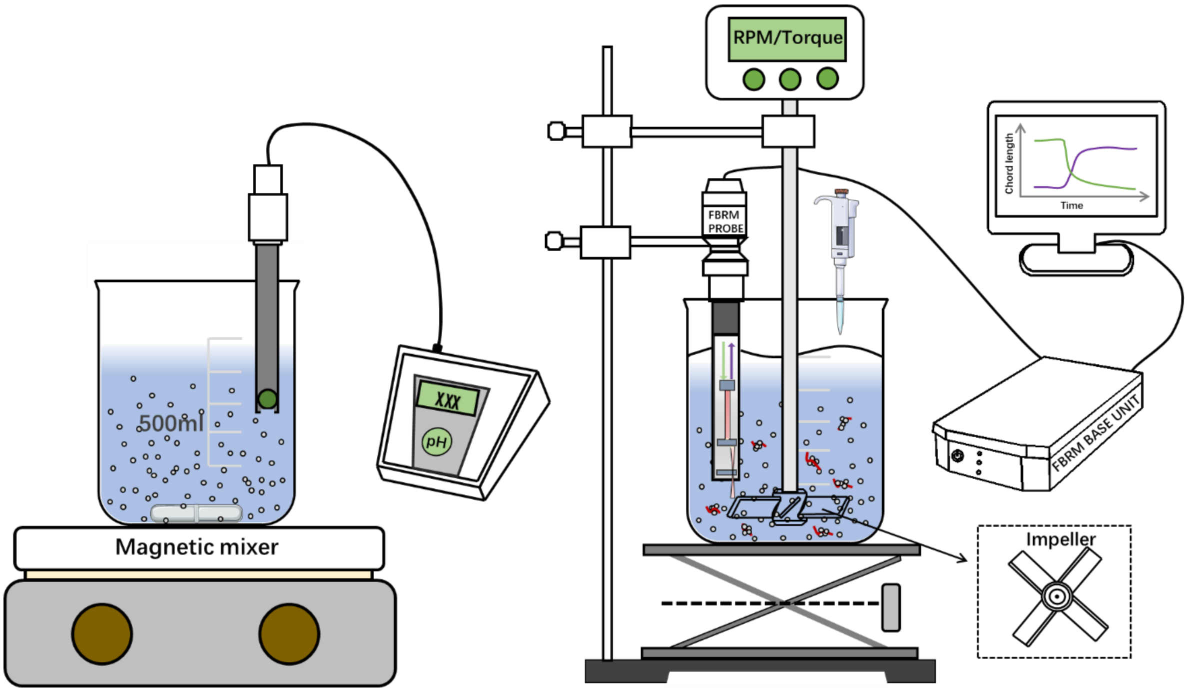

Figure 4.2 Schematics of flocculation process setup by employing in-situ focused beam reflectance measurement.

4.2.2.2 Settling test and turbidity measurement

Settling test was performed in a 250-mL graduated cylinder with a solid content of 1 wt%. The suspension was prepared by mixing 2.5 g quartz powder in deionized water in a 250-mL beaker, and the pH of the suspension was adjusted with 0.5 M HCl or NaOH solutions. The conditioned suspension was transferred to the graduated cylinder. Flocculant with the desired amount was added to the suspension using an adjustable-volume pipette. The cylinder was then sealed, inverted 10 times for good mixing, then placed on a flat surface to allow the suspension to settle for 10 mins. Afterwards, a sample of 40 mL supernatant was siphoned out from a fixed depth (15 cm from the top) and its turbidity was measured using a HACH turbidimeter. The measurement under the same condition was repeated three times and the average turbidity value was reported.

4.2.2.3 Zeta potential measurement

Electrical properties of quartz/liquid interface in the presence of different reagents were studied by measuring the zeta potential with a ZetaPALS analyzer (Brookhaven Instruments Corporation, USA). A stock quartz suspension (5 g/L) was prepared in 0.001 M KCl solution and kept stirred for 24 hours. On measurement, 20 mL of the stock solution was withdrawn and diluted to 100 mL using 0.001 M KCl solution. The pH was adjusted to desired values with HCl or NaOH, and then PEO, TAN, or TAN followed by PEO were added to the suspension and conditioned for 10 mins. After conditioning, 1.5 mL of the suspension was pipetted into a sample cuvette for measurement. The Smoluchowski model was used to calculate the zeta potentials from the measured electrophoretic mobilities. The reported zeta potential was the average of 10 runs, with 10 measurement cycles per run.

4.2.2.4 Adsorption density measurement

The adsorption density of PEO and TAN on quartz surface was measured using a total organic carbon (TOC-L) analyzer (Shimadzu, Japan) and a Lambda 365 Ultraviolet-visible (UV-Vis) spectrophotometer (Perkin-Elmer Inc., USA), respectively. Before measurement, standard calibration curves were established using a set of PEO or TAN samples prepared with known concentrations. To prepare samples for the adsorption density measurements, PEO or TAN solution of certain concentrations (5 mg/L and 10 mg/L in the present study) was added to 250-mL Erlenmeyer flasks containing 1wt% quartz suspension at different pH. The Erlenmeyer flasks were then placed in a benchtop shaking incubator (Corning Inc., USA) and oscillated for 2 hours at 20°C. The suspension was then centrifuged for 30 mins at 7000 rpm using a model 5430 centrifuge (Eppendorf, Germany). To obtain the carbon content, about 40 mL of supernatant was taken and injected into the 50-mL vials of the autosampler for TOC analysis. UV-Vis spectra were acquired in the wavelength range 200-500 nm by pipetting 3 mL supernatant into a quartz cuvette (100-QS, Hellma), with a slit width of 2 nm and a scan speed of 120 nm/min. The TAN concentration in the supernatant was obtained by the intensity of absorbance peaks at the wavelength of ~213 nm. The adsorption density of polymers on quartz surface was calculated by the depletion method using the following equation,

$$\tau = \frac{V(C_0 - C_e)}{m \cdot S} \tag{4.3}$$

where τ is the adsorption density on quartz surface (mg/m^2); C_0 is the initial concentration of PEO or TAN (mg/L); C_e is the equilibrium concentration of reagents in the supernatant (mg/L); V is the total volume of suspension (L); m is the mass of quartz (g); S is the specific surface area of quartz (m^2/g).

4.2.2.5 Formation of TAN-PEO associative complex and viscosity measurement

TAN and PEO solutions of the same concentration were mixed at a 1:1 mass ratio in vials at room temperature. The mixed solution was allowed to react for 20 mins under different pH values. After that, the viscosity of the solution was measured using a laboratory Ostwald viscometer. Deionized water with standard viscosity and density was used as the reference liquid. Detailed test procedure and calculation method have been introduced in our previous work [4].

4.2.2.6 Floc structure characterization

The microstructures of flocs generated by PEO and dual TAN-PEO polymers were investigated using confocal scanning microscopy (Axio CSM700) and freeze-drying-SEM imaging methods. PEO or TAN-PEO was added to dilute quartz suspension (0.1 wt%) with stirring, and then a small drop of the suspension was taken and deposited on a sample cell which was then observed under the CSM with a 10× objective magnification (image field 1168 μm × 938 μm). The Z scanning function was used so that topographical measurements can be performed to obtain the height profile of flocs in suspensions. For freeze-drying-SEM imaging, samples in the suspension state were deposited on the sample stubs and then were rapidly frozen in liquid nitrogen. Following that, the samples were transferred into vials and freeze-dried overnight using a SuperModulyo freeze dryer (Thermo Electron Corporation). In this cryodesiccation process, the ice water in the sample was removed directly by sublimating into vapor under a low pressure without destroying the original structure of the flocs. After freeze-drying, the samples were loaded to an Au sputtering deposition unit (Denton Vacuum) for 120 s, and a thin gold film coating was deposited on the sample surface for conducting purpose. Finally, the samples were placed into the chamber of SEM (Zeiss EVO MA10) for imaging.

4.3 Results and Discussion

4.3.1 Effect of solution pH on quartz flocculation using PEO and dual TAN-PEO polymers

Figure 4.3 shows the mean chord length evolution as a function of time for the quartz suspension. As can be seen from Figure 4.3a, a dramatic increase of mean chord length was observed immediately upon the addition of PEO (at 2 min) at pH 3.1 and 6.3 at a dosage of 0.1 mg PEO per g of quartz (100 g/t). It indicated that relatively strong flocculation of quartz by PEO occurred at neutral and acidic pH. The steady-state floc size reached ~120 μm at pH 3.1, which was the largest and slightly higher than that formed at pH 6.3. In contrast, weaker flocculation of quartz was observed under alkaline conditions, with a much smaller mean chord length (less than 40 μm) at pH 9.4. Hydrogen bonding is well-known to be an important mechanism that contributes to the adsorption of non-ionic polymers on oxide minerals [13, 24]. Considering that PEO mainly interacted with quartz by forming hydrogen bonds between the ether oxygen of PEO and silanol groups on quartz, it can be seen that an acidic pH would favor the hydrogen bonds formation because of the larger quantities of silanol groups –OH on the quartz surface at the acidic pH. With increasing pH, ionization of the silanol groups occurred, and numerous ionized silanol groups $–O^-$ may present on quartz surface at alkaline conditions, which was not favorable for the formation of hydrogen bonds with PEO, thus the decreased flocculation of quartz by PEO at pH 9.4. In addition, flocs formed by PEO did not experience significant breakage at the turbulence intensity used ($G = 476\ s^{-1}$), suggesting a certain degree of shear resistance capability.

Figure 4.3b shows the results when the TAN and PEO dual polymer system was used for quartz flocculation. TAN was added at 2 min and PEO was added at 3 min, and both were used at a dosage of 0.1 mg/g quartz (i.e., a TAN/PEO ratio of 1). As can be seen, the particle size did not change in the period of time between 2 and 3 min, indicating that TAN alone was incapable of flocculating quartz particles. Upon the addition of PEO at 3 min, the mean chord length increased sharply to more than 200 μm at neutral and alkaline pH, especially at pH 9.4 under which the maximum floc size (~ 275 μm at steady-state) was obtained, while quartz was only weakly flocculated by PEO alone at this pH (Figure 4.3a). This difference in floc sizes illustrated that tannic acid could substantially improve the flocculation of quartz by PEO under neutral and alkaline conditions. On the other hand, at the acidic pH of 3.1, the floc size of quartz stayed at around 100-120 μm and did not change markedly whether tannic acid was used or not. The observed synergistic effect of the dual polymers leading to larger floc size was likely due to the complexation between TAN and PEO, and the formed TAN-PEO associative complexes acted as more effective flocculants for quartz than PEO alone. The complexation between TAN and PEO seemed to depend on the pH of the solution.

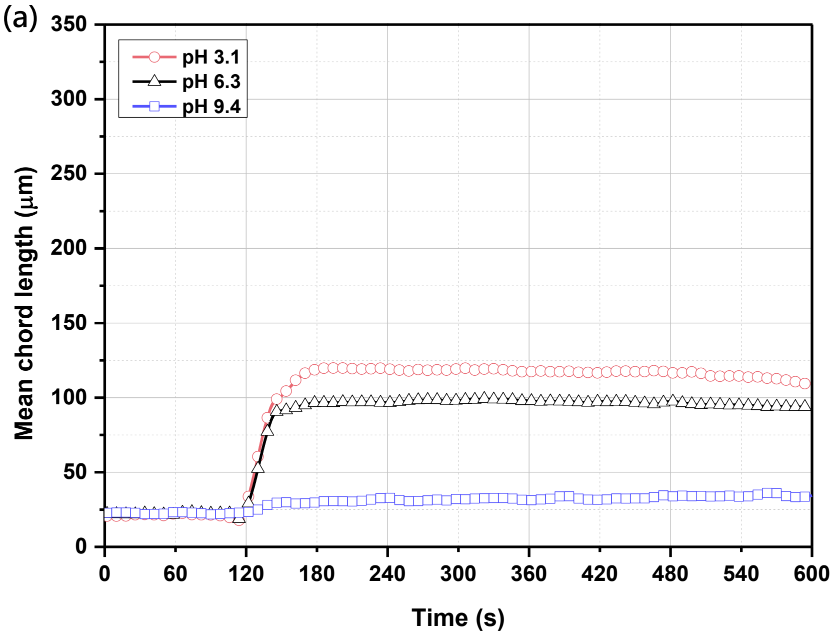

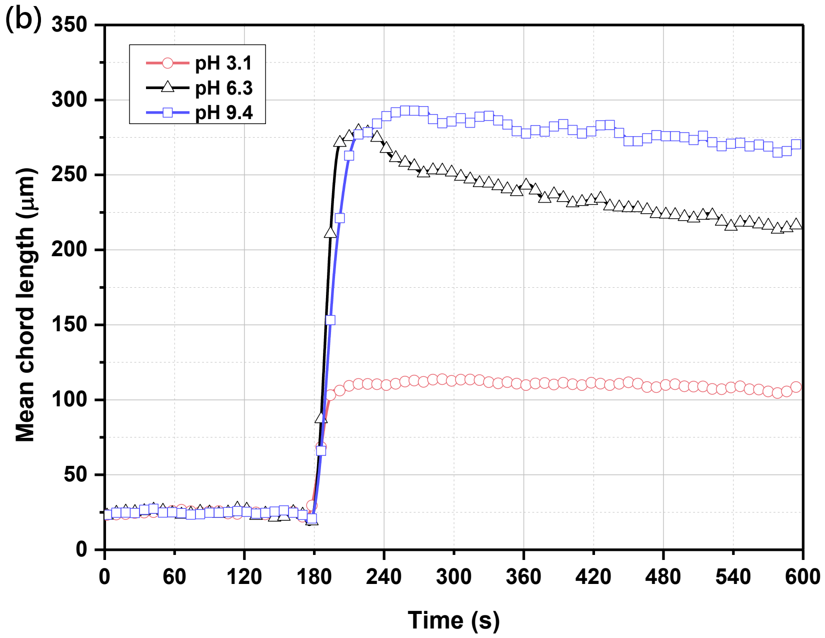

Figure 4.3 Flocculation of quartz with PEO only (a) and the dual TAN-PEO polymers system (b) at different pH, [PEO] = 0.1 mg/g quartz, TAN/PEO mass ratio is 1:1, G = 476 s^{-1}.

4.3.2 Effect of TAN/PEO mass ratio on quartz flocculation

Figure 4.4 shows the chord length distribution (CLD) of quartz flocculation at pH ~9.4 when different TAN/PEO ratios were used. PEO was fixed at a constant dosage of 0.1 mg/g quartz (100 g/t) and TAN concentrations were varied. During the flocculation process, the square weighted counts of CLD were recorded the moment when the mean chord length reached a steady state at each TAN/PEO mass ratio. As can be seen, with a low mass ratio of 0.2 (Figure 4.4a), the peak intensity of the CLD curve was low (<10 counts·s^{-1}) and chord lengths were predominantly less than 100 μm. This was caused by the insufficient amount of TAN. When a higher TAN/PEO mass ratio was applied, such as 0.5, the cps peak height increased sharply and the CLD shifted to larger chord lengths, indicating the formation of a greater number of larger flocs. The growing trend remained until the TAN/PEO mass ratio reached 2.0, after which higher TAN/PEO ratios did not further increase the flocculation efficiency of quartz. As shown in Figure 4.4b, the cps peak height gradually decreased with the increasing TAN/PEO mass ratio from 4 to 10, and the curves also slightly moved to the direction of lower chord lengths in that interval. It appears that an optimal TAN/PEO ratio (i.e., 2.0) existed for the optimum flocculation performance of quartz under the experimental conditions. Too low or too high TAN/PEO ratios induced lower degrees of flocculation of quartz. We hypothesize that a synergistic effect was at work between TAN and PEO for quartz flocculation. According to the literature, TAN has minor adsorption capability, if any, on quartz surface [29]. Thus, the role of TAN was mainly a “cofactor” that can associate with PEO so that PEO chains could be cross-linked, to form expanded configuration in solutions due to the high negative charge of the TAN. In this way, more quartz particles were captured by PEO to develop into larger flocs. Considering that a relatively low PEO dosage was used in this study, most functional adsorption sites of PEO molecules may have been occupied by TAN at high TAN/PEO ratios, and the excess TAN molecules may freely disperse in the solution. Due to the dispersing capability and negative charges of TAN in basic conditions [28], which may increase the repulsion interaction among particles, the flocculation efficiency was reduced at high TAN/PEO ratios. Noting that the concentration of PEO was also an important factor affecting flocculation, it was uncertain whether the optimum TAN/PEO ratio of 2 would remain if higher PEO dosages were used. The question was interesting but out of the scope of the current investigation.

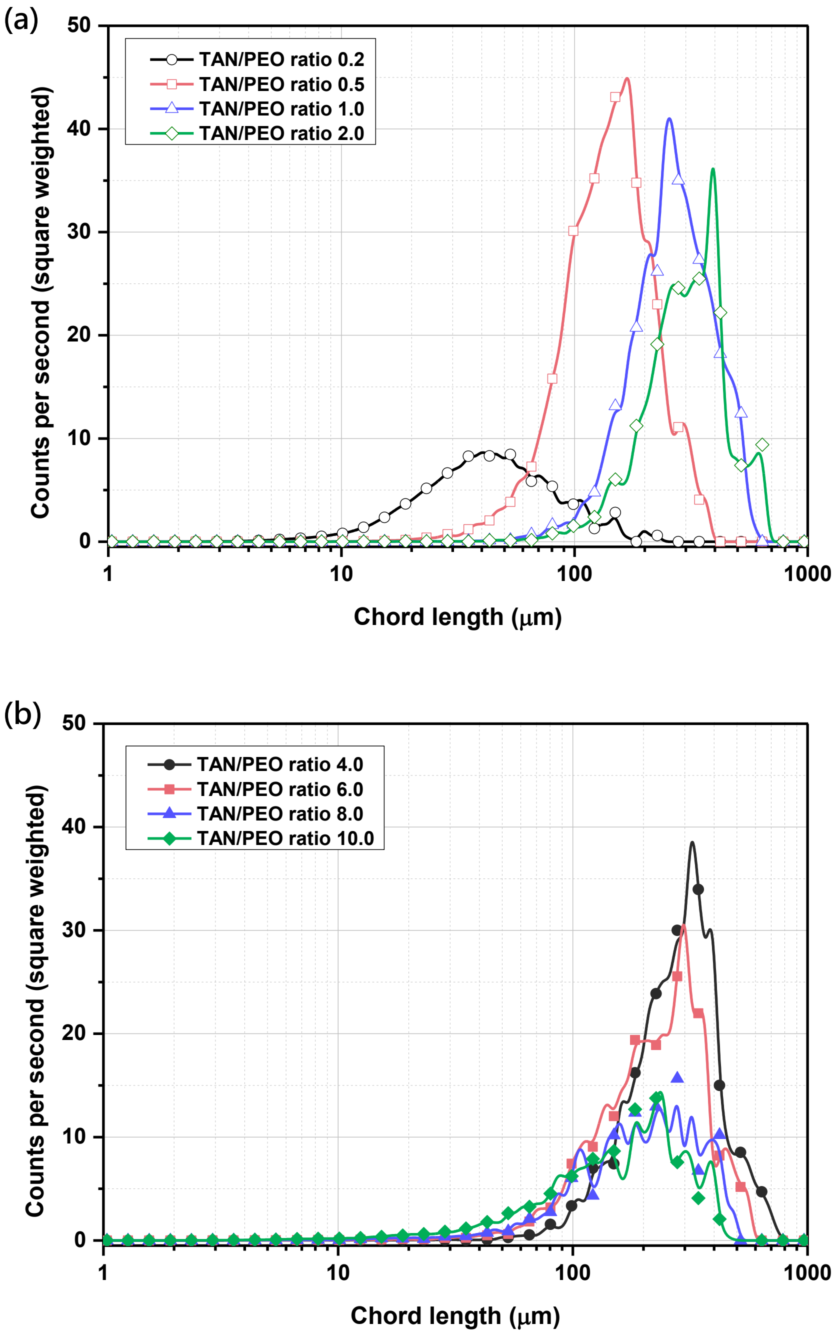

Figure 4.4 Chord length distribution of quartz suspension as a function of TAN/PEO mass ratio, [PEO] = 0.1 mg/g quartz, G = 476 s^{-1}, pH ~9.4.

4.3.3 Effect of turbulence intensity on quartz flocculation

In addition to the aforementioned physicochemical variables such as pH and polymer mass ratio, flocculation process is also affected by hydrodynamics, such as turbulence intensity. Flocs tend to break into smaller fragments when subjected to high shear. In some cases, the suspension shows reversible floc dynamics, namely that the broken flocs can regrow and attain the original flocculation size when the previous lower shear rate is resumed. But not all the flocs can be re-flocculated after breakage, and it largely depends on the action mechanism of flocculants [37]. Applying a cycled shear scheme has proven to be a good approach to study the floc properties (e.g., floc size, floc strength, and floc reversibility) under different turbulent shear [38-40]. Herein, the flocculation, deflocculation, and re-flocculation of quartz were investigated under cycled shear rates using PEO and TAN-PEO as flocculants, and the results are shown in Figure 4.5.

As can be seen from Figure 4.5a, during the flocculation stage (3-8 min, G = 476 s^{-1}), the flocs rapidly grew to reach steady-state floc size after the addition of PEO. The steady-state floc size was about 120 μm at pH 3.1 and about 100 μm at pH 6.3. The floc size then experienced a continuous decrease on exposure to a higher shear rate (G = 1103 s^{-1}). At the end of this breakage period (8-13 min), the mean floc size decreased to ~60 μm and ~35 μm, respectively, at pH 3.1 and 6.3. When the lower shear rate of G = 476 s^{-1} was restored, no re-flocculation was observed, and the floc size remained unchanged or slightly further decreased. This indicated that PEO-induced flocculation was irreversible upon high shear, and floc size formed was dependent on shear intensity. According to the literature, whether or not the flocs are reversible after breakage by turbulence is related to the particle-flocculant bonding [41]. It has been shown that re-flocculation can occur if the flocs are formed predominantly through charge neutralization (e.g., aggregation using coagulants or polyelectrolytes with high charge densities) [39, 42]. Here the PEO molecules were non-ionic and linear, and bridging flocculation by PEO for quartz suspension was generally driven via hydrogen bonds formed between the PEO's ether oxygen and quartz surface silanol groups. Due to the low binding energy, they could not withstand the high shear rates such that PEO chains detached from quartz particles. Once broken, these bonds may not be able to be reformed, so that the broken quartz flocs could no longer be held together. Previous research also suggested that turbulent flow can cause chain scission of polymer chains near the midpoint [43], and this may also happen for PEO chains at high shear rates and was another likely reason limiting the re-flocculation process. While different results have been reported that some non-ionic polymers may induce limited flocs regrowth after cycled shear in the literature, it was probably due to a much shorter breakage period, in contrast to 5 min that was used in the current investigation. It has been demonstrated that the steady-state floc size and the floc reversibility are both dependent upon breakage time [39].

Flocculation using dual TAN-PEO polymers, on the other hand, showed interesting phenomena. As can be seen in Figure 4.5b, a similar trend was observed for TAN/PEO flocculation at pH 3.1 as when PEO was used alone, and the flocs did not regrow after breakage. However, certain degrees of flocs re-flocculation were observed under neutral and especially under alkaline conditions. After resuming the initial lower shear rate, the maximum mean floc size regrew from 102 μm to 124 μm at pH 6.3 during the re-flocculation stage, and from 129 μm to 165 μm at pH 9.4. The result revealed that the introduction of TAN could not only promote the formation of larger floc size by PEO but also endow the PEO the capability of re-flocculation after floc breakage, and the effects were pH-dependent.

It seems that flocculation of quartz induced by the combined use of TAN and PEO differed from traditional polymer bridging. Inter-polymer complexation between TAN and PEO somewhat resembled the supramolecular interaction, where numerous hydrogen bonds participated [44, 45]. The composite materials formed in such a way display automatic self-healing/repair features in response to the mechanical or other disruptive forces [46]. Indeed, it has been found that in aqueous suspensions the hydrogen-bonded assemblies of tannic acid and polyethylene glycol (PEG), another term of PEO with smaller molecular weight, could self-repair after being physically damaged [47]. For TAN-PEO flocculation of quartz, the floc size was reduced by high shear rates, during which the TAN-PEO polymer associative complex may be disrupted after the 5-min exposure to higher turbulent shear. As the lower shear rate was restored, some hydrogen bonds between TAN and PEO molecules may be rebuilt so that new complexes were formed. In this process, the broken quartz-TAN-PEO fragments were captured by the crosslinked polymer complex and regrew to larger-sized flocs. Since PEO was the polymer that adsorbed on quartz, and since PEO alone did not demonstrate the ability to re-flocculate quartz once the PEO-quartz flocs were broken, it may be inferred that the hydrogen bonds between TAN and PEO were weaker than the hydrogen bonds between quartz and PEO. At the higher turbulence of G = 1103 s^{-1}, some of the hydrogen bonds between TAN and PEO were broken preferentially leaving the hydrogen bonds between quartz and PEO intact. The quartz-TAN-PEO fragments were re-connected by the "healing" effect of the hydrogen bonds between TAN and PEO when the shear rate was reduced, causing the quartz to re-flocculate. Indeed, this could only happen when the TAN-PEO hydrogen bonds were not overly strong, such as in the neutral and alkaline pH. At acidic pH, the hydrogen bonds between TAN and PEO were very strong (discussed below), so that the high turbulence broke the quartz-PEO bonds, and re-flocculation could not occur.

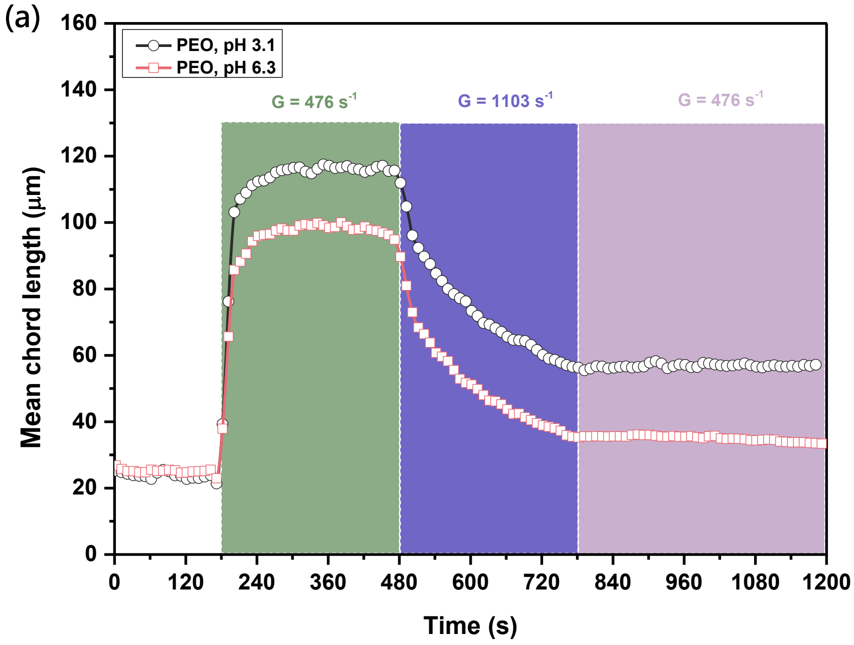

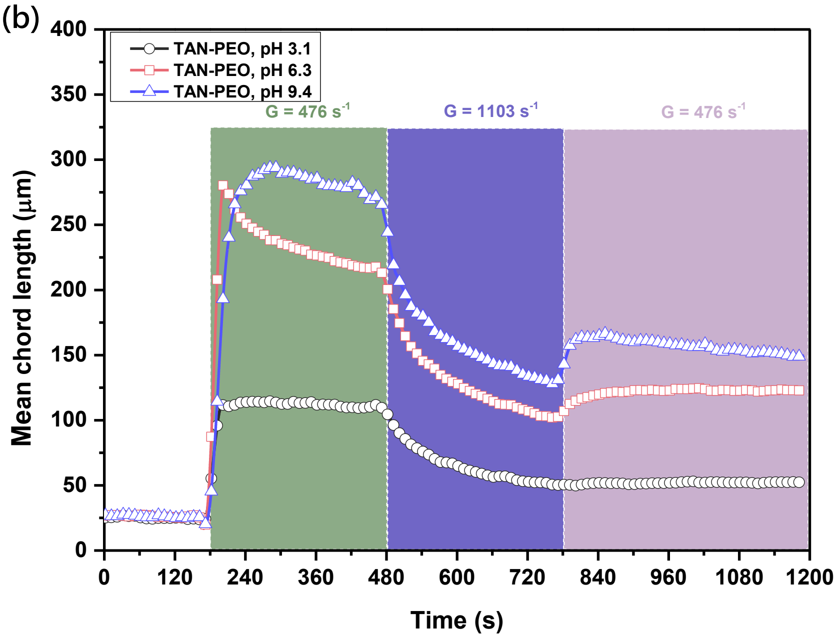

Figure 4.5 Effect of the cycled shear rates on quartz flocculation, deflocculation, and re-flocculation using PEO or TAN-PEO as flocculants at different pH, [PEO] = 0.1 mg/g quartz, TAN/PEO mass ratio is 1:1.

Floc properties as a function of TAN/PEO ratio were investigated under turbulent conditions. Table 1 shows the steady-state mean floc sizes at different stages of flocculation with various TAN/PEO mass ratios. The term $\frac{D_{de-floc}}{D_{floc}}$ was used to indicate the floc strength index when exposed to turbulence, and $\frac{D_{re-floc}}{D_{de-floc}}$ was used to describe floc reversibility after high shear. Higher values of $\frac{D_{de-floc}}{D_{floc}}$ suggested a better capability to withstand shear force and thus more resistant floc structures [39]. Likewise, higher values of $\frac{D_{re-floc}}{D_{de-floc}}$ suggested better flocs regrowth after breakage. As can be seen, when the TAN/PEO ratio was zero, namely the PEO-only flocculation system, flocs formed at pH 3.1 was stronger than that at pH 6.3. This could be seen not only by the larger average floc size at the initial flocculation stage but also by the higher strength index at pH 3.1 (0.49) than that at pH 6.3 (0.37). It was probably due to the stronger adsorption of PEO on quartz surface at acidic pH. For the TAN-PEO flocculation system, the effect of TAN/PEO ratio was examined at pH 9.4. As can be seen, the strength index generally increased with the increasing mass ratio of TAN/PEO, indicating that the addition of TAN could enhance the floc strength by PEO, and flocs seemed more robust with higher TAN/PEO ratios. It was proposed that phenolic compounds can increase the stiffness of PEO chains and make them adsorb more readily onto fines [14]. Regarding the structure of TAN-PEO associative complex, the initially flexible linear PEO chains may become rigid by association with TAN such that they bonded more firmly with quartz particles (or less likely to desorb), developing flocs that were more resistant against hydrodynamic force. A higher TAN/PEO ratio indicated more hydrogen bonding interactions within the complex, giving rise to a stronger adhesive force within the supramolecular and thus the floc structure. Consequently, the flocs showed better capability to resist high shear. For example, when the TAN/PEO ratio was 10, the flocs formed were believed to be more compact than that under lower ratios despite the smaller size (181.2 μm), and they showed the best shear resistance with a floc strength index of 0.80. On the other hand, it was interesting to see that flocs regrowth rate only peaked at low TAN/PEO ratios (0.2-2.0), and diminished as the ratio went above 2.0. This was likely due to the saturated adsorption of PEO chains by tannic acid at high concentrations. The complex would carry a large number of negative charges that caused increased electrostatic repulsion. Once the flocs were broken, the repulsive force may hinder the reformation of hydrogen bonds, thus preventing the re-flocculation at higher TAN/PEO ratios. At low and intermediate TAN/PEO ratios, there would be unreacted PEO chains or free ether oxygen groups, plus the weaker electrostatic repulsion force at the lower TAN concentration, both of which favoring the re-establishment of hydrogen bonding. Apart from the above analysis, the reduced particle-particle collision probability may also in part affect the possible flocs regrowth with high TAN/PEO ratios, because increased shear resistance resulted in fewer fragmented flocs at the re-flocculation stage.

Table 4.1 The steady-state mean chord length at different stages of flocculation with various TAN/PEO mass ratios. PEO concentration was constant at 0.1 mg/g quartz.

pH	TAN/ PEO ratio	Floc size $D_{floc}/\mu m$ (G = 476 s^{-1})	Floc size $D_{de-floc}/\mu m$ (G = 1103 s^{-1})	Floc size $D_{re-floc}/\mu m$ (G = 476 s^{-1})	$\frac{D_{de-floc}}{D_{floc}}$	$\frac{D_{re-floc}}{D_{de-floc}}$
3.1	0	115.7	56.5	56.7	0.49	1.00
6.3	0	95.2	35.3	33.4	0.37	0.95
9.4	0.2	49.5	33.1	44.5	0.67	1.34
	0.5	149.8	61.9	94.7	0.41	1.53
	1.0	271.3	129.2	163.9	0.48	1.27
	2.0	300.9	153.1	177.6	0.51	1.16
	3.0	344.6	187.4	187.4	0.54	1.00
	4.0	308.3	165.1	169.2	0.54	1.02
	5.0	278.1	181.4	178.1	0.65	0.98
	6.0	233.2	138.3	139.9	0.59	1.01
	8.0	218.9	165.8	158.8	0.76	0.96
	10.0	181.2	145.5	116.3	0.80	0.80

D_{floc} denotes the steady-state mean floc size at the flocculation period, and the value was taken at the end of the flocculation stage; $D_{de-floc}$ denotes the mean floc size after breakage, and the value was taken at the end of the de-flocculation stage; $D_{re-floc}$ denotes the maximum mean floc size that can be reached at the re-flocculation stage.

In comparison with the conventional polyaluminum chloride (PAC) coagulant and polyacrylamide (PAM) flocculant, the use of non-ionic PEO as a flocculant has both advantages and disadvantages for industrial operations that rely on polymer flocculation. First, PEO flocculation can better tolerate the interfering species in suspension, such as dissolved metal ions in mineral flotation slurry and the so-called “anionic trash” in papermaking process water. Otherwise, these interfering species would lower flocculation efficiency and consume a significantly higher amount of chemicals, a phenomenon that is often seen when coagulants or polyelectrolytes are used. Take the quartz flocculation as an example. It was found that equivalent or larger floc size was obtained using PEO than using PAC [48] despite a much lower concentration of PEO. Second, PEO was found to induce more compact floc structures upon shear than the anionic PAM due to PEO's flexible (elastic) molecular structure [5]. The unique property of PEO can enable improved pulp dewatering and consolidation of clay tailings [5]. Studies on the dewatering of oil sands mature fine tailings also indicated that PEO could yield higher solid content in pressure plate filtration cake together with another anionic polymer A3335 [49]. The disadvantages of PEO lie in its economic viability and unstable flocculation performance. Selectivity would also be a concern if PEO was used in mineral flotation separation as it interacts with many minerals (both hydrophilic and hydrophobic ones) by hydrogen bonding and hydrophobic association. Here we provided evidence that the resistance of PEO-induced flocs can be further strengthened with appropriate concentrations of tannic acid. This finding may be of significance to flocculation flotation in mechanical flotation machines, an environment where turbulent flows typically prevail by impeller agitation [1] and robust flocs are required. It was also noted that the use of tannic acid changed the optimum flocculation pH from acidic to alkaline, which made the process more practical since most industrial flotation is carried out in an alkaline flotation pulp.

4.3.4 Supernatant turbidity measurement in settling tests

The settling behaviors of quartz suspension were studied to further examine the flocculation efficiency of PEO and TAN-PEO polymers system. The supernatant turbidity of 1 wt% quartz suspension is shown in Figure 4.6. When PEO was used alone, the lowest turbidity was obtained at pH 3.1 after 10 min settling, followed by pH 6.3, while the turbidity of supernatant was significantly higher at pH 9.4 (more than 5000 NTU). Smaller values of turbidity indicated better clarity of the supernatant, implying that a smaller number of fine particles were left in the supernatant after flocculation and settling. Based on turbidity results, PEO was proved more efficient to flocculate quartz particles in acidic and neutral media and had the least flocculation efficiency of quartz at basic pH. On the other hand, when the TAN-PEO was used, the turbidity of supernatant was found to decrease dramatically to lower than 1000 NTU at pH 6.3 and 9.4. It suggested that tannic acid could promote larger floc sizes of quartz by PEO at neutral and alkaline conditions, causing faster settling rates and entrapping more fine suspended quartz. However, tannic acid failed to increase the floc size of quartz by PEO in acidic conditions as reflected by the higher supernatant turbidity treated by TAN-PEO than that using only PEO at pH 3.1. The results of turbidity measurement corresponded well with flocculation results from FBRM. It indicated that TAN and PEO acted synergistically to create a larger floc size of quartz suspension, meanwhile, the synergistic effect of the two polymers was affected by solution pH.

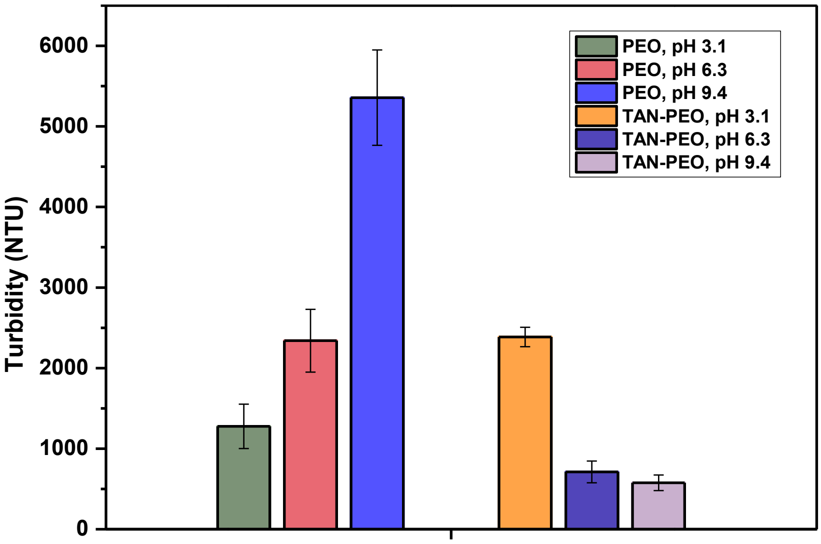

Figure 4.6 Supernatant turbidity of quartz suspension after 10 min settling at different pH using PEO and TAN-PEO as flocculants, [PEO] = 0.1 mg/g quartz, TAN/PEO mass ratio is 1:1.

4.3.5 Zeta potential measurement

Zeta potential is an important indicator of the stability of colloidal suspensions and is often used to study aggregation/dispersion behavior of particles. In this study, the zeta potential of quartz suspension was measured after interaction with polymers in 0.001 M KCl solutions. Figure 4.7a shows the zeta potential of quartz as a function of PEO concentration under different pH. As can be seen from Figure 4.7a, quartz was negatively charged (≤ -50 mV) at the three tested pH, thus quartz suspension should be stable without PEO due to the electrostatic repulsion. A rapid reduction in the magnitude of the negative zeta potential was observed with the increasing PEO concentration, especially in acidic and neutral conditions. The results showed that 5 mg/L PEO was enough to change the zeta potential from approximately -50 mV to nearly 0 mV at pH 3.1, and the value remained close to 0 mV at higher PEO concentrations. The absence of electrostatic repulsion would cause the system to aggregate under van der Waals attractive forces [50]. Quartz suspension was therefore destabilized by PEO adsorption in acidic and neutral conditions, due to both a reduction of the magnitude of the surface charge and bridge flocculation. Note that the reduction in the magnitude of the zeta potential by the non-ionic PEO was due to the expansion of the Stern layer caused by PEO adsorption. In contrast, the decrease in the magnitude of the zeta potentials at the alkaline pH of 9.4 was much less than at pH 3.1 and 6.3, indicating the weaker adsorption of PEO in alkaline solutions. This explained the pH dependence of flocculation efficiency by PEO from the electrokinetic perspective.

The prior addition of tannic acid significantly improved the flocculation efficiency by PEO. To achieve the synergistic function of the two polymers in quartz flocculation, several pathways were possible. One way is that TAN could adsorb onto quartz surface acting as the bridge which can facilitate the adsorption of PEO for flocculation. Another possible way is that TAN had a negligible affinity for quartz, and in such circumstances, TAN interacted with PEO to form associative polymer complexes which then adsorbed onto quartz surface through PEO. Therefore, whether or not TAN could adsorb on quartz determines which route was more likely. To check the adsorption of TAN on quartz, the zeta potential of quartz was measured at different TAN concentrations and pH and the results are shown in Figure 4.7b. The results showed that zeta potentials only fluctuated within a narrow range of ±5 mV as TAN concentration increased from zero to 20 mg/L. The trend was the same for all the three tested pH values. This indicated that TAN barely adsorbed on quartz, a conclusion that was also drawn in previous research [29].

Figure 4.7c shows the zeta potentials of quartz in the presence of both TAN and PEO (1:1 ratio) as a function of pH. As can be seen, with dual polymers treatment at pH 3.1 (regardless of concentration), the values of zeta potential were somewhere between that using the individual PEO and TAN. When the pH increased to 6.3, the measured zeta potentials were only slightly decreased compared with that using only PEO of the same concentration. At pH 9.4, the result was different in that dual polymers treatment could induce a reduction of the magnitude of the negative zeta potentials than that using only PEO. For example, the zeta potential was -21 mV at pH 9.4 in the presence of 5 mg/L PEO and 5 mg/L TAN, compared with -38 mV (red dash line in Figure 4.7c) in the case of only 5 mg/L PEO. This shows that TAN could join PEO and help decrease the electrostatic repulsion between quartz particles, thus promoting flocculation, particularly in neutral and alkaline suspension, whereas the effect was not as equally efficient in acidic solutions due to the more negative zeta potential by TAN.

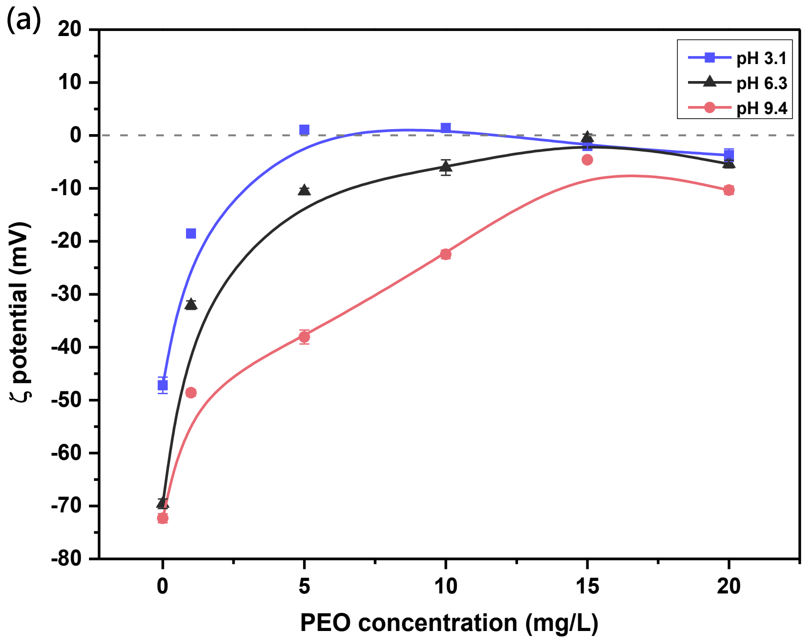

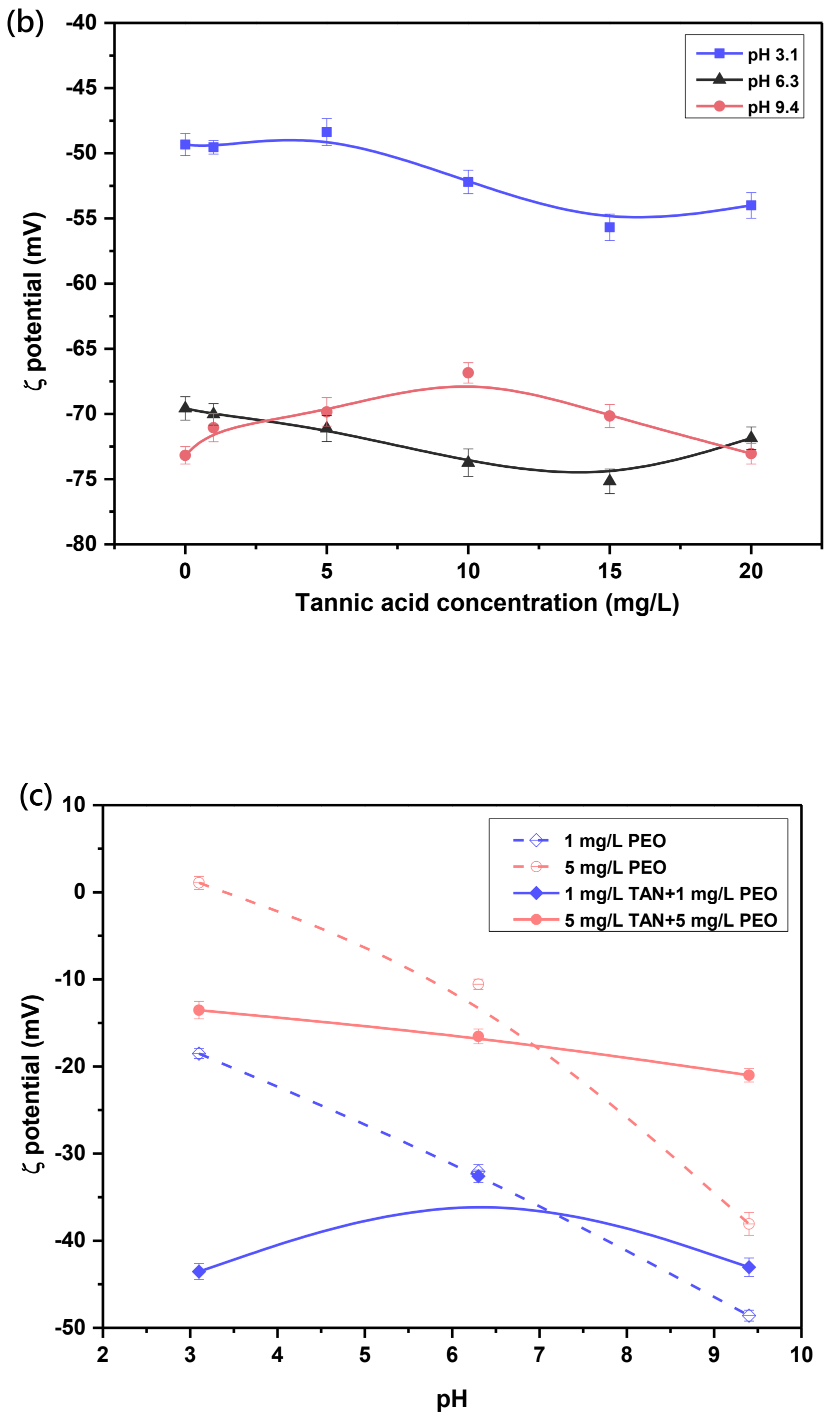

Figure 4.7 Zeta potential of quartz treated with PEO (a), TAN (b), and both PEO and TAN (c) at different pH in 0.001 mol/L KCl solutions.

4.3.6 Adsorption measurement

The adsorption behavior of PEO and TAN on quartz surface was measured at different pH and the results are shown in Figure 4.8. As can be seen from Figure 4.8a, the highest PEO adsorption density on quartz was found at pH 3.1, with 0.13 and 0.25 mg/m^2, respectively, for 5 and 10 mg/L PEO concentrations. With increasing pH, PEO adsorption decreased, and the lowest adsorption density (less than 0.075 mg/m^2) was observed at pH 9.4. The results were consistent with zeta potential measurements and flocculation tests. Higher adsorption density of PEO contributed to forming larger flocs in acidic and neutral solutions, while lower adsorption in basic solutions caused inferior flocculation of quartz due to insufficient polymer bridging. Figure 4.8b shows the adsorption of tannic acid. The results indicated that only a small amount of TAN adsorbed on quartz regardless of solution pH or TAN concentration. Despite a slight increase of adsorption density at pH 9.4, it was still lower than 0.01 mg/m^2.

On the basis of zeta potential and adsorption measurements, it can be seen that TAN interacted weakly with quartz. As a result, TAN should mainly disperse in solution and associate with PEO to form TAN-PEO associative complexes, which then induced more efficient flocculation of quartz suspension by the PEO.

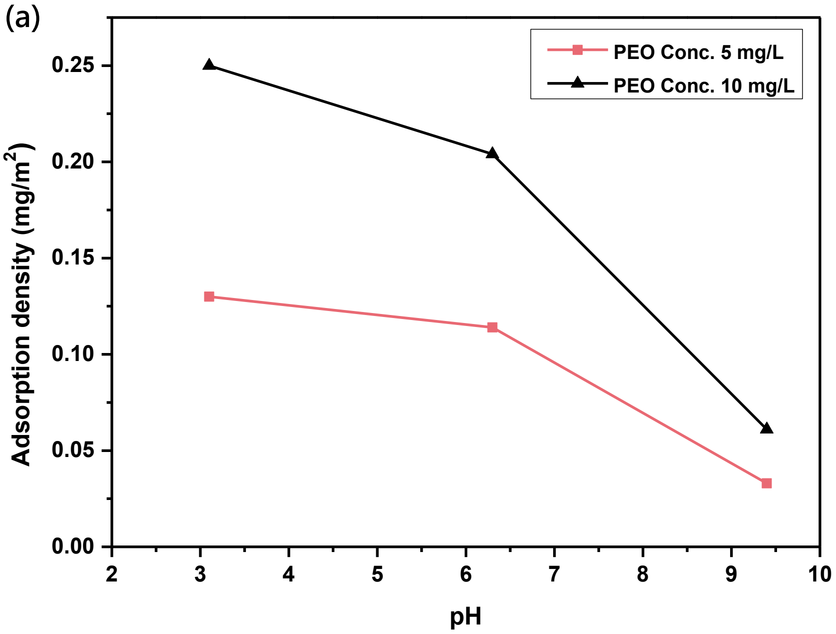

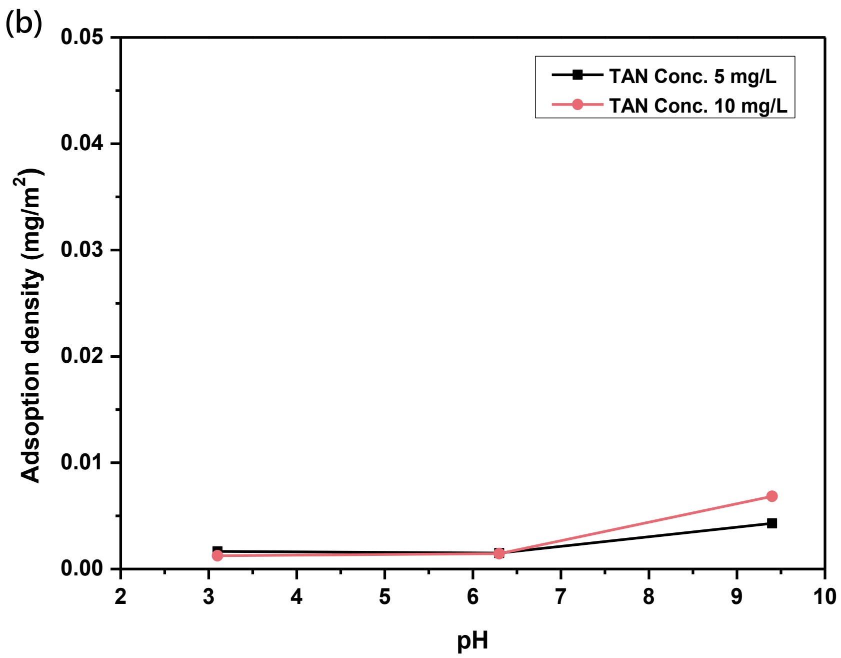

Figure 4.8 Adsorption density of PEO (a) and tannic acid (b) on quartz surface at different pH.

4.3.7 Analysis of TAN-PEO associative complexes and their property at different pH

So far, we have concluded that TAN-PEO associative complexes account for the enhanced flocculation of quartz, yet the effect of pH on TAN-PEO associative complex flocculation has not been investigated. As shown in flocculation experiments, flocs induced by the dual polymer system were not always in larger sizes than that using the individual PEO in different solutions. Previous research suggested that pH and ionic strength affect the complexation between PEO and phenolic compounds [17]. It is assumed that connections exist for flocculation behavior and complex properties that may vary upon solution pH. Here a facile method was used by mixing TAN and PEO solutions in vials at different pH such that complexes formation could be visualized. As can be seen from Figure 4.9, TAN interacted with PEO at pH 3.1 immediately upon mixing (Figure 4.9c), and the formed complexes rapidly contracted to a spherical shape and precipitated out of solution. Since tannic acid was not dissociated at this pH, it could strongly interact with PEO forming a large number of hydrogen bonds. However, the structure of the formed complexes collapsed at a fast pace and polymers bonded firmly with each other, the conformation of which would prevent the segmental mobility of PEO [21] to capture quartz particles in suspension effectively. That explained why TAN did not improve quartz flocculation by PEO in acidic media. With an increase in pH, some phenolic hydroxyls of TAN could dissociate. Thus, the complexation was not so intense at pH 6.3 as shown in Figure 4.9d. The formed complexes were larger in size and had an expanded configuration, and such a complex structure was more efficient to increase the floc size. Similar complexes were not observed at pH 9.4 (Figure 4.9e). However, the mixed polymer solution at pH 9.4 showed a yellowish coloration indicating the formation of possibly a different complex. It is known that tannic acid is a weak acid having low dissociation constant (pK_a ~6). Titration experiment reported in the literature has indicated that phenolic hydrogens of TAN were intact at acidic and neutral pH but gradually became dislodged when pH reached 9 or higher [27]. Figure 4.9f shows the UV-Vis spectra of tannic acid and TAN-PEO mixtures in aqueous solutions. As can be seen, tannic acid at natural pH exhibited two peaks located at around 213 and 275 nm, which was in accordance with literature [51]. At the higher pH of 9.4, the broad peak at 275 nm shifted its position to a larger wavelength (about 321 nm), likely resulting from the deprotonation of TAN molecules. When the HOMO-LUMO energy band gap was calculated in the position of the broad peak, it can be seen that a narrowed energy band gap (3.86 eV) was obtained at pH 9.4 versus that (4.51 eV) at the natural pH of 6.3, indicating more conjugated π electrons in TAN molecules at pH 9.4. Deprotonated TAN at high pH caused the formation of nucleophiles, increasing the HOMO energy level so that it became more readily to “donate” the electrons to form coordination bonds. Previous research suggested that the high pH-stability of hydrogen-bonded assemblies of tannic acid with non-ionic polymers was partially due to the suppressed ionization (deprotonation) of TAN [52]. Likewise, the addition of PEO in this study appeared to suppress the deprotonation of TAN because the broad peak in the UV-Vis spectrum of TAN-PEO mixture shifted to a lower wavelength (about 317 nm) compared with that of TAN at pH

9.4. This indicated the complexation interaction between TAN and PEO. Meanwhile, it can be inferred from the UV-Vis spectrum that tannic acid molecules retained partial protonated states upon mixing with PEO at high pH, and the protons may act as a link and form hydrogen-centered bonds between the ether oxygen of PEO and tannic acid within TAN-PEO associative complex. Besides, there are also reports that TAN was partially hydrolyzed under alkaline conditions and released gallic acid [53, 54], which is a trihydroxy benzoic acid containing phenolic hydroxyls. In other words, the phenolic hydroxyls did not entirely disappear and complexation would happen between TAN and PEO at high pH. According to the previous investigation, the phenolic compounds-PEO associative complexes were likely in the gel state under basic conditions, with better solubility and stability than at neutral and acidic conditions [17]. From the UV-Vis spectra and the above analysis, the presence of TAN-PEO associative complex seems logical as observed in Figure 4.9e.

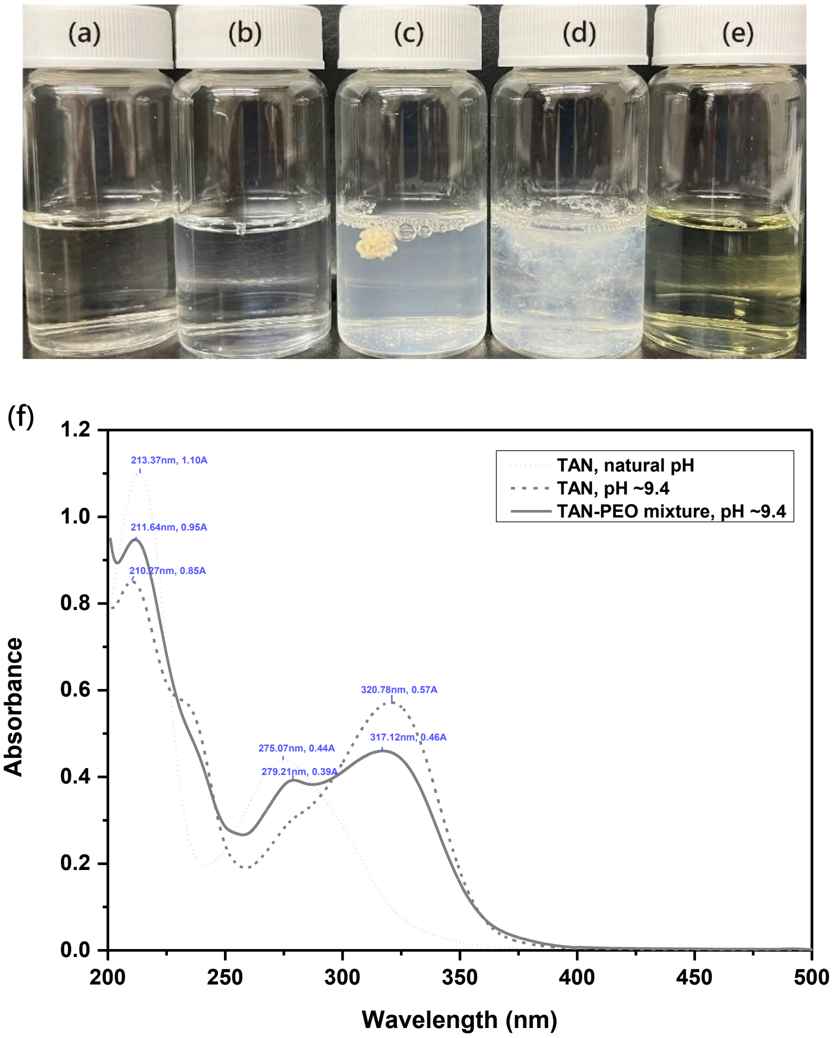

Figure 4.9 Tannic acid (a) and PEO solutions (b) with a concentration of 0.1wt%. Mixtures of TAN and PEO solutions at 1:1 ratio at pH 3.1 (c), 6.3 (d), and 9.4 (e). (f) the UV-Vis absorption spectra of tannic acid and TAN-PEO mixtures, and the TAN concentration was 10 mg/L.

Table 4.2 shows the viscosity of TAN and PEO solutions as well as their mixtures corresponding to the pictures shown in Figure 4.9. At room temperature, pure PEO solution had the highest viscosity (4.7×10^{-3} Pa·s) among the tested combinations. While the viscosity dramatically decreased upon mixing PEO with TAN at pH 3.1, likely due to the intense complexation interaction in acidic conditions and the removal of the polymers from solution by precipitation. In contrast, the viscosity of TAN-PEO mixtures was higher (2.2×10^{-3} Pa·s) at pH 9.4. This illustrated that the gel-like complex of TAN-PEO possessed better viscous properties, especially in the basic solution. Similar findings were also reported that crosslinked TAN-PEO associative complex could function as a highly adhesive agent (binder) for cathode materials in Li-S batteries [55]. Such a property of the complexes was deemed significant in promoting flocculation efficiency. According to the work by Lu and Pelton [20], the sticky PEO/cofactor complex was critical for efficient flocculation, while flocculation would become less efficient with the deactivation (decrease in stickiness) of the complex. More importantly, many studies have correlated the self-healing capability of polymers with their viscoelasticity property [44, 45, 56]. From this point of view, TAN-PEO associative complexes formed in alkaline solution might exhibit specific viscoelastic characteristics in flocculation, displaying the self-healing capability after exposure to high shear rates. That was likely the reason why the best flocs reversibility was observed in alkaline solutions as shown in Figure 4.5b.

Table 4.2 Viscosity of TAN and PEO solutions and their mixtures (mass ratio 1:1) at different pH. The concentrations of TAN and PEO were both 0.1 wt%.

Sample	Time of flow (s)			Mean time (s)	Density (kg/m^3)	Viscosity ($\times 10^{-3}$ Pa·s)
	1	2	3			
Deionized water	92	93	93	92.7	1000	1.0
TAN solution	92	94	94	93.3	995.8	1.0
PEO solution	427	441	443	437	989.4	4.7
TAN-PEO mixtures, pH 3.1	102	104	105	103.7	999.6	1.1
TAN-PEO mixtures, pH 6.3	118	121	122	120.3	980.5	1.3
TAN-PEO mixtures, pH 9.4	216	210	205	210.3	975.3	2.2

4.3.8 Flocs structure characterization

4.3.8.1 Structural investigation of flocs in the suspension using confocal scanning microscopy (CSM)

Figure 4.10 shows floc images observed in the suspension using different scanning modes of confocal scanning microscopy. As can be seen, flocs induced by PEO alone were in smaller sizes compared with that by TAN-PEO as shown in the 2D images (Figs. 10a and 10d). Moreover, most PEO-induced flocs were found to be in elongated shapes (Figure 4.10a), which was likely related to the linear structure of PEO chains. Such slender structures may make PEO-induced flocs easier to break on exposure to high shear, as indicated in Table 1. Associative TAN-PEO complex induced flocs, on the other hand, showed more expanded structures (Figure 4.10d). From Z images of flocs, it was found that flocs induced by PEO generally exhibited a uniform black color (Figure 4.10b). Interestingly, flocs formed by TAN-PEO, however, showed a non-uniform color distribution with white regions in the middle being surrounded by black edges (Figure 4.10e). It is noted that different color tones indicate height differences rather than different materials from CSM Z imaging. As shown in the height profile diagrams, flocs formed by PEO were of lower height and with less fluctuated topographical distribution (Figure 4.10g), indicating more uniform and compact floc structures. In contrast, flocs formed by dual TAN-PEO polymers possessed structures with a greater height of middle areas versus the much lower edges of the surrounding (Figure 4.10h). The relative height within the flocs could be as high as ~150 μm, significantly larger than that of PEO-induced flocs (about 130 μm), and this may indicate a comparatively more expanded floc structure. Such differences of topographic distribution in flocs could also be clearly seen from the 3D views in Figs. 10c and 10f. It was unclear why such a structural specificity showed for flocs formed by TAN-PEO. As explained earlier, the expanded flocs structure may be attributed to the repulsion force that tannic acid imparted to PEO chains. The possible reason for the specific topographic distribution of flocs would be caused by a certain preferred configuration of PEO molecules [17] during complexation with TAN.

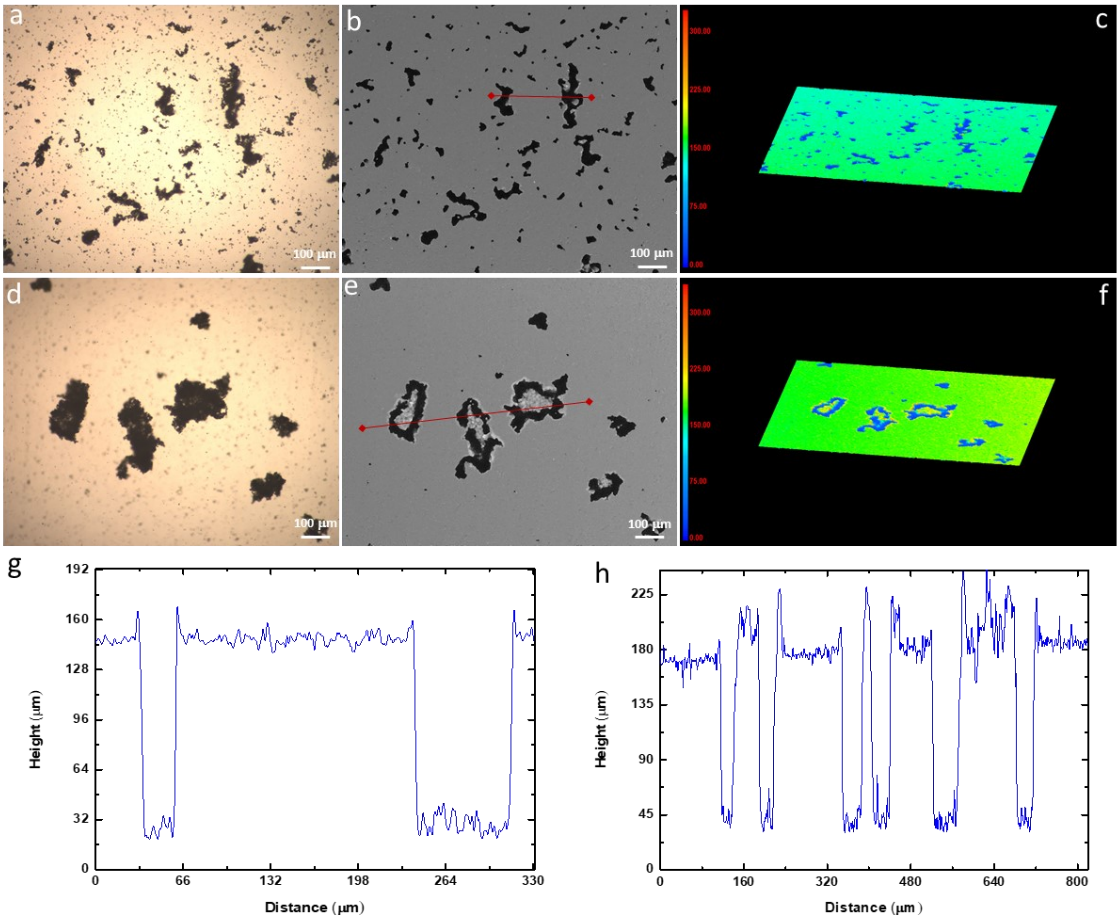

Figure 4.10 Confocal scanning microscope images of flocs formed using only PEO (a, b, and c) and TAN-PEO dual polymers (d, e, and f). Figs. 10a and 10d are 2D images, 10b and 10e are Z images obtained by performing a Z scan, and 10c and 10f are 3D topography showing flocs images. Figs. 10g and 10h are height profile diagrams of the regions chosen in Figs. 10b and 10e, respectively.

4.3.8.2 Structural observation of flocs using freeze-drying-SEM imaging

Figure 4.11 shows the freeze-dried flocs observed using SEM secondary electron images except for Figure 4.11a which shows the sediment of 5 wt% quartz suspension after settling overnight. The advantage of the freeze-drying technique is that the intact structure of flocs upon flocculation can be preserved which allows the possible pores (or cavities) to be analyzed. As can be seen, more loose flocs were formed by TAN-PEO dual polymers (Figs. 11c and 11f) compared with PEO alone (Figs. 11b and 11e). In fact, dual polymer TAN-PEO induced flocs appeared to be more swelled and more porous in structure. This may be resulted from the non-uniform floc structures observed by CSM. The specific floc structure of quartz by TAN-PEO dual polymer flocculation could well explain the phenomenon shown in Figure 4.11a, that a higher quartz sediment volume was observed in TAN-PEO dual polymer flocculated quartz after overnight settling despite the same solid content in the two cylinders.

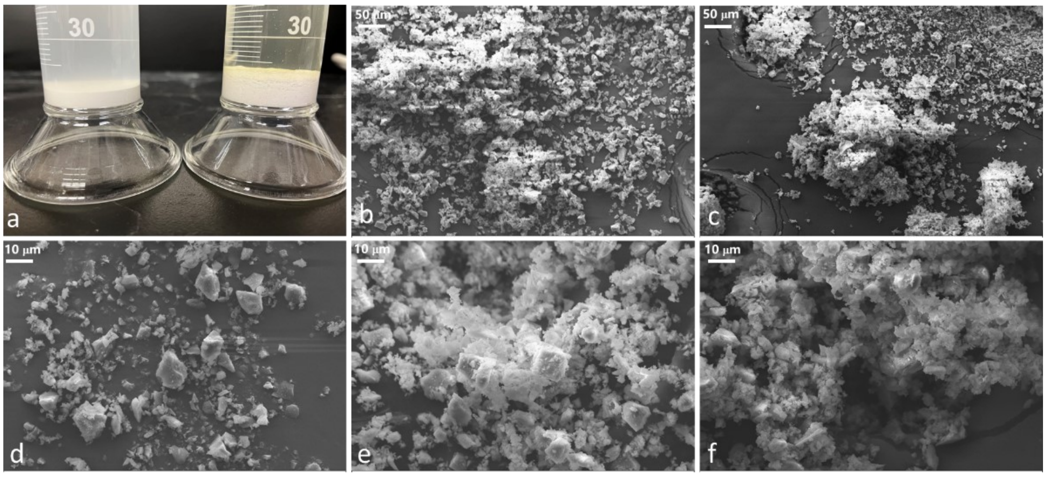

Figure 4.11 (a) Sedimentation of 5 wt% quartz suspension; PEO (0.1 mg/g quartz) was used in the left graduated cylinder and TAN-PEO was used in the right cylinder; (b) freeze-drying-SEM image of quartz flocculated by PEO (0.1 mg/g quartz); (c) freeze-drying-SEM image of quartz flocculated by 1:1 mixtures of TAN-PEO (PEO at 0.1 mg/g quartz); (d) freeze-drying-SEM image of quartz particles without flocculant; (e) and (f) are higher magnification images of (b) and (c), respectively.

In summary, flocculation of quartz by PEO alone or TAN-PEO dual polymers displayed completely different patterns. When PEO was used alone, the flocculation mechanism was polymer bridging via the long chains of PEO molecules. Specifically, the ether oxygens of PEO, which act as proton acceptors, form hydrogen bonds with hydrogen of the isolated silanol groups on quartz [57]. In an aqueous solution, protonation and deprotonation of quartz induced by pH change can affect the number densities of the isolated silanol groups that react with PEO. This therefore determines that the PEO adsorption densities and flocculation efficiency decreased with an increase in solution pH. On the other hand, flocculation of quartz by the TAN-PEO dual polymers was attributed to the complexation interaction between tannic acid and PEO, and then bridging of quartz particles by the TAN-PEO associative complexes. Flocculation performance by TAN-PEO associative complexes was affected by both physicochemical variables (e.g., solution pH, polymers ratio) and hydrodynamics (e.g., shear intensity). In this scenario, solution pH was found to affect the PEO flocculation of quartz in an opposite manner due to the prior addition of tannic acid TAN. The complexation interaction between TAN and PEO and the configuration of the formed associative complexes were pH-dependent. At neutral and alkaline pH, the tannic acid-PEO associative complexes took an expanded cross-linked configuration caused by the intermolecular or/and intramolecular repulsive forces [14] that arose from the partially deprotonated tannic acid. Moreover, the associative complexes were slightly viscous and possessed self-healing properties because the broken hydrogen bonds could be formed again. Tannic acid-PEO associative complexes of such a configuration and property, when adsorbed onto quartz, could enhance the flocculation efficiency and contribute to the shear resistance and re-flocculation of flocs in response to turbulence. Based on the results of this investigation, a schematic illustration was given to differentiate the flocculation mechanisms of quartz suspension by PEO alone and by TAN-PEO dual polymers as shown in Figure 4.12.

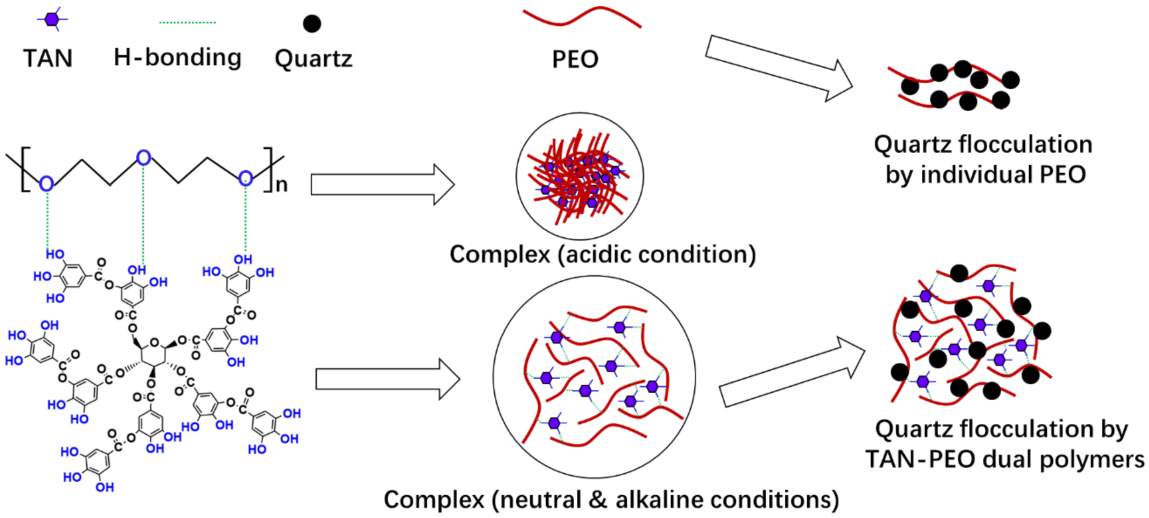

Figure 4.12 Schematics of quartz flocculation by PEO alone and by TAN-PEO dual polymers.

4.4 Conclusions

The flocculation behaviors of a < 12 μm high purity quartz sample by poly(ethylene oxide) (PEO), with a molecular weight of 8 million, with and without the co-presence of tannic acid (TAN) were investigated in this study. Floc size was monitored dynamically using an in-situ focused beam reflectance measurement technique. Interactive effects of solution pH, TAN/PEO ratio, and shear intensity on the flocculation were investigated. Floc properties under turbulent conditions were correlated to different structures of TAN-PEO associative complexes. Floc structure was characterized using confocal scanning microscopy in suspension as well as freeze-drying-SEM imaging. The main observations and conclusions were summarized as follows.

(1) Using PEO alone as a flocculant, the floc size and flocculation effectiveness of quartz decreased in the order of pH 3.1 > pH 6.3 >> pH 9.4. However, the prior addition of tannic acid reversed this trend so that floc size decreased in the order of pH 9.4 > pH 6.3 >> pH 3.1. Accordingly, supernatant clarity was higher at alkaline and neutral pH than at acidic pH when tannic acid and PEO were used together. The optimum mass ratio of tannic acid and PEO was 2.0 under the experimental conditions.

Tannic acid was found to increase the strength of quartz flocs formed by PEO, and the shear resistance of flocs increased with increasing TAN/PEO ratio under the investigated turbulent conditions. The quartz flocs formed by the combined use of tannic acid and PEO were found to have the capability of re-flocculation after breakage. When a cycled shear scheme was used, it was observed that flocs induced by PEO alone could not be re-flocculated once broken. However, quartz flocs formed by TAN-PEO mixtures could re-flocculate to some extent, especially in alkaline suspensions. Furthermore, the ability to re-flocculate was only observed when the TAN/PEO ratio was between 0.2 and 2.0. At higher TAN/PEO ratios, the floc's regrowth capability disappeared.

(2) Zeta potential and adsorption density measurements indicated that the adsorption density of PEO on quartz was highest in acidic pH and decreased with increasing pH. Tannic acid could not adsorb on the quartz surface nor induce quartz flocculation. Its beneficial effect in the PEO-quartz flocculation process was through the formation of a PEO-tannic acid associative complex, possibly through hydrogen bonding of the PEO's ether oxygen and tannic acid's vast number of hydroxyl groups. The associative PEO-tannic acid complex probably rendered the PEO molecular chain more rigid and more extended in the aqueous solution, both of which helped PEO's flocculation function.

(3) The structure of the TAN-PEO associative complex varied with pH, possibly due to different levels of hydrogen bonding interaction, and the structural difference affected floc properties. Under acidic conditions, the strong complexation between tannic acid and PEO resulted in the precipitated and smaller-sized complex, which was less effective for quartz flocculation. The associative tannic acid and PEO complex formed in alkaline solutions was gel-like and soluble, showing greater flocculation effectiveness for quartz suspension. Meanwhile, the tannic acid and PEO associative complex formed in alkaline solutions

showed better viscoelastic characteristics, and possessed self-healing properties that contributed to the re-flocculation after floc breakage.

PEO-induced quartz flocs were generally in elongated shapes and more uniform and compact in structure. Flocs induced by TAN-PEO dual polymers were more porous and took up a larger volume. This may be caused by the more rigid structure of the PEO-tannic acid associative complexes. The higher porosity and the more rigid polymer complex may be beneficial to subsequent filtration of the flocculated slurries.

4.5 References

[1] D. Wang, Q. Liu, Hydrodynamics of froth flotation and its effects on fine and ultrafine mineral particle flotation: A literature review, Minerals Engineering 173 (2021) 107220.

[2] J. Gong, Y. Peng, A. Bouajila, M. Ourriban, A. Yeung, Q. Liu, Reducing quartz gangue entrainment in sulphide ore flotation by high molecular weight polyethylene oxide, International Journal of Mineral Processing 97(1-4) (2010) 44-51.

[3] D. Liu, Y. Peng, Reducing the entrainment of clay minerals in flotation using tap and saline water, Powder Technology 253 (2014) 216-222.

[4] D. Wang, Q. Liu, Influence of aggregation/dispersion state of hydrophilic particles on their entrainment in fine mineral particle flotation, Minerals Engineering 166 (2021) 106835.

[5] J. Addai-Mensah, Enhanced flocculation and dewatering of clay mineral dispersions, Powder Technology 179(1-2) (2007) 73-78.

[6] M. Cadotte, M.E. Tellier, A. Blanco, E. Fuente, T.G. Van De Ven, J. Paris, Flocculation, retention and drainage in papermaking: a comparative study of polymeric additives, The Canadian Journal of Chemical Engineering 85(2) (2007) 240-248.

[7] M.R. Wu, J. Paris, T.G. van de Ven, Flocculation of papermaking fines by poly (ethylene oxide) and various cofactors: Effects of PEO entanglement, salt and fines properties, Colloids and Surfaces A: Physicochemical and Engineering Aspects 303(3) (2007) 211-218.

[8] H. Shi, P. Fatehi, H. Xiao, Y. Ni, Optimizing the poly ethylene oxide flocculation process for isolating lignin of prehydrolysis liquor of a kraft-based dissolving pulp production process, Industrial & engineering chemistry research 51(14) (2012) 5330-5335.

[9] S. Li, L. Gao, J. Wang, H. Zhou, Y. Liao, Y. Xing, X. Gui, Y. Cao, Polyethylene oxide assisted separation of molybdenite from quartz by flotation, Minerals Engineering 162 (2021) 106765.

[10] A. Alvarez, L. Gutierrez, J.S. Laskowski, Use of polyethylene oxide to improve flotation of fine molybdenite, Minerals Engineering 127 (2018) 232-237.

[11] A.M. Bodratti, B. Sarkar, P. Alexandridis, Adsorption of poly (ethylene oxide)-containing amphiphilic polymers on solid-liquid interfaces: Fundamentals and applications, Advances in colloid and interface science 244 (2017) 132-163.

[12] J. Rubio, J. Kitchener, The mechanism of adsorption of poly (ethylene oxide) flocculant on silica, Journal of Colloid and Interface Science 57(1) (1976) 132-142.

[13] J. Rubio, The flocculation properties of poly (ethylene oxide), Colloids and surfaces 3(1) (1981) 79-95.

[14] T.G. van de Ven, Association-induced polymer bridging by poly (ethylene oxide)–cofactor flocculation systems, Advances in colloid and interface science 114 (2005) 147-157.

[15] E. Koksal, R. Ramachandran, P. Somasundaran, C. Maltesh, Flocculation of oxides using polyethylene oxide, Powder technology 62(3) (1990) 253-259.

[16] C. Negro, E. Fuente, A. Blanco, J. Tijero, Flocculation mechanism induced by phenolic resin/PEO and floc properties, AIChE journal 51(3) (2005) 1022-1031.

[17] K.R. Stack, L.A. Dunn, N.K. Roberts, Study of the interaction between poly (ethylene oxide) and phenol-formaldehyde resin, Colloids and surfaces 61 (1991) 205-218.

[18] T. Lindström, G. Glad-Nordmark, Flocculation of latex and cellulose dispersions by means of transient polymer networks, Colloids and surfaces 8(4) (1984) 337-351.

[19] A.E. Imel, A.K. Naskar, M.D. Dadmun, Understanding the impact of poly (ethylene oxide) on the assembly of lignin in solution toward improved carbon fiber production, ACS applied materials & interfaces 8(5) (2016) 3200-3207.

[20] C. Lu, R. Pelton, Flocculation with poly (ethylene oxide)/tyrosine-rich polypeptide complexes, Langmuir 21(9) (2005) 3765-3772.

[21] C. Maltesh, P. Somasundaran, R. Kulkarni, S. Gundiah, Polymer-polymer complexation in dilute aqueous solutions: poly (acrylic acid)-poly (ethylene oxide) and poly (acrylic acid)-poly (vinylpyrrolidone), Langmuir 7(10) (1991) 2108-2111.

[22] K. Khoultchaev, P. Pang, R. Kerekes, P. Englezos, Enhancement of the retention performance of the poly (ethylene oxide)—tannic acid system by poly (diallyldimethyl ammonium chloride), The Canadian Journal of Chemical Engineering 76(2) (1998) 261-266.

[23] R. Gaudreault, T.G. van de Ven, M. Whitehead, Salt necessary for PEO-cofactor association: The role of molecular modelling in PEO flocculation mechanisms, Proc. First Applied Pulp and Paper Molecular modelling symposium, 2005.

[24] S. Mathur, B.M. Moudgil, Adsorption mechanism (s) of poly (ethylene oxide) on oxide surfaces, Journal of colloid and interface science 196(1) (1997) 92-98.

[25] E. Antunes, F.A. Garcia, P. Ferreira, A. Blanco, C. Negro, M.G. Rasteiro, Effect of water cationic content on flocculation, flocs resistance and reflocculation capacity of PCC induced by polyelectrolytes, Industrial & engineering chemistry research 47(16) (2008) 6006-6013.

[26] C. Negro, A. Blanco, I. San Pío, J. Tijero, Methodology for flocculant selection in fibre–cement manufacture, Cement and Concrete Composites 28(1) (2006) 90-96.

[27] J.D. Hem, Complexes of ferrous iron with tannic acid, US Government Printing Office1960.

[28] J. Rutledge, C.G. Anderson, Tannins in mineral processing and extractive metallurgy, Metals 5(3) (2015) 1520-1542.

[29] A. Tohry, R. Dehghan, L. de Salles Leal Filho, S.C. Chelgani, Tannin: An eco-friendly depressant for the green flotation separation of hematite from quartz, Minerals Engineering 168 (2021) 106917.

[30] S. Cowen, H.A. Al-Abadleh, DRIFTS studies on the photodegradation of tannic acid as a model for HULIS in atmospheric aerosols, Physical Chemistry Chemical Physics 11(36) (2009) 7838-7847.

[31] A. Ricci, K.J. Olejar, G.P. Parpinello, P.A. Kilmartin, A. Versari, Application of Fourier transform infrared (FTIR) spectroscopy in the characterization of tannins, Applied Spectroscopy Reviews 50(5) (2015) 407-442.

[32] I. Pucić, T. Jurkin, FTIR assessment of poly (ethylene oxide) irradiated in solid state, melt and aqeuous solution, Radiation Physics and Chemistry 81(9) (2012) 1426-1429.

[33] A. Blanco, E. Fuente, C. Negro, J. Tijero, Flocculation monitoring: focused beam reflectance measurement as a measurement tool, The Canadian Journal of Chemical Engineering 80(4) (2002) 1-7.

[34] Y. Kyoda, A. Costine, P. Fawell, J. Bellwood, G. Das, Using focused beam reflectance measurement (FBRM) to monitor aggregate structures formed in flocculated clay suspensions, Minerals Engineering 138 (2019) 148-160.

[35] A. Blanco, C. Negro, A. Hooimeijer, J. Tijero, Polymer optimization in paper mills by means of a particle size analyser: an alternative to zeta potential measurements, Appita journal 49(2) (1996) 113-116.

[36] J.S. Pérez, E.R. Porcel, J.C. López, J.F. Sevilla, Y. Chisti, Shear rate in stirred tank and bubble column bioreactors, Chemical Engineering Journal 124(1-3) (2006) 1-5.

[37] J. Nan, M. Yao, T. Chen, S. Li, Z. Wang, G. Feng, Breakage and regrowth of flocs formed by sweep coagulation using additional coagulant of poly aluminium chloride and non-ionic polyacrylamide, Environmental Science and Pollution Research 23(16) (2016) 16336-16348.

[38] W.-z. Yu, J. Gregory, L. Campos, G. Li, The role of mixing conditions on floc growth, breakage and re-growth, Chemical Engineering Journal 171(2) (2011) 425-430.

[39] P. Jarvis, B. Jefferson, S.A. Parsons, Breakage, regrowth, and fractal nature of natural organic matter flocs, Environmental science & technology 39(7) (2005) 2307-2314.

[40] C. Wang, C. Sun, Q. Liu, Formation, breakage, and re-growth of quartz flocs generated by non-ionic high molecular weight polyacrylamide, Minerals Engineering 157 (2020) 106546.

[41] P.T. Spicer, S.E. Pratsinis, J. Raper, R. Amal, G. Bushell, G. Meesters, Effect of shear schedule on particle size, density, and structure during flocculation in stirred tanks, Powder Technology 97(1) (1998) 26-34.

[42] V. Chaignon, B. Lartiges, A. El Samrani, C. Mustin, Evolution of size distribution and transfer of mineral particles between flocs in activated sludges: an insight into floc exchange dynamics, Water Research 36(3) (2002) 676-684.

[43] A. Horn, E. Merrill, Midpoint scission of macromolecules in dilute solution in turbulent flow, Nature 312(5990) (1984) 140-141.

[44] A. Faghihnejad, K.E. Feldman, J. Yu, M.V. Tirrell, J.N. Israelachvili, C.J. Hawker, E.J. Kramer, H. Zeng, Adhesion and surface interactions of a self-healing polymer with multiple hydrogen-bonding groups, Advanced Functional Materials 24(16) (2014) 2322-2333.

[45] I. Gadwal, A brief overview on preparation of self-healing polymers and coatings via hydrogen bonding interactions, Macromol 1(1) (2020) 18-36.

[46] V.K. Thakur, M.R. Kessler, Self-healing polymer nanocomposite materials: A review, Polymer 69 (2015) 369-383.

[47] Y. Du, W.Z. Qiu, Z.L. Wu, P.F. Ren, Q. Zheng, Z.K. Xu, Water-Triggered Self-Healing Coatings of Hydrogen-Bonded Complexes for High Binding Affinity and Antioxidative Property, Advanced Materials Interfaces 3(15) (2016) 1600167.

[48] C. Wang, P. Wang, X. Tan, G. Huang, J. Kou, C. Sun, Q. Liu, Selective aggregation of fine quartz by polyaluminum chloride to mitigate its entrainment during fine and ultrafine mineral flotation, Separation and Purification Technology 279 (2021) 119606.

[49] R. Loerke, X. Tan, Q. Liu, Dewatering of oil sands mature fine tailings by dual polymer flocculation and pressure plate filtration, Energy & Fuels 31(7) (2017) 6986-6995.

[50] B. Salopek, D. Krasic, S. Filipovic, Measurement and application of zeta-potential, Rudarsko-geolosko-naftni zbornik 4(1) (1992) 147.

[51] T. Shutava, M. Prouty, D. Kommireddy, Y. Lvov, pH responsive decomposable layer-by-layer nanofilms and capsules on the basis of tannic acid, Macromolecules 38(7) (2005) 2850-2858.

[52] V. Kozlovskaya, E. Kharlampieva, I. Drachuk, D. Cheng, V.V. Tsukruk, Responsive microcapsule reactors based on hydrogen-bonded tannic acid layer-by-layer assemblies, Soft Matter 6(15) (2010) 3596-3608.

[53] R. Osawa, T.P. Walsh, Effects of acidic and alkaline treatments on tannic acid and its binding property to protein, Journal of Agricultural and Food Chemistry 41(5) (1993) 704-707.

[54] F. Weber, E. Sagstuen, Q.-Z. Zhong, T. Zheng, H. Tiainen, Tannic acid radicals in the presence of alkali metal salts and their impact on the formation of silicate-phenolic networks, ACS applied materials & interfaces 12(47) (2020) 52457-52466.

[55] H. Zhang, X. Hu, Y. Zhang, S. Wang, F. Xin, X. Chen, D. Yu, 3D-crosslinked tannic acid/poly (ethylene oxide) complex as a three-in-one multifunctional binder for high-sulfur-loading and high-stability cathodes in lithium-sulfur batteries, Energy Storage Materials 17 (2019) 293-299.

[56] A.M. Grande, R. Martin, I. Odriozola, S. Van Der Zwaag, S.J. Garcia, Effect of the polymer structure on the viscoelastic and interfacial healing behaviour of poly (urea-urethane) networks containing aromatic disulphides, European Polymer Journal 97 (2017) 120-128.

[57] J. Gong, The role of high molecular weight polyethylene oxide in reducing quartz gangue entrainment in chalcopyrite flotation by xanthate collectors, PhD Thesis, University of Alberta, Edmonton, Alberta, Canada (2011).

CHAPTER 5 Effects of Agitation Intensity and Foaming Property on the Flocculation Flotation of Fine and Ultrafine Minerals Using a Laboratory-Scale Flotation Column

Abstract

In the present study flocculation flotation of fine and ultrafine hematite and quartz was investigated in a laboratory-scale flotation column. Direct flotation route was applied to float hematite using in-house synthesized n-octyl hydroxamic acid (OHA) as a collector. A polymer system containing tannic acid (TAN) and poly(ethylene oxide) (PEO) was used to flocculate quartz particles to reduce their entrainment. The effects of agitation intensity and foaming property on floc size distribution, entrainment degree, and flotation kinetics/recovery were investigated for the quartz and hematite flotation systems. The results indicated that the dual polymer system of TAN-PEO was effective to flocculate quartz and reduce its entrainment, however, the reduced degree of entrainment was affected by agitation intensity. A preliminary correlation was established between mean floc size and reduced degree of quartz entrainment using TAN-PEO as flocculants. Moreover, TAN-PEO dual polymer system was also found to enhance the flotation kinetics and recovery of hematite by OHA in single hematite flotation, benefitting from a synergistic effect between PEO and OHA. Better separation efficiency was obtained from synthetic fine hematite and quartz mixtures flotation with TAN-PEO added after OHA. The underlying reason for the observations was explained by studying the floc size distribution with FBRM, and measuring the surface tension, foaming property, and mean bubble size at water-air phases under different conditions. This work helps to understand the relationship between hydrodynamic condition, flocs size, and mechanical entrainment when polymeric flocculation is used for entrainment reduction purposes in fine and ultrafine minerals flotation.

Keywords

Column flotation; floc property; agitation intensity; foam stability; polymer flocculation; mechanical entrainment

5.1 Introduction

Low flotation kinetics of fine hydrophobic mineral particles and high mechanical entrainment of fine hydrophilic mineral particles are two major problems facing mineral processing industry. They limit efficient recovery of value minerals and meanwhile affect the quality of concentrate when froth flotation is used to separate fine and ultrafine minerals. Many factors have contributed to the two problems, but particle size is the most important one [1]. With the depletion of rich ore resources, the two problems are more pronounced due to the need of ultrafine grinding for target minerals liberation. As a consequence, finding effective strategies to mitigate the two problems is essential and significant for processing low-grade and finely disseminated ore deposits.

In response to the two problems, we attempted to use a two-stage aggregation flotation strategy. Essentially the idea is to combine the hydrophobic (shear, agglomeration) flocculation and selective polymer flocculation to separately aggregate the hydrophobic and hydrophilic fine particles, and in the ideal circumstance, they would form both hydrophobic and hydrophilic flocs in the slurry, then the normal flotation procedure can be applied to separate the hydrophobic flocs from the hydrophilic flocs [2]. By finding appropriate ways to increase the apparent size of both hydrophobic and hydrophilic particles, it is expected to improve the flotation rate/recovery of hydrophobic particles and at the same time reduce the degree of entrainment of hydrophilic particles.

Floc properties (e.g., floc size, shape, density, porosity, shear resistance, etc.) have been found to be important factors that influence flocculation flotation [3]. For the sub-processes of flocculation flotation, such as inter-particle collision and particle-bubble interactions, hydrodynamic and interfacial forces play the main role [4, 5]. Accordingly, the floc property would be mainly dependent on variables of hydrodynamic and physicochemical aspects. A number of literature reports have investigated the effect of hydrodynamic conditions (e.g., agitation intensity, kinetic energy input and energy dissipation rate) on hydrophobic flocculation and the subsequently enhanced flotation efficiency of fine minerals [6-8]. It was found that sufficient shear strength is necessary for hydrophobic particles to overcome the energy barrier and form flocs by hydrophobic association, and the needed shear strength varies according to different mineral types [6]. However, few studies have examined the flocs property in selective polymer flocculation and the associated flotation performance under different hydrodynamic and physiochemical conditions. For example, there is not yet evidence illustrating how agitation intensity in the conditioning stage would affect the sizes of hydrophilic flocs and their potential effect on fine particle entrainment. Considering the intention of generating both hydrophobic and hydrophilic flocs for flotation, delicate control of agitation intensity is necessary because forming the two types of flocs does not share the same requirement of a hydrodynamic regime. High shear strength would destroy floc structure and impede the flocculation process by polymers [9]. Although previous studies proved that entrainment of ultrafine hydrophilic particles can be reduced by aggregating those using appropriate coagulants/polymers [10, 11], it is unclear if this function remains under moderate or high agitation intensities. Therefore, one objective of the present study is to examine the effect of agitation intensity on hydrophilic floc property in the polymeric system and the resulting entrainment behavior in flotation. On the other hand, polymer chemistry is also an important aspect that affects floc property, and those variables include polymer molecular weight, type, charge density, configuration, polymer combination, and so on [12, 13]. It should be mentioned that some polymers (e.g., amphiphilic polymers) possess surface active function, and they can adsorb at the gas-liquid interface and act together with surfactants as foaming reagents [14, 15]. This might change the froth stability and thus improve or impede processes of entrainment and bubble-particle interaction. Consequently, foaming capability should be considered when such polymers are used for flocculation purposes in flotation.

Hematite and quartz with particle size less than 20 μm were used as model minerals. In beneficiation plants reverse cationic flotation is mostly used by floating siliceous gangue minerals with amine collectors and depressing iron oxide minerals with starch to achieve separation [16]. Apart from that, the direct flotation routes are also applied by floating iron ores with anionic collectors such as fatty acids or hydroxamates [17]. In the present study, an in-house synthesized n-octyl hydroxamic acid (OHA) was used as the collector of hematite. As a chelating reagent, hydroxamic acid can form stable complexes with cations of mineral lattice [18] and it showed superiority in collecting fine minerals [19]. In floating an iron ore of ultrafine size (ground to 70% -15 μm), Fuerstenau et al. [20] compared the efficacy of hydroxamate and fatty acids as collectors. They found that hydroxamate could generate a concentrate with satisfactory grade and recovery even at a relatively small dosage, whereas fatty acids did not seem to work. They also found that prolonging conditioning time and increasing pulp temperature promoted the flotation recovery of iron ore by hydroxamate, possibly due to higher concentrations of $Fe(OH)_{3\,(aq)}$ arising from iron dissolution. Li et al. [21, 22] also indicated that OHA was effective to collect -20 μm hematite. In their batch flotation of hematite-quartz mixtures, despite a high recovery of hematite by OHA, however, substantial quartz was entrained into the concentrate (about 50% at 500 g/t OHA) [22]. The main reason for the high entrainment was attributed to the ultrafine size of quartz (D_{90}, 10.6 μm) used in their work. Plus no pre-treatment was conducted for these ultrafine quartz particles; they were in a dispersion state during flotation and easily followed the water flow into concentrate. Following the concept of two-stage hydrophobic and hydrophilic aggregation flotation, if the ultrafine quartz was pre-aggregated to a larger size by coagulants/flocculants, it would decrease the probability of entrainment and thus improve the separation efficiency of hematite-quartz mixtures in OHA flotation systems. Previous research proved that using nonionic poly(ethylene oxide) (PEO) of high molecular weight helped improve the concentrate grade of chalcopyrite-quartz mixtures and a commercial Au-Cu sulfide ore [23]. However, it was also found that flotation performance was quite sensitive to PEO concentration, and a slightly higher addition of which can adversely increase the entrainment of hydrophilic particles. This was because PEO are amphiphilic molecules and can adsorb at air-water interface [24-26], and its application in flotation may increase the foaming and frothing stability. The improved froth capability/stability by PEO can likely impede drainage behaviors of hydrophilic particles and increase water recovery, both of which will contribute to increased entrainment in flotation. In the previous chapter, it was reported that using a dual polymer system, namely introducing the tannic acid (TAN) prior to PEO, significantly enhanced the flocculating capability and floc strength of quartz by PEO at alkaline conditions. Following that work, the polymer combination of tannic acid and PEO was used for the first time for fine minerals flotation in the present investigation. It was assumed that the complex interaction of the two polymers (TAN and PEO) not only can improve the flocculating properties of PEO but also reduce its foaming characteristics in flotation. Influences of the two aspects would benefit reducing entrainment recovery of ultrafine quartz.

This research employed a column for flotation and a baffled tank for slurry conditioning. Different from the turbulent environment in mechanical flotation cells, the flotation column created quiescent hydrodynamic conditions that favour the investigation of how floc properties may affect flotation performance. Based on the two-stage aggregation flotation concept, the current study aimed to improve the separation efficiency of -20 μm hematite-quartz mixtures using a direct flotation route. An emphasis was placed in the investigation of floc properties of hydrophilic particles and foaming characteristics under different agitation intensities and chemical conditions and the corresponding response of flotation efficiency.

5.2 Materials and Methods

5.2.1 Materials

Mineral samples used in this research included quartz and hematite. Quartz sample with high purity (>98% SiO_2) was purchased from US Silica with a vendor-specified particle size smaller than 15 µm. Hematite sample was provided by an iron ore mine in eastern Canada. The received sample was collected in the form of spiral concentrates and had an approximate Fe_2O_3 content of 91%. Besides, it contained small amounts of pyrolusite and quartz as impurities. The hematite sample was ground in a laboratory ball mill using mild steel balls, and the grinding discharge was wet screened using a 635-mesh sieve (aperture 20 µm). The -20 µm hematite was collected, dried, and sealed for flotation. Particle size distribution of both the hematite and quartz samples was analyzed using a Malvern Mastersizer 3000 and the results are shown in Figure 5.1. As can be seen, the 80% passing size was about 9 µm for quartz and 15 µm for hematite, and the medium size was about 5 µm and 8 µm for quartz and hematite, respectively.

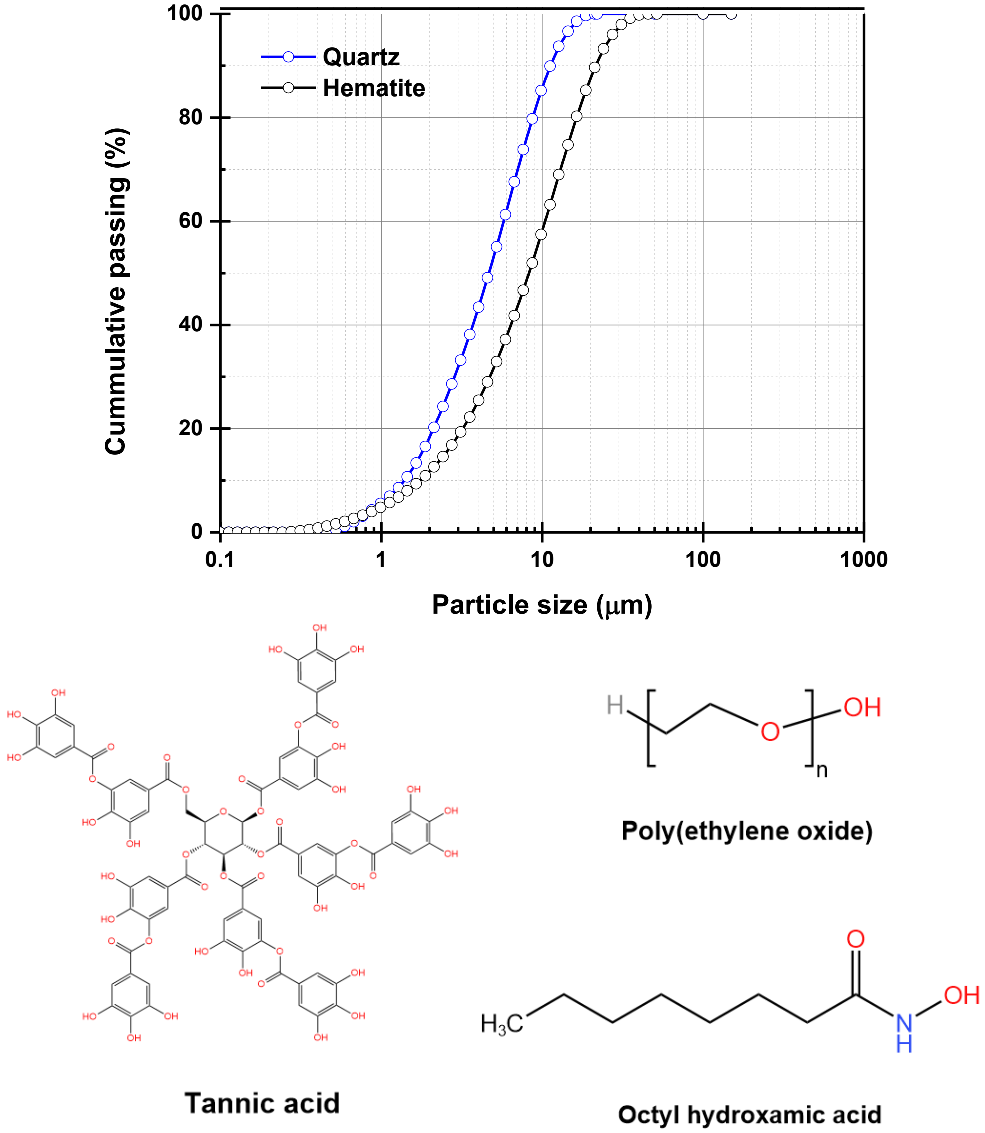

Figure 5.1 Particle size distribution of quartz and hematite samples measured by Malvern mastersizer 3000; Structure and functional groups of the main chemicals used in this work: tannic acid, poly(ethylene) oxide, and n-octyl hydroxamic acid.

Chemicals used in this research included n-octyl hydroxamic acid (OHA), tannic acid (TAN), poly(ethylene oxide) (PEO) with different molecular weights (8 MDa and 1 MDa) and Dowfroth 250 (DF250). The OHA was synthesized in our lab following the procedure in the literature [27] and the detailed ingredients and synthesis route have been introduced in previous work [28]. Tannic acid was purchased from Fisher Scientific, and PEOs were obtained from Polysciences Inc., and both were of analytical grade and used as received. DF250 was provided by Dow Chemical Canada Inc. Sodium hydroxide (NaOH, Fisher Scientific) was used to adjust the pH of slurry. Deionized water (Millipore water purification system) was used for all the experiments.

5.2.2 Methods

5.2.2.1 Column flotation

Flotation experiments were conducted using a column which was custom-made by the Glass Shop at the University of Alberta. Figure 5.2 (top panel) shows the basic structure and according dimensions of the column and it has a total volume of approximately one litre. A sintered glass frit that has micro-sized pores (4-5.5 μm) was in the base of the column and through which gas bubbles were generated by injecting compressed nitrogen gas. A magnetic stir bar was used to gently stir the slurries and enable mineral particles suspension within the column.

The slurry was conditioned in a baffled tank as shown in the top panel of Figure 5.2. The purpose of installing baffles was to reduce slurry swirling and promote axial circulation, thus increasing turbulence levels upon high-speed stirring. It was expected that flocs could be broken into smaller fragments more efficiently with the aid of baffles under intense agitation. The mixing system consisted of an overhead stirrer (Hei-TORQUE 100) with a wide speed range (10-2000 rpm) and a pitch blade impeller (4 blades, 30° pitch) having a diameter of 5 cm. In the conditioning stage, two levels of agitation intensities were investigated for single mineral flotation with a lower agitation level from 500 to 700 rpm and a higher agitation level from 1000 to 1500 rpm. The term of average shear rate (G, s^{-1}) was calculated using the torque readout values under a certain agitation speed as introduced in the last chapter. In the case of quartz slurry, if the slurry viscosity was assumed as about 1.0×10^{-3} Pa·s, the average shear rate in the tank ranged from 652.4 to 1260.7 s^{-1} at the lower level agitation and from 1845.4 to

2526.9 s^{-1} at the higher level of agitation intensities. After conditioning under different hydrodynamic conditions, the slurry was transferred into the flotation column via a peristaltic pump (Cole Parmer) at a maximum flow rate of ~70 mL per minute. The Tygon flexible tubing equipped with the pump had an inside diameter of 1/8 inch (equivalent to 3.2 mm). Considering that the diameter of the tubing was much larger than flocs size (in the micron range), it was hypothesized that the compressing effect of the pump would minimally affect the floc structures when slurry moved through it.

The bottom panel of Figure 5.2 presents the instrumental assembly in the lab. In single mineral flotation, 50 grams of pure quartz or hematite was mixed with 350 mL of deionized water and conditioned in the tank. The chemicals were added in the sequence of tannic acid (80 g/t), PEO (40 g/t), OHA (300 g/t) and DF250 (30 µL/L). It is noted that concentrations of chemicals were determined based on relevant work in literature, and they may not represent the optimum flotation conditions in this study. For comparison purposes, only OHA and DF250 were added for the test series that flocculation was not required. Variables such as agitation intensity and agitation time were controlled. Then the conditioned slurry was pumped into the column which was pre-loaded with 300 mL of DI water. As the suspension level reached a fixed mark line (about 15 cm below the concentrate launder) in the column, nitrogen gas flow was turned on, and the superficial gas velocity was strictly controlled at 0.2 - 0.3 cm/s since it was observed that the gas flow velocity is an important hydrodynamic parameter that affected gas holdup, water recovery, and mineral entrainment [29, 30]. At the same time, another 300 mL of DI water was added to the baffled tank and provided as make-up water as the flotation proceeded. Flotation time lasted for three minutes, and four froth products were continuously collected at 30, 60, 120 and 180 second. Water and minerals solid content in these samples were determined by wet weighing, vacuum filtration, and dry weighing. The slurry pH in the column was controlled between 8.5 and 9.0 using NaOH. For mixed minerals flotation separation, the same procedure was followed except that quartz and hematite were artificially mixed proportionally and loaded as flotation feed. The contents of Fe and SiO_2 in concentrates and tailings were analyzed using a benchtop CBX 810 X-ray fluorescence spectrometer (Bruker, USA) and used to evaluate the separation efficiency.

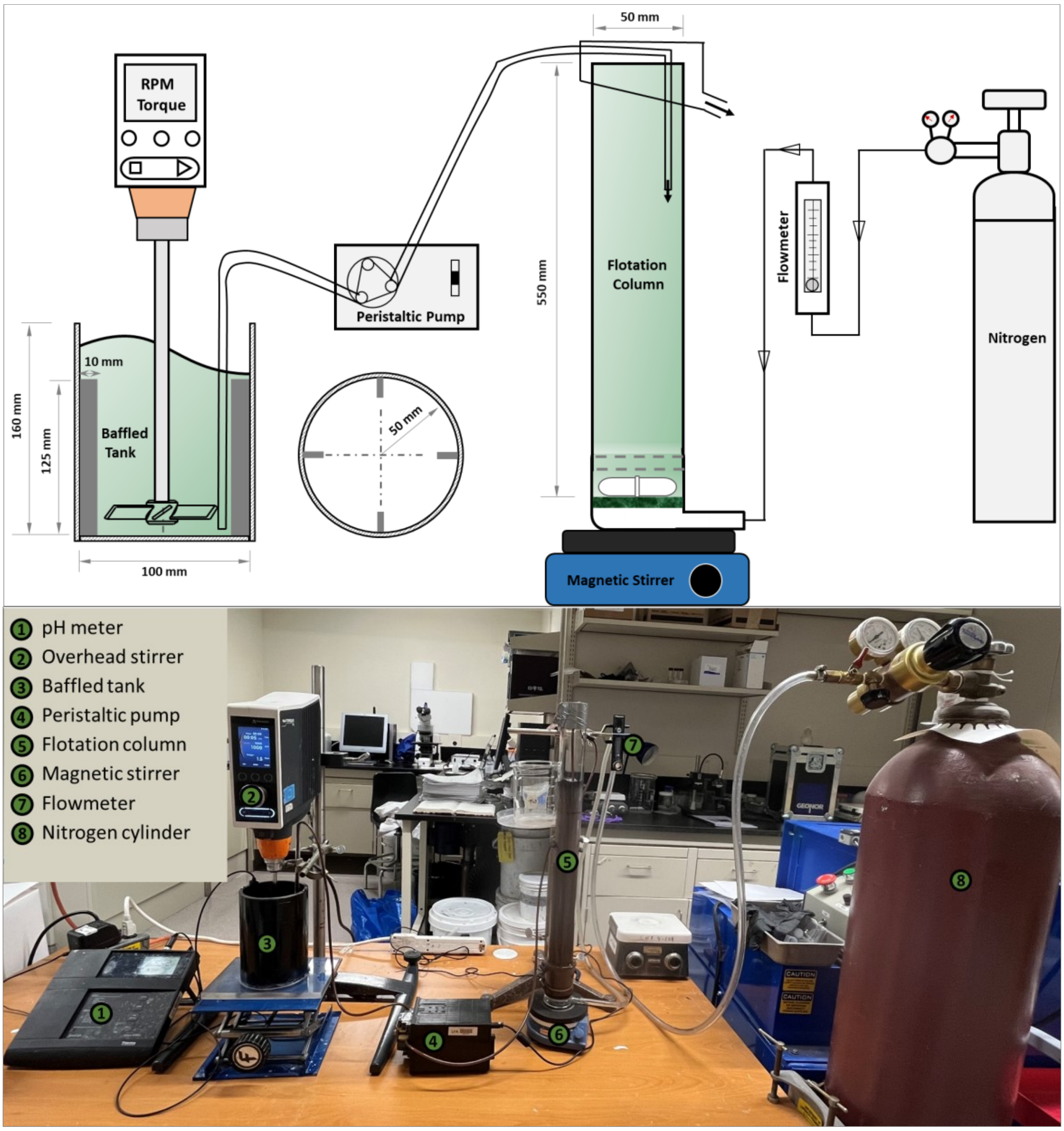

Figure 5.2 Schematic setup of column flotation experiment (top panel) and the instrumental assembly in the lab (bottom panel).

5.2.2.2 Floc size analysis by focused beam reflectance measurement

Floc size distribution was analyzed by FBRM, an in-situ technique for real-time particle size and count tracking. It can detect particle size populations ranging from 0.5 to 1000 µm. The process of FBRM test followed the same procedure as column flotation. For each test condition, 10 grams of sample was used, and the amount of chemicals was reduced accordingly but kept at the same concentration as in the flotation tests. The slurry transported through the peristaltic pump was discharged into a beaker which was placed on a magnetic stirrer, and the probe of FBRM was immersed in water just above the magnetic stir bar. After the suspension was stable in the beaker, the peristaltic pump was stopped, and floc size distribution was measured.

5.2.2.3 Surface tension measurement

Surface tension of aqueous solutions of different chemicals was measured with a surface tensiometer (KRÜSS Scientific) that utilized the Wilhelmy plate method. Before the measurement, the equipment was calibrated by measuring the surface tension of pure deionized water at room temperature. Solutions of single chemical and different chemicals combination were prepared with desired concentrations and proportions. The pH of the solutions was maintained the same as in column flotation. The prepared sample solution was placed in a solvent vessel to initiate measurement. For procedure control, the detection speed was set as 10 mm/min, the immersion depth was 2.0 mm, and the measurement time was 1 min. When the measurement was finished, software could calculate and output mean values of surface tension and standard deviation. After each test, the platinum plate was cleaned thoroughly with DI water and then dried with pressurized air. The dry plate was heated using a butane torch to burn off any remaining contaminants before conducting the next measurement.

5.2.2.4 Foaming property and bubble size measurement

The foaming property of different chemical regents was studied in two phases containing water and gas. On one hand, the formation and decay processes of foam were investigated using the flotation column. Following the procedure of column flotation, single chemical or their combinations were added at a certain dosage, and an equilibrium foam height and decay time were recorded after aeration for the same period with a fixed airflow rate. The test for each condition was repeated three times and the average result was taken. On the other hand, mean bubble size was measured employing FBRM for different chemical conditions. To measure bubble size, the FBRM probe was inserted into a small column containing DI water and chemicals. After aeration for two minutes at a fixed air rate, bubbles were generated by getting through the fine frit in the column base and reaching a stable state. Then the measurement was started and the mean bubble size was tracked over time with FBRM probe and software.

5.3 Results and Discussion

5.3.1 Column flotation in single quartz system

Results in Figure 5.3 show the cumulative quartz recovery in the froth as a function of water recovery by only OHA or in the presence of TAN-PEO polymers. Before the quartz suspension was pumped to the column, it was conditioned in the tank under two groups of hydrodynamic agitation, with results shown in Figure 5.3a (lower levels) and Figure 5.3b (higher levels) respectively. With only OHA, it can be seen that quartz recovery generally increased linearly with water recovery regardless of agitation intensity, indicating that quartz was recovered by mechanical entrainment. The trend was consistent with literature studies on the relationship between entrainment and water recovery [31] and was logical considering that hydroxamate collectors can hardly adsorb onto quartz surface and render it hydrophobic to attach to air bubbles [32, 33]. In general, the agitation intensity did not affect quartz and water recoveries significantly in the presence of only OHA except that they both decreased slightly when the agitation speed was 1500 rpm (2526.9 s^{-1}), which was likely due to a different slurry viscosity at high turbulent conditions. On the other hand, when the dual TAN-PEO polymers were added as flocculants of quartz, quartz recovery was seen to decrease from approximately 33% to about 21% when conditioning at lower levels of agitation intensities (Figure 5.3a), and the water recoveries were also reduced simultaneously. Reduction of quartz recoveries was still observed when agitation intensity was at higher levels (Figure 5.3b) in the presence of TAN-PEO, however, it was not as efficient in contrast with that at lower levels of agitation. Table 5.1 shows a comparison of the total entrainment recovery of quartz at the end of column flotation in the absence and presence of TAN-PEO polymers under different agitation intensities. It is clear that the reduced degree of quartz entrainment was dependent on agitation intensity. At lower levels of agitation, the reduced quartz entrainment could be as high as about 34% using 80 g/t tannic acid and 40 g/t PEO, and that value decreased with increasing agitation intensity of conditioning and was only 7.5% at 1500 rpm (2526.9 s^{-1}). Investigation in chapter 4 has proved that combining tannic acid and PEO could increase the size of quartz flocs in alkaline solutions. It was assumed that hydrophilic flocs of quartz were formed in flotation column by TAN-PEO polymers, and enlarged particle size of quartz can reduce their transfer probability along with water or promote their drainage rate once entrained into the froth phase, and the phenomenon was particularly pronounced when the agitation intensity was not too vigorous. Besides, the changes in frothing property may also be responsible for the reduced entrainment of quartz in flotation. As has been observed, less water was recovered in general when TAN-PEO polymers were used.

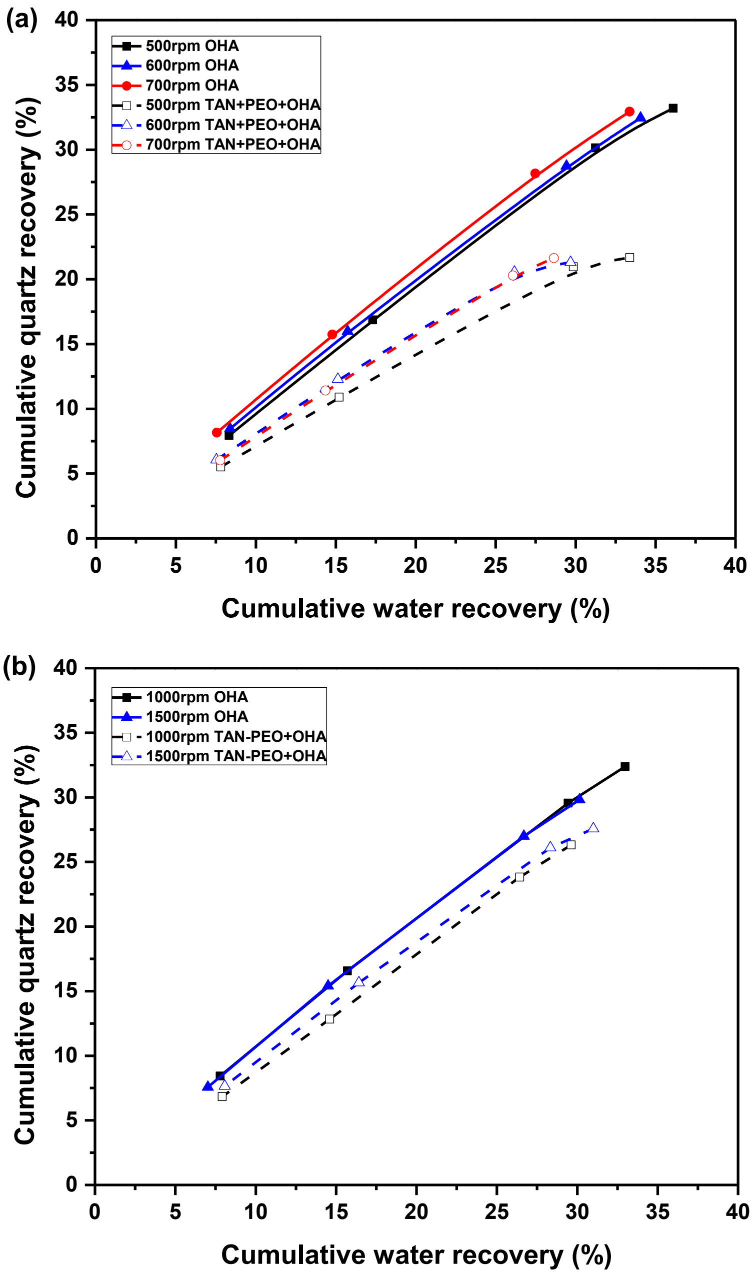

Figure 5.3 Cumulative quartz recovery in the froth as a function of water recovery at low levels of agitation intensities (a) and high levels of agitation intensities (b). The solid lines show the condition with only OHA and the dash lines show the condition where TAN-PEO polymers were used. [TAN] = 80 g/t, [PEO] = 40 g/t, [OHA] = 300 g/t.

Table 5.1 A comparison of entrainment recovery of quartz in the absence and presence of TAN-PEO polymers under different agitation intensities.

	500 rpm (625.4 s^{-1})	600 rpm (857.7 s^{-1})	700 rpm (1260.7 s^{-1})	1000 rpm (1845.4 s^{-1})	1500 rpm (2526.9 s^{-1})
QRZ Entrainment, % (without TAN-PEO)	33.20	32.45	32.94	32.39	29.82
QRZ Entrainment, % (with TAN-PEO)	21.67	21.31	21.63	26.32	27.57
Reduced degree of QRZ Entrainment, %	34.7	34.3	34.3	18.7	7.5

Figure 5.4 shows the effect of conditioning time on quartz recovery using TAN-PEO polymers. This shows the potential influence of energy input by mechanical stirring on flocs property and thus on quartz entrainment. The agitation intensity was kept at 700 rpm (1260.7 s^{-1}). The time referred to the interval from PEO addition till the peristaltic pump began to pump the slurry. It can be seen that over the conditioning time of 2-20 minutes, no significant difference was observed in quartz recovery. This indicated that the flocs generated could withstand the hydrodynamic forces under the investigated agitation intensity. The size distribution of flocs may attain a balanced state and did not vary largely with prolonged conditioning time.

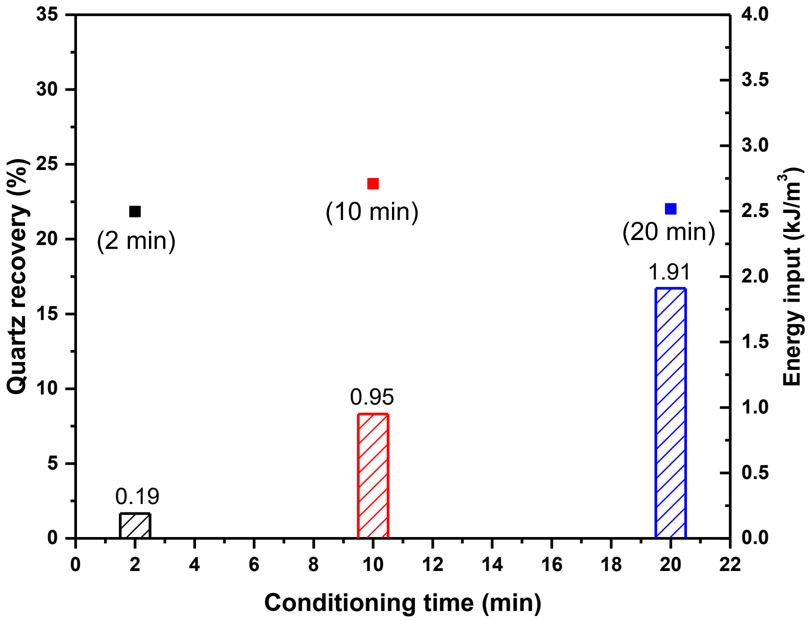

Figure 5.4 Effect of conditioning time with TAN-PEO polymers on quartz entrainment recovery under the agitation intensity of 700 rpm (1260.7 s^{-1}). The bars at the different conditioning time indicate the total energy input in kJ/m^3. [TAN] = 80 g/t, [PEO] = 40 g/t. pH 8.5-9.0.

5.3.2 Column flotation in single hematite system

Figure 5.5 shows the results of cumulative recovery of hematite by OHA as a function of flotation time under two different levels of agitation intensity. In the absence of TAN-PEO polymers, hematite recovery was found to increase with agitation intensity as seen from the solid lines. After 3 min flotation, the highest recovery of hematite was approximately 70% by using 300 g/t OHA. The improved hematite recovery at higher levels of agitation may be partially due to the possible aggregation of fine hematite particles by high shear forces. On the other hand, the frothing property may also contribute to improving hematite recovery to a certain degree, and this claim was made since a stronger frothing capability and more abundant air bubbles were observed within the column when conditioned with high levels of agitation intensity in the tank. When TAN-PEO polymers were present, it can be seen that both flotation rate and flotation recovery increased as shown from the dash lines. The increased hematite recovery seemed to be independent of agitation intensity. For example, almost equivalent increment was obtained at 700 rpm (an increase from 62.4% to 82.5%) compared with that at 1500 rpm (an increase from 67.8% to 88.2%) for the final hematite recoveries. Furthermore, with TAN-PEO polymers the trend still remain that higher agitation intensity was favourable to better recoveries like the situation using only OHA. The beneficial effect of TAN-PEO polymers on hematite recovery was somewhat unexpected due to the concern that the addition of tannic acid would depress hematite flotation by OHA. Previous study has indicated that tannins can be adsorbed onto hematite surface and hinder the function of collectors [34]. However, it was not the case in the present study, likely because a relatively small concentration (80 g/t) of TAN was used or because OHA was a different collector from the one used in [34] and could bond more firmly with hematite surface. Regarding the beneficial effect of hematite recovery by TAN-PEO polymers, there may be several conjectures. One was the possible flocculation of fine hematite by TAN-PEO polymers so that larger flocs may interact with bubbles more efficiently. Another was attributed to the surface active/frothing functions of PEO molecules, which may act collaboratively with OHA as an auxiliary collector/frother for hematite flotation.

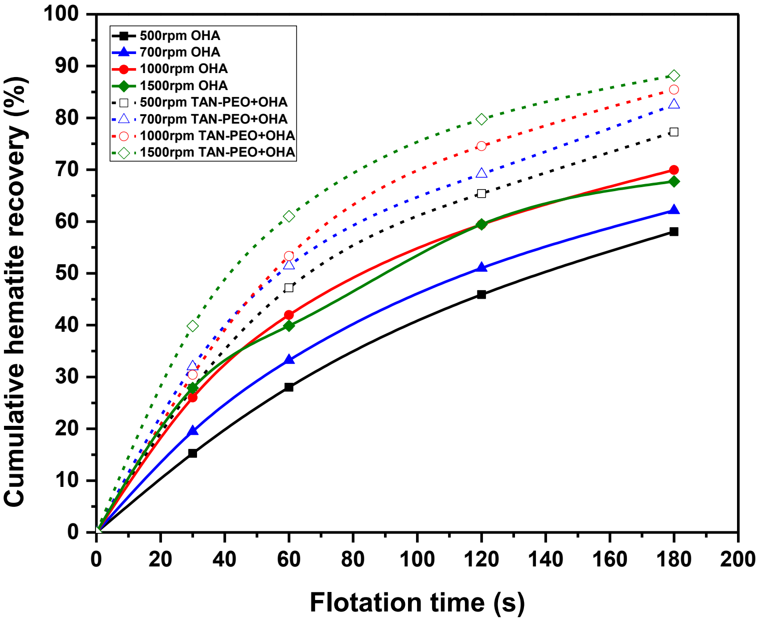

Figure 5.5 Cumulative recovery of hematite by OHA with and without TAN-PEO polymers as a function of flotation time under different agitation intensities. [TAN] = 80 g/t, [PEO] = 40 g/t, [OHA] = 300 g/t.

Figure 5.6 shows stage-wise water recoveries in the process of hematite flotation, corresponding to the experimental conditions in Figure 5.5. As can be seen at a certain agitation intensity (1500 rpm excluded) higher water recovery was found for almost all four intervals in the presence of TAN-PEO polymers (patterned columns), which is more obvious when the slurry was conditioned at lower levels of agitation (500 and 700 rpm). With increased stirring intensity, such as at 1500 rpm, the rheological behavior of slurry or froth may be different from that at lower agitation. That was reflected by a substantially higher amount of froth generated by high shear, and the apparent viscosity of the whole slurry tended to increase since it took a longer time for the peristaltic pump to transfer slurry of the same volume. Given so, the froth velocity became slower in flotation column and resulted in a decrease in water recovery. From the perspective of differences in water recovery, it can be inferred that TAN-PEO polymers may promote entrainment recovery of fine hematite, thus contributing to the total hematite recovery in concentrate. But it was confusing that hematite recovery also increased at 1500 rpm with TAN-PEO polymers despite less water recovery. In addition to the possible shear flocculation, this was more likely related to the viscosity of the slurry of that condition. It has been reported that bubble-particle aggregates tend to be more stable with increasing viscosity of suspending media in flotation [35, 36].

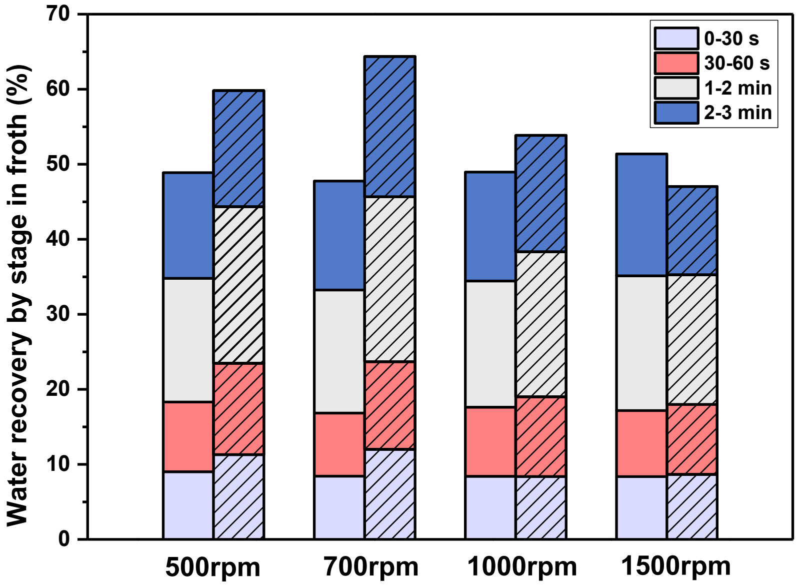

Figure 5.6 Water recovery by stage in hematite flotation by OHA in the absence (non-pattern columns) and presence of TAN-PEO polymers (patterned columns). [TAN] = 80 g/t, [PEO] = 40 g/t, [OHA] = 300 g/t.

Figure 5.7 shows the effect of conditioning time on hematite recovery by OHA under the agitation speed of 1000 rpm. In the presence of only OHA, hematite recovery was found to decrease gradually with conditioning time. As can be seen, when prolonging the conditioning time from 5 minutes to 30 minutes, hematite recovery dropped from 68.9% to 54.4%. This may indicate that no significant aggregation of hematite by OHA occurred in flotation, for shear flocculation usually benefits from long conditioning time [37]. Increasing the conditioning time may affect the adsorption behavior of OHA with hematite and further adversely affect the stability of hematite-bubble aggregates. It was interesting to discover that the adverse effect of conditioning time on hematite recovery seemed to be eliminated by the prior addition of TAN-PEO polymers. Over the 5-30 minutes of conditioning, hematite recoveries remained constant around 80% and did not experience dramatic declines by introducing the TAN-PEO polymers. The underlying reason was unclear but might be resulted from the properties of PEO polymer, as mentioned earlier its surfactant-like function may be helpful for the stability of particle-bubble aggregates in hematite flotation.

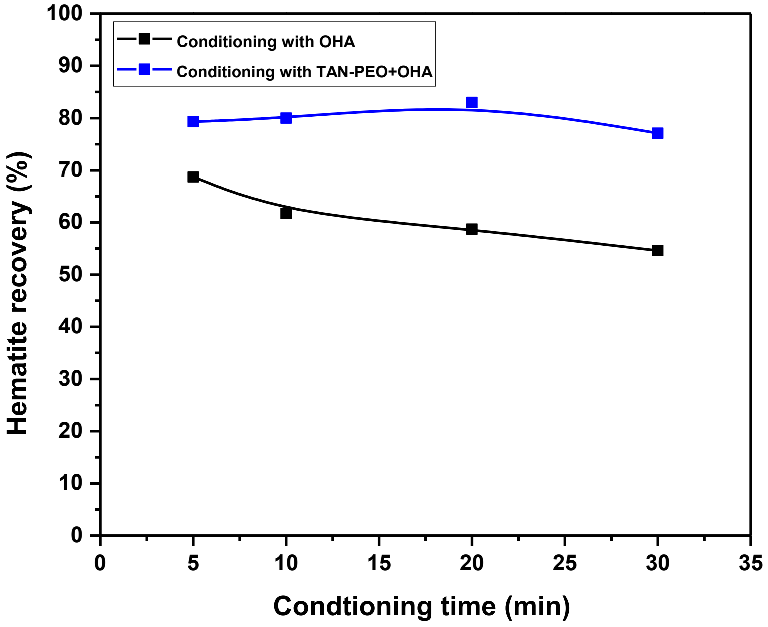

Figure 5.7 Effect of conditioning time on hematite recovery by OHA with or without TAN-PEO polymers under the agitation intensity of 1000 rpm. [TAN] = 80 g/t, [PEO] = 40 g/t, [OHA] = 300 g/t.

5.3.3 Floc size distribution measurement

Aggregation behavior of quartz and hematite particles was measured using FBRM technique. Figure 5.8 shows the floc size distribution of the two minerals as a function of agitation intensity using different chemicals. In Figure 5.8a, measurement with only OHA was conducted for contrast purpose and quartz particles could not be aggregated by OHA. At 500 rpm, after the addition of TAN-PEO polymers, peak of the chord length distribution curve became much broader with a lower percentage of <10 μm particle counts (unweighted), plus a dramatic increase of squared weighted particle counts, indicating that TAN-PEO polymers combination was effective to flocculate fine quartz under that hydrodynamic condition. The conclusion was in agreement with the investigation of chapter 4. With an increase in agitation intensity, peaks of both unweighted and square weighted chord length curves were found to shift from right to left, suggesting that flocs of smaller sizes were formed at high shear rates. For example, when average shear rate was 2526.9 s^{-1} (1500 rpm), the shape and trend of chord length distribution curves almost overlap with that using only OHA. That partially explained why entrainment reduction of quartz was not obvious in flotation at that condition since flocs were intensely broken by excessive shear force. Figure 5.8b indicates the aggregation/dispersion behavior of hematite by TAN-PEO polymers and by OHA. By comparing the chord length distribution curves of pure hematite and hematite with TAN-PEO polymers, it can be seen that hematite was very weakly flocculated by the two polymers, if any. This was because PEO molecules cannot adsorb at hematite surface as has been revealed in the literature [38, 39]. It seems that the presence of TAN together with PEO did not change the flocculation property of hematite by PEO, which provided the potential selective separation window for hematite-quartz mixtures. On the other hand, only weak aggregation of hematite particles by OHA at higher agitation intensity was observed, indicated by increased peaks of square weighted counts of chord length distribution curve (dash line in Figure 5.8b). The FBRM results ruled out the possibility that improved hematite recovery by OHA at high levels of agitation was mainly by shear flocculation. This may be due to that OHA has a short hydrocarbon chain and could not provide sufficient surface hydrophobicity with the dosage (300 g/t) used in present study.

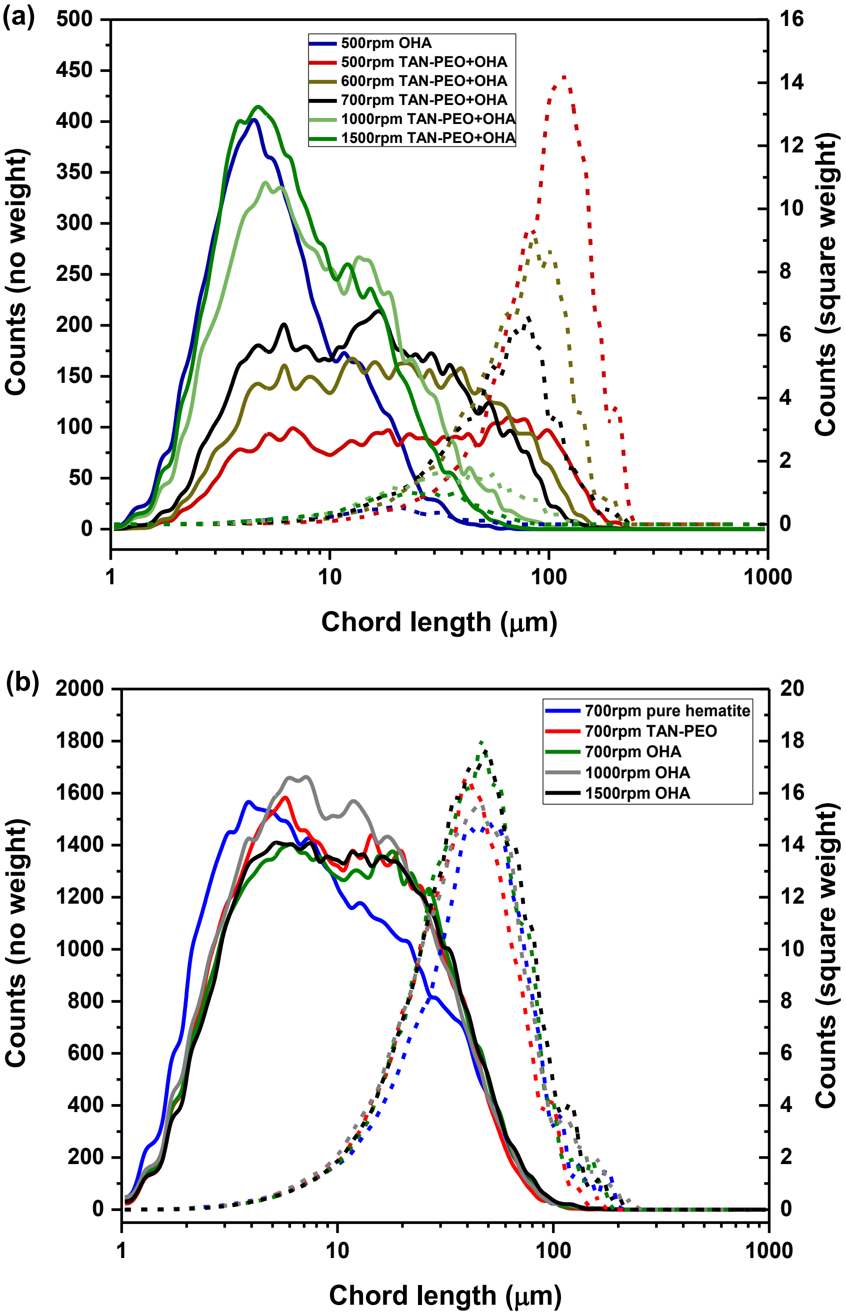

Figure 5.8 (a) Chord length distribution of quartz with TAN-PEO polymers under different agitation intensities; (b) Chord length distribution of hematite with OHA or TAN-PEO polymers under different agitation densities. Solid lines represent unweighted counts and dot lines represent square weighted counts. [TAN] = 80 g/t, [PEO] = 40 g/t, [OHA] = 300 g/t.

Table 5.2 shows the average floc size (unweighted and square weighted) of quartz in FBRM measurement under various conditions. The values were obtained at the equilibrium state of flocculation. It is clear to see that large flocs were formed under low levels of agitation intensities, with the square weighted mean floc size above 60 μm. At high levels of agitation, mean floc size began to decrease below 50 μm. Since FBRM measurement shared the same procedure and experimental conditions as column flotation, it was therefore logical to claim that measured floc size distribution and average floc size can reflect the flocculation status within the flotation column. As such it might be possible to establish a correlation between the floc size of hydrophilic fine particles and their degree of entrainment when polymers are used for entrainment reduction purpose. Figure 5.9 shows the reduced degree of quartz entrainment as a function of mean floc size in column flotation when TAN-PEO polymers were used. As can be seen, quartz entrainment was reduced more with larger floc size between an approximate range from 26 to 68 μm. Beyond that range, a further increase of floc size from 68 to 108 μm did not cause an extra reduction of quartz entrainment. It suggested that very large flocs (hundreds of microns) are not necessary when polymeric flocculation is used in flotation. In fact, raw materials used for beneficiation flotation usually contain complicated mineral components, and excessively large polymer flocs are detrimental to the selectivity of flotation as they tend to trap hydrophobic particles [40]. From Figure 5.9 it can also observe that reduced degree of quartz entrainment showed a linear relationship with mean floc size when they were less than 68 μm. Linear regression analysis was performed on the data to obtain the fitted curve as shown by the blue line. It can be seen that the two variables had good linear correlation, and the fitted line intersected the mean floc size at 13.5 μm when reduced quartz entrainment was zero. This indicated that polymeric flocculation would not take effect in reducing quartz entrainment when floc size was smaller than 13.5 μm for the present investigation. Considering that the quartz sample used for flotation was mostly smaller than 15 μm, the discovery was consistent since effective polymer flocculation would have barely occurred if the mean floc size was less than 13.5 μm. The above analyses suggest that if polymers are used to flocculate hydrophilic particles, too small or too large flocs would not benefit the optimal entrainment reduction/elimination and flotation selectivity for fine and ultrafine flotation. Therefore, it requires delicate adjustment of agitation intensity for slurry conditioning to control the floc size in an appropriate range, maximizing the efficiency of polymers. Furthermore, the correlation between the agitation intensity, mean floc size, and entrainment reduction is unlikely to be identical and would vary according to different mineral/polymer systems under different flotation conditions.

Table 5.2 Average floc size (unweighted and square weighted) of quartz at equilibrium by TAN-PEO-OHA under various agitation intensities. [TAN] = 80 g/t, [PEO] = 40 g/t, [OHA] = 300 g/t.

Impeller speed (rpm)	Average shear rate (G, s^{-1})	Chemical conditions	Mean size, μm (no weight)	Mean size, μm (square weight)
500	652.4	OHA	7.38	19.94
500	652.4	TAN-PEO-OHA	37.45	107.97
600	857.7	TAN-PEO-OHA	25.93	80.39
700	1260.7	TAN-PEO-OHA	21.99	68.27
1000	1854.4	TAN-PEO-OHA	12.08	42.04
1500	2526.9	TAN-PEO-OHA	9.28	26.09

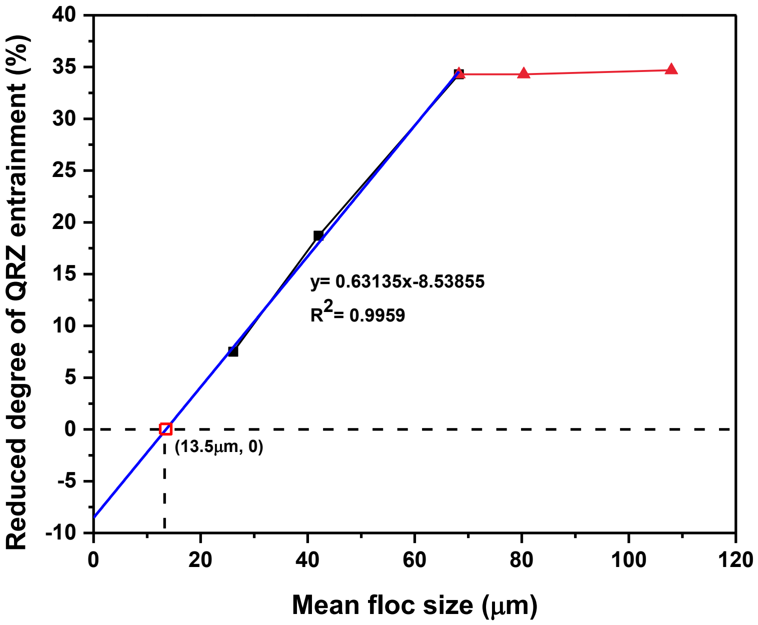

Figure 5.9 Reduced degree of quartz entrainment as a function of mean floc size (square weight) using TAN-PEO polymers in flotation column. [TAN] = 80 g/t, [PEO] = 40 g/t, [OHA] = 300 g/t.

5.3.4 Surface tension measurement

In the single flotation system of quartz and hematite, it was observed that frothing property was different in cases with or without TAN-PEO polymers. This may arise from the chemical environment changes that polymers bring, especially PEO. Herein surface tension was measured at the air/water interface to investigate the surface active properties of the single polymer or their combinations as shown in Figure 5.10. For pure PEO solution, it was observed that surface tension decreased dramatically with PEO concentration. The surface tension was reduced to 62.97 mN/m when the PEO concentration was 15 mg/L, which may be close to the critical micelle concentration because the surface tension could be barely changed by further increasing PEO concentration. The result indicated that PEO had a strong function of surface activity, which was in part due to the hydrophobic chains. Literature research has also revealed that the component (CH_2CH_2) in the PEO structure is sufficiently hydrophobic to form a spreading monolayer adsorption at the air/water interface [41]. Consequently, PEO in the flotation system could function like a frothing reagent apart from its flocculating capability, resulting in more air bubbles generated and reduced possibility of bubble coalescence [24]. It also explained the phenomena in previous research that PEO of a higher dosage caused high water recovery and adversely affect the entrainment of hydrophilic particles in flotation [23, 42]. Figure 5.10a shows that the surface tension of tannic acid aqueous solutions did not vary with concentration and remained steady between 72-73 mN/m, the value is similar to the surface tension of pure water, suggesting that TAN was not surface active. When combining the PEO with TAN at a mass ratio of 1:1 in aqueous solutions, it can be seen that surface tension increased at certain concentrations of PEO. For example, the value of surface tension rose from 63.48 to 66.51 mN/m for 10 mg/L PEO in the presence of TAN. This implied that TAN was able to interfere with the surface activity of PEO. The underlying reason may be related to the complex interaction between the two polymers. It is well known that hydrogen bonding interaction between PEO and water molecules is responsible for PEO solubility in water. Macromolecules of TAN can compete with water molecules and interact with PEO, as a result, there would be less PEO molecules adsorbed at the air/water interface. It means that in flotation system the surface activity of PEO was weakened by TAN and thus the decreased frothing capability and water recovery. On the other hand, TAN could assist to obtain a more robust floc structure of quartz via the formation of associative complexes with PEO and then complex bridging, as shown in the previous chapter. In contrast, the circumstance was different for the hematite flotation. In that case, the pre-added TAN will firstly adsorb on the hematite surface, the process of which can consume part of TAN hydroxyl groups to form Fe-O bonds [34], resulting in less of them available to complex with PEO. Therefore, more free PEO molecules in the slurry may increase the frothing property and contribute to hematite recovery by OHA.

Figure 5.10b shows the surface tension of OHA solutions in the absence and presence of PEO or TAN-PEO polymers. As a surfactant, the surface tension of pure OHA solutions decreased consistently with increasing concentration, however, no micelle formation was observed until 500 mg/L OHA, which was likely due to the electrostatic repulsion between ionic groups of OHA molecules under alkaline solutions [43]. In the presence of 5 mg/L PEO, it can be seen that the surface tension decreased, especially at lower OHA concentrations (≤ 100 mg/L). Compared with the surface tension value of a single 5 mg/L PEO solution (indicated by the dash line in Fig. 5.10b), it may be inferred that PEO can work synergistically with OHA to bring an additional reduction of surface activity. In the present investigation, 300 g/t OHA (about 23 mg/L) was used in column flotation. OHA of that dosage may have limited surface active function and PEO could dominantly influence the frothing properties as a whole. Additionally, when both 5 mg/L TAN and PEO were present, the surface tension can find a slight increase for OHA solutions within the range of 50 mg/L. This indicated the disturbing effect of tannic acid on the whole system.

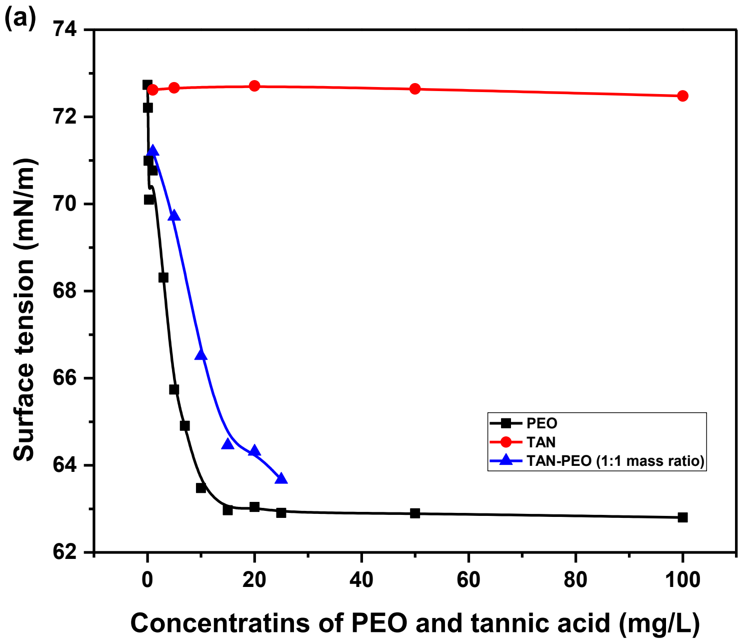

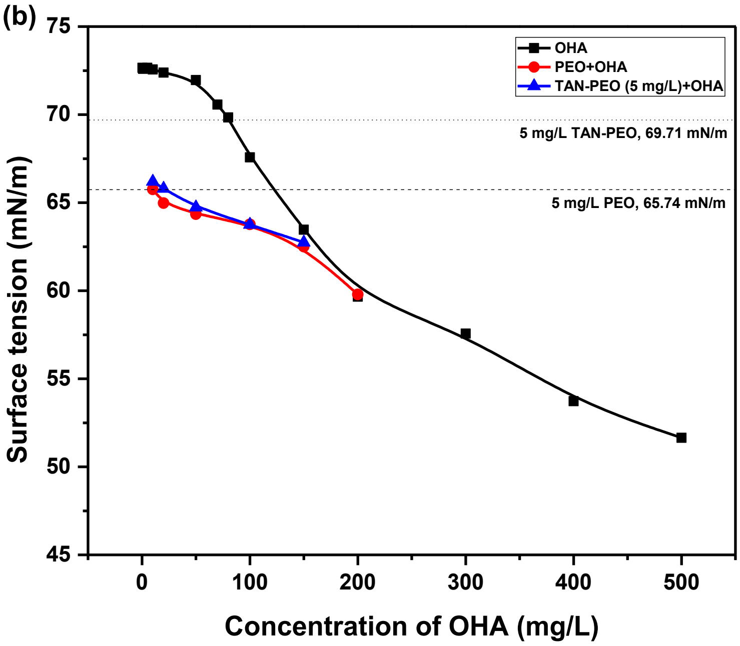

Figure 5.10 (a) Surface tension of PEO, tannic acid, and TAN-PEO at different concentrations; (b) surface tension of OHA with and without PEO (5 mg/L) at different concentrations. The dash line and dot line were drawn indicating surface tension values of 5 mg/L PEO and 5 mg/L TAN-PEO (1:1 mass ratio), respectively, to guide comparison.

5.3.5 Measurement of foam height and decay time

Foaming property under different chemical conditions was investigated by measuring the height and decay time of the foam layer at a fixed aeration rate (0.2 L/min). Here the decay time referred to the time since aeration was stopped, foam collapsed, until the liquid surface began to appear, and a longer decay time suggests better foam stability. Figure 5.11a illustrates the foamability observation in a two-phase (water/air) system and Figure 5.11b shows the corresponding foam height and decay time. As can be seen, PEO could act as a good foam reagent and generated abundant foam, which was about 120 mm in height at a concentration of 10 mg/L. The behavior was consistent with surface tension measurement that revealed the strong surface activity of PEO at that concentration. Given so, PEO used alone in flotation may bring more water upward to the froth phase. In contrast, OHA formed only small-volume foam with the least foam height (<10 mm) at 50 mg/L. However, foamability was dramatically increased in the presence of both PEO and OHA, indicating that they can work together to facilitate foam stability as reflected by the longest foam decay time (about 55 s). Indeed, it has been reported that polyglycol ether type of frother was efficient to prevent bubble coalescence and generate more stable and viscous foams [44]. Besides, the introduction of tannic acid seemed to deteriorate the foam structure and stability of PEO and PEO-OHA systems. From Figure 5.11a it can be seen that the foam height of TAN-PEO solution was reduced compared with pure PEO solution. Further, the foam stability was weakened and foam decayed much faster. Unlike the relatively uniform and compact foam structure in the PEO solution, there appeared to be large cavities in the foam layer for TAN-PEO system. This proved that the addition of TAN can partially decrease the surface activity of PEO, which agreed well with surface tension results. A similar phenomenon was observed for the TAN-PEO-OHA system, although the foam tended to grow higher it had an unstable structure and broke quickly. It was also noted that the foam might be more viscous in the presence of TAN since the broken residual foam could stick to the column wall for a long time. The investigation of foaming property was performed in the two-phase system that did not contain mineral solids. Results of the current investigation may not perfectly explain the observations in column flotation due to the differences between foam property and frothing property, and the latter is largely affected by particle amount and particle surface nature [45].

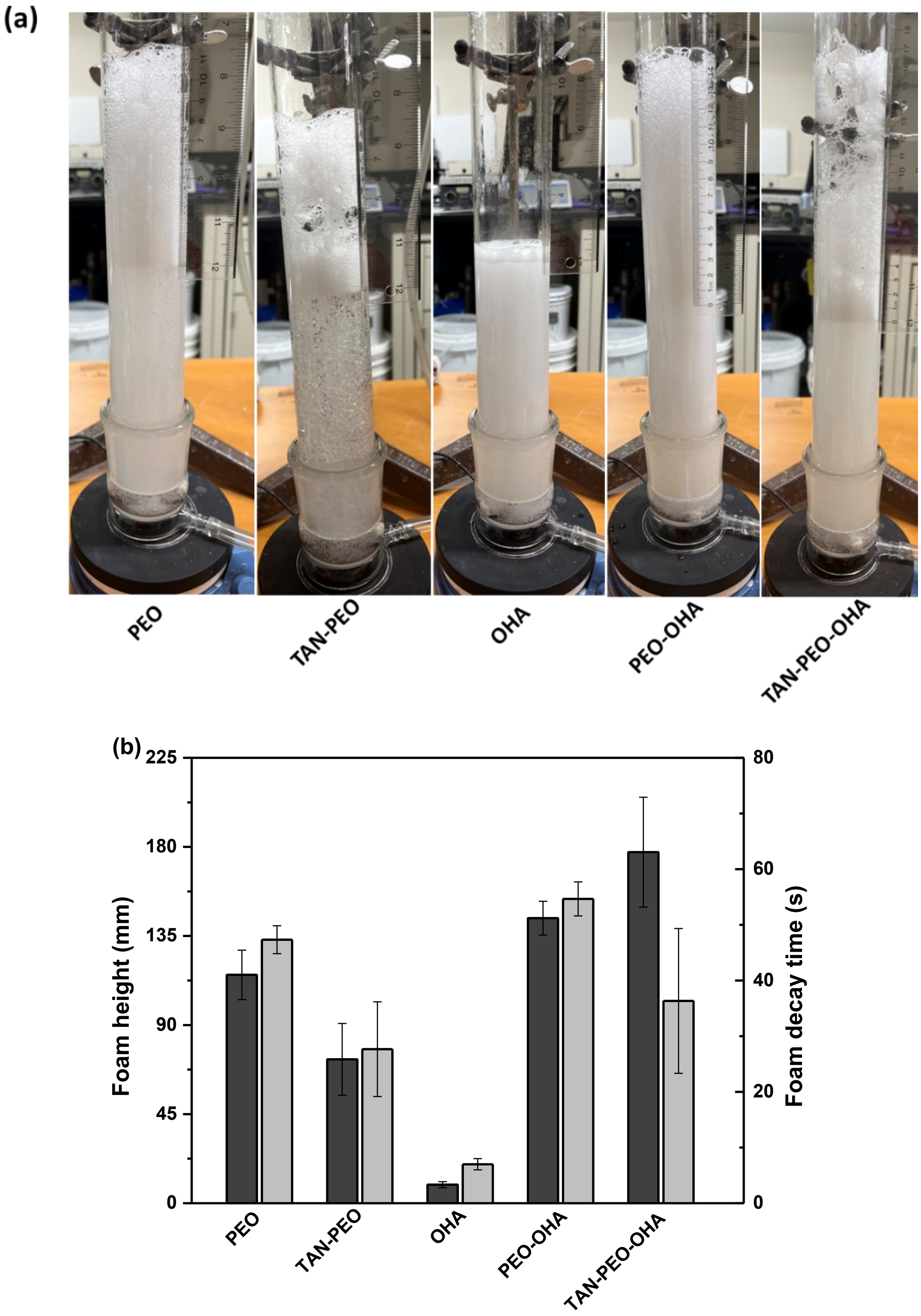
(a)
PEO
TAN-PEO
OHA
PEO-OHA
TAN-PEO-OHA
(b)
Foam height (mm)
0
45
90
135
180
225
Foam decay time (s)
0
20
40
60
80
PEO
TAN-PEO
OHA
PEO-OHA
TAN-PEO-OHA

Figure 5.11 (a) Illustration of foamability in flotation column under different chemical conditions; (b) corresponding foam height (black column) and decay time (gray column). [OHA]=50 mg/L, [PEO]=10 mg/L, [TAN]=10 mg/L.

5.3.6 Bubble size measurement

Differences in foam structures of foamability investigation motivated us to further study the bubble size under the above various chemical conditions. It was also carried out in air-water phases employing the FBRM probe. Figure 5.12a indicated that the mean bubble size in pure water was generally large and it fluctuate widely in a range between 90 and 140 μm. As a surface-active compound, PEO assisted to generate smaller bubbles, with the mean bubble size between 60 and 90 μm. This was similar to the function of frother a proper dosage of which can reduce the bubble size and hinder bubble coalescence. There were indeed reports regarding the application of PEO as a frother in flotation [25, 46]. It was also found that mean bubble size increased for PEO coupled with TAN, likely due to the decreased surface activity and improved bubble coalescence. The measurement in part corresponded to the foam structure observed in Figure 5.11a. Results in Figure 5.12b indicate that smaller bubbles (55-70 μm) were generated with both PEO and OHA. Moreover, PEO was found to enable the bubbles to fluctuate in a less narrow range working together with OHA, suggesting the stabilization effect on the air-liquid interface by the two chemicals. Based on that, the addition of TAN increased the mean bubble size slightly, which was similar to the results of the surface tension test.

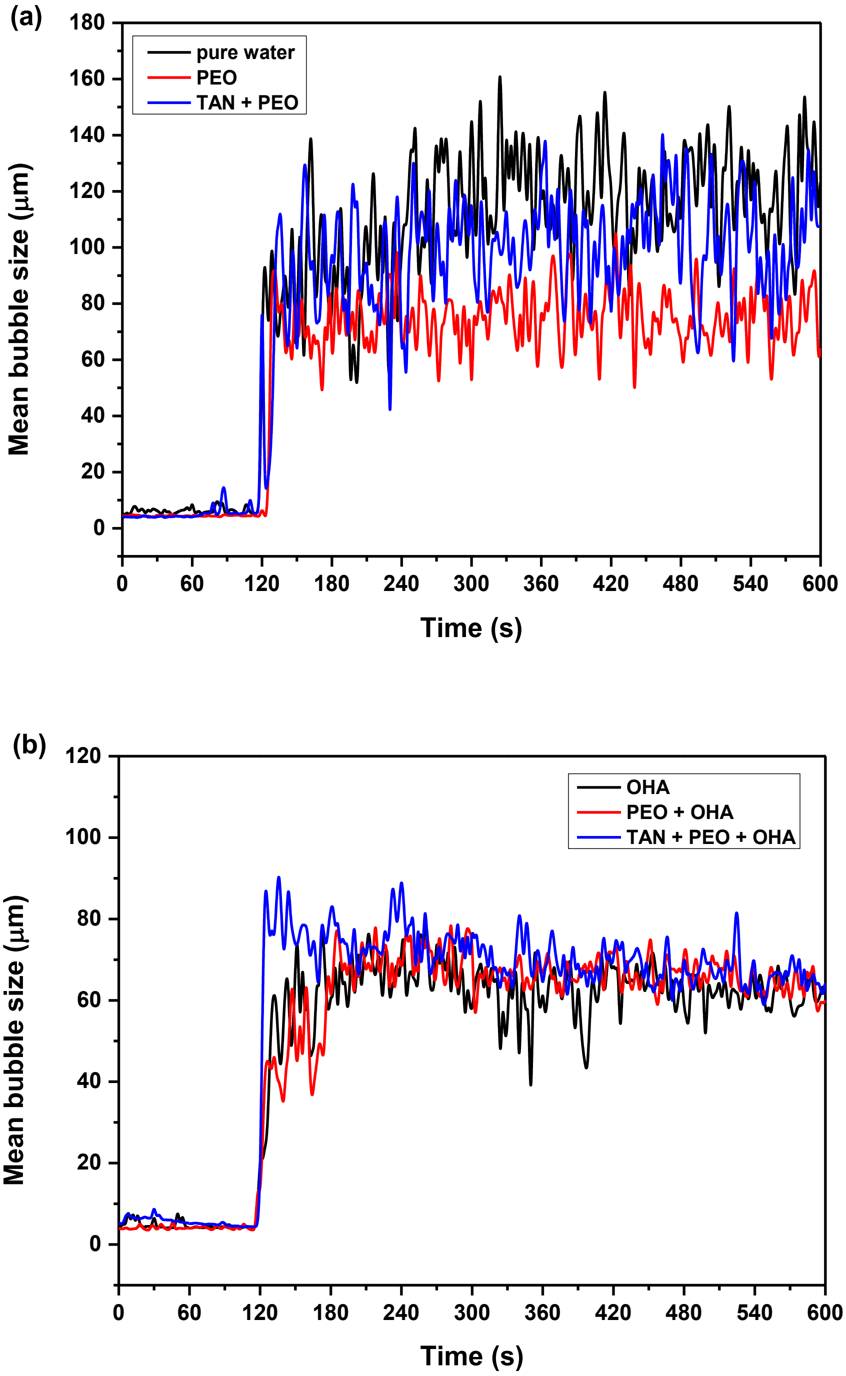

Figure 5.12 (a) and (b) Mean bubble size in air-water phases under different chemical conditions.

5.3.7 Column flotation separation of synthetic mixtures of hematite and quartz

Separation of synthetic mineral mixtures (50 g hematite and 50 g quartz) by column flotation was carried out in two series. In the first series, hematite and quartz were mixed and conditioned in the stirred tank sequentially with OHA and TAN-PEO, and then pumped into the column for flotation separation. In the second series, quartz was separately aggregated by TAN-PEO polymers in the column, and hematite was conditioned in the tank with OHA. After conditioning, the hematite slurry was pumped into the column to mix with the quartz slurry followed by flotation separation. The series two was designed to reduce the adsorption of TAN on hematite so that it can work with PEO to flocculate quartz, and also minimize the hetero-aggregation of hematite and quartz. Figure 5.13 shows the results of the two series, with the cumulative Fe and SiO_2 recoveries versus water recovery (Fig. 5.13a) and grade-recovery curves of Fe in the concentrate (Fig. 5.13b). As can be seen, in series one (solid lines), the separation efficiency of hematite-quartz mixtures was improved slightly with TAN-PEO polymers added together after OHA, with higher Fe recovery and grade especially in the first minute of flotation. In series two, the flotation concentrate had higher mass pulls and hematite recovery under the same conditions compared with tests in series one. Moreover, the quartz entrainment was reduced more efficiently by TAN-PEO polymers and comparatively better separation efficiency was achieved, reflected by the grade-recovery curve (red dash line) moving further upwards in Fig. 5.13b.

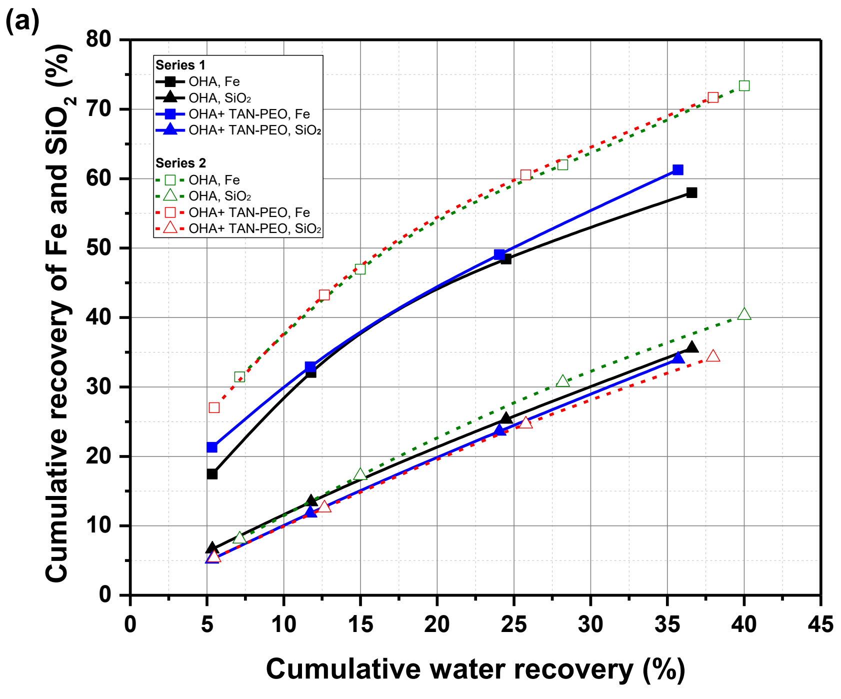

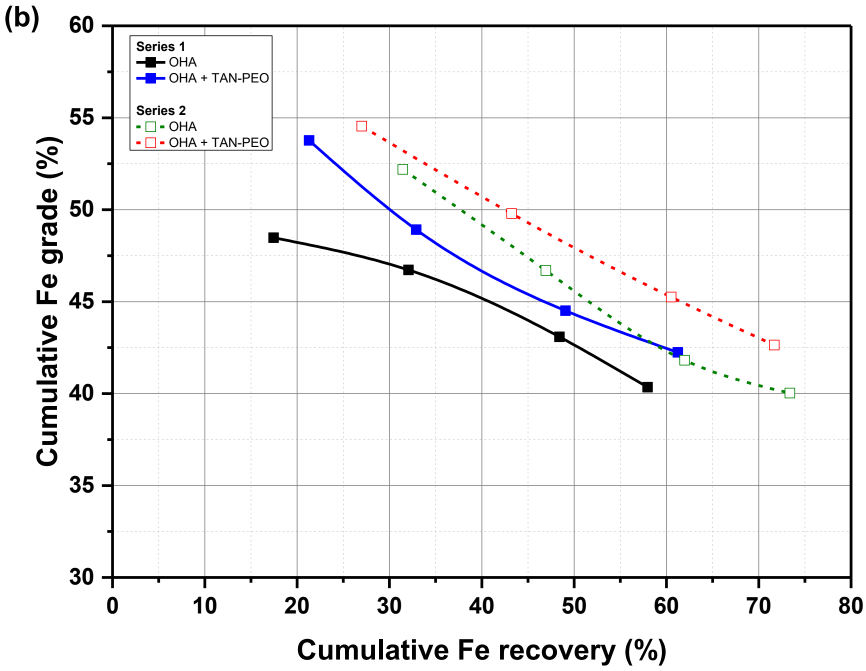

Figure 5.13 (a) Cumulative recovery of Fe and SiO_2 as a function of water recovery; (b) grade-recovery curves of cumulative Fe in the concentrate. [TAN] = 80 g/t, [PEO] = 40 g/t, [OHA] = 300 g/t.

The series two aggregation-flotation tests were designed to demonstrate the effects of the separate hydrophobic and hydrophilic aggregation on the subsequent flotation separation. In practice, series one was closer to reality. The results showed that the beneficial effects of two-stage aggregation did exist, but they need to be capitalized by careful control and adjustment of process conditions such as reagent addition sequences, dosages, and so on.

5.4 Conclusions

The present work investigated the flotation performance of fine and ultrafine hematite and quartz mineral system in a flotation column. Direct flotation route was applied to float hematite using n-octyl hydroxamic acid (OHA) as a collector. A combined polymer system containing tannic acid (TAN) and poly(ethylene oxide) (PEO) was used to flocculate quartz particles to reduce their entrainment. In particular, the effects of agitation intensity and foaming property of the reagents on floc size distribution, entrainment degree, and flotation kinetics/recovery were revealed for quartz and hematite flotation. The main observations and conclusions were summarized as follows.

(1) Flocculating quartz by TAN-PEO polymer system to form hydrophilic flocs was effective to reduce the mechanical entrainment of quartz. The reduced degree of quartz entrainment was dependent on agitation intensity applied for slurry conditioning. FBRM measurements indicated the formation of large flocs (> 68 μm) within the column at low levels of agitation intensities, which lowered the percentage of quartz that entrained into the froth. However, at high levels of agitation intensities, smaller-sized flocs (< 50 μm) were formed which resulted in a lower degree of quartz entrainment reduction. Under current experimental conditions, a linear correlation was established between mean floc size and the degree of entrainment reduction when the average size of quartz flocs was less than 68 μm.

(2) Increasing the agitation intensity can improve the flotation recovery of hematite by OHA. The addition of TAN-PEO polymers enhanced both flotation kinetics and recovery for hematite flotation, with an approximate 20% increase in overall hematite recovery using OHA. The hematite recovery was found to decrease with prolonged conditioning time with OHA, whereas the decreasing trend was eliminated when TAN-PEO polymers were added. FBRM measurement proved that TAN-PEO polymers had limited flocculation selectivity towards hematite particles. Higher water recoveries were observed in the presence of TAN-PEO polymers, especially with low levels of agitation intensity, therefore, the increased recovery of hematite in single hematite flotation was likely due to the frothing property changes brought by PEO, i.e., by entrainment.

(3) Surface tension measurement confirmed that PEO had strong surface activity, and it can work together with OHA to gain a further decrease in the surface tension of water. Tannic acid did not show surface activity, but it could increase the surface tension of PEO solutions,

i.e., decreasing PEO's surface activity. Foaming property investigation in water/air phases indicated that PEO had good foamability and it could function synergistically with OHA to improve the foam stability. It was also found that TAN could destroy the foamability and foam structures of PEO and PEO-OHA systems to a certain degree. The bubble size measurement suggested that bubbles generated with PEO or PEO-OHA had smaller mean bubble size, while the introduction of TAN can increase the mean bubble size.

(4) Batch flotation of synthetic mineral mixtures indicated that the addition of TAN-PEO polymers together following OHA benefited the separation of fine hematite and quartz, and the beneficial effect in separation efficiency was more pronounced when the quartz was separately pre-aggregated within the column to minimize the possible interactions between hematite and tannic acid.

The current study has indicated the potential flocculation selectivity of TAN-PEO polymer system in the hematite/quartz mineral system. It provides an opportunity to better manage the mechanical entrainment of flocculating ultrafine hydrophilic particles and a window for more efficient separation of fine hematite and quartz by direct flotation. In addition, when coupled with results reported in the previous chapter, this work also revealed that tannic acid had dual functions when added together with PEO. It not only can improve the flocculation property of quartz by PEO and help to obtain robust flocs, but also weaken the surface activity and foaming stability of PEO, both of which are advantageous to reduce the entrainment recovery of quartz. Lastly, the correlations between agitation intensity, mean floc size, and degree of entrainment of hydrophilic particles were established when polymeric flocculation is applied in the two-stage aggregation flotation process. Neither the absence of polymer flocculation nor the generation of large polymer flocs of hydrophilic particles was beneficial to lower the entrainment of the hydrophilic particles and improve flotation efficiency. To our knowledge, this has rarely been reported in the literature. Results in this work revealed the relationship among them and inspired that the hydrodynamic conditions can be manipulated to control polymer flocculation and floc size evolution to go along with the proposed concept of two-stage aggregation flotation strategy.

5.5 References

[1] W. Trahar, A rational interpretation of the role of particle size in flotation, International Journal of Mineral Processing 8 (1981) 289-327.

[2] D. Wang, Q. Liu, Influence of aggregation/dispersion state of hydrophilic particles on their entrainment in fine mineral particle flotation, Minerals Engineering 166 (2021) 106835.

[3] S. Liao, L. Ou, Flocs Properties and Flotation Performance of Fine Diaspore with Energy Input Pretreatment Induced Using Sodium Oleate, Minerals 9 (2019) 433.

[4] Y. Hu, G. Qiu, J. Miller, Hydrodynamic interactions between particles in aggregation and flotation, International journal of mineral processing 70 (2003) 157-170.

[5] B. Oyegbile, P. Ay, S. Narra, Flocculation kinetics and hydrodynamic interactions in natural and engineered flow systems: A review, Environmental Engineering Research 21 (2016) 1-14.

[6] S.-x. Song, A. Lopez-Valdivieso, J. Reyes-Bahena, C. Lara-Valenzuela, Floc flotation of galena and sphalerite fines, Minerals Engineering 14 (2001) 87-98.

[7] W. Chen, Q. Feng, G. Zhang, L. Li, S. Jin, Effect of energy input on flocculation process and flotation performance of fine scheelite using sodium oleate, Minerals Engineering 112 (2017) 27-35.

[8] S. Zou, X. Ma, S. Wang, H. Zhong, W. Qin, Flotation of rhodochrosite fines induced by octyl hydroxamic acid as hydrophobic agglomerates, Powder Technology 392 (2021) 108-115.

[9] D. Bache, Floc rupture and turbulence: a framework for analysis, Chemical Engineering Science 59 (2004) 2521-2534.

[10] L. Liang, J. Tan, B. Li, G. Xie, Reducing quartz entrainment in fine coal flotation by polyaluminum chloride, Fuel 235 (2019) 150-157.

[11] J. Gong, Y. Peng, A. Bouajila, M. Ourriban, A. Yeung, Q. Liu, Reducing quartz gangue entrainment in sulphide ore flotation by high molecular weight polyethylene oxide, International Journal of Mineral Processing 97 (2010) 44-51.

[12] M. Lapointe, B. Barbeau, Dual starch–polyacrylamide polymer system for improved flocculation, Water research 124 (2017) 202-209.

[13] J. Gregory, S. Barany, Adsorption and flocculation by polymers and polymer mixtures, Advances in colloid and interface science 169 (2011) 1-12.

[14] A. Cervantes-Martínez, A. Maldonado, Foaming behaviour of polymer–surfactant solutions, Journal of Physics: Condensed Matter 19 (2007) 246101.

[15] R. Petkova, S. Tcholakova, N. Denkov, Foaming and foam stability for mixed polymer–surfactant solutions: effects of surfactant type and polymer charge, Langmuir 28 (2012) 4996-5009.

[16] L. Filippov, V. Severov, I. Filippova, An overview of the beneficiation of iron ores via reverse cationic flotation, International journal of mineral processing 127 (2014) 62-69.

[17] X. Zhang, X. Gu, Y. Han, N. Parra-Álvarez, V. Claremboux, S. Kawatra, Flotation of iron ores: A review, Mineral processing and extractive metallurgy review 42 (2021) 184-212.

[18] S. Assis, L. Montenegro, A. Peres, Utilisation of hydroxamates in minerals froth flotation, Minerals engineering 9 (1996) 103-114.

[19] M. Liu, H. Li, T. Jiang, Q. Liu, Flotation of coarse and fine pyrochlore using octyl hydroxamic acid and sodium oleate, Minerals Engineering 132 (2019) 191-201.

[20] M. Fuerstenau, R. Harper, J. Miller, Hydroxamate vs fatty-acid flotation of iron oxide, TRANS SOC MINING ENG AIME 247 (1970) 69-73.

[21] H. Li, M. Liu, Q. Liu, The effect of non-polar oil on fine hematite flocculation and flotation using sodium oleate or hydroxamic acids as a collector, Minerals Engineering 119 (2018) 105-115.

[22] H. Li, M. Liu, Q. Liu, Oil-assisted flotation of fine hematite using sodium oleate or hydroxamic acids as a collector, Physicochemical Problems of Mineral Processing 54 (2018).

[23] J. Gong, The role of high molecular weight polyethylene oxide in reducing quartz gangue entrainment in chalcopyrite flotation by xanthate collectors, (2011).

[24] D. Liu, Y. Peng, Foaming and aggregation behaviours of polyethylene oxide and polyacrylamide in inhibiting mechanical entrainment of kaolinite in flotation using saline water, Journal of Molecular Liquids 359 (2022) 119299.

[25] R. Pugh, Non-ionic polyethylene oxide frothers in graphite flotation, Minerals Engineering 13 (2000) 151-162.

[26] J. Israelachvili, The different faces of poly (ethylene glycol), Proceedings of the National Academy of Sciences 94 (1997) 8378-8379.

[27] M.C. Pirrung, J.H.-L. Chau, A convenient procedure for the preparation of amino acid hydroxamates from esters, The Journal of Organic Chemistry 60 (1995) 8084-8085.

[28] X. Ni, Q. Liu, The adsorption and configuration of octyl hydroxamic acid on pyrochlore and calcite, Colloids and Surfaces A: Physicochemical and Engineering Aspects 411 (2012) 80-86.

[29] D. Wang, Q. Liu, Hydrodynamics of froth flotation and its effects on fine and ultrafine mineral particle flotation: A literature review, Minerals Engineering 173 (2021) 107220.

[30] S. Neethling, J. Cilliers, The entrainment factor in froth flotation: Model for particle size and other operating parameter effects, International Journal of Mineral Processing 93 (2009) 141-148.

[31] Z. Konopacka, J. Drzymala, Types of particles recovery—water recovery entrainment plots useful in flotation research, Adsorption 16 (2010) 313-320.

[32] C. Marion, A. Jordens, R. Li, M. Rudolph, K.E. Waters, An evaluation of hydroxamate collectors for malachite flotation, Separation and Purification Technology 183 (2017) 258-269.

[33] F. Li, X. Zhou, G. Zhao, R. Lin, A novel decyl-salicyl hydroxamic acid flotation collector: Its synthesis and flotation separation of malachite against quartz, Powder Technology 374 (2020) 522-526.

[34] A. Tohry, R. Dehghan, L. de Salles Leal Filho, S.C. Chelgani, Tannin: An eco-friendly depressant for the green flotation separation of hematite from quartz, Minerals Engineering 168 (2021) 106917.

[35] S. Farrokhpay, I. Ametov, S. Grano, Improving the recovery of low grade coarse composite particles in porphyry copper ores, Advanced Powder Technology 22 (2011) 464-470.

[36] D. Xu, I. Ametov, S. Grano, Detachment of coarse particles from oscillating bubbles—The effect of particle contact angle, shape and medium viscosity, International Journal of Mineral Processing 101 (2011) 50-57.

[37] S. Bilgen, B. Wills, Shear flocculation—A review, Minerals Engineering 4 (1991) 483-487.

[38] S. Mathur, B.M. Moudgil, Adsorption mechanism (s) of poly (ethylene oxide) on oxide surfaces, Journal of colloid and interface science 196 (1997) 92-98.

[39] E. Koksal, R. Ramachandran, P. Somasundaran, C. Maltesh, Flocculation of oxides using polyethylene oxide, Powder technology 62 (1990) 253-259.

[40] K. Ding, J. Laskowski, Effect of conditioning on selective flocculation with polyacrylamide in the coal reverse flotation, Mineral Processing and Extractive Metallurgy 116 (2007) 108-114.

[41] M. WonáKim, Molecular weight dependence of the surface tension of aqueous poly (ethylene oxide) solutions, Faraday Discussions 98 (1994) 245-252.

[42] D. Liu, Y. Peng, Reducing the entrainment of clay minerals in flotation using tap and saline water, Powder Technology 253 (2014) 216-222.

[43] F.K.G. Santos, E.L.B. Neto, M.C.P. Moura, T.N.C. Dantas, A.A.D. Neto, Molecular behavior of ionic and nonionic surfactants in saline medium, Colloids and Surfaces A: Physicochemical and Engineering Aspects 333 (2009) 156-162.

[44] I. Solomentseva, S. Bárány, J. Gregory, The effect of mixing on stability and break-up of aggregates formed from aluminum sulfate hydrolysis products, Colloids and Surfaces A: Physicochemical and Engineering Aspects 298 (2007) 34-41.

[45] S. Farrokhpay, The significance of froth stability in mineral flotation—A review, Advances in colloid and interface science 166 (2011) 1-7.

[46] E. Manev, R. Pugh, Frother/collector interactions in thin froth films and flotation, Colloids and Surfaces A: Physicochemical and Engineering Aspects 70 (1993) 289-295.

CHAPTER 6 Conclusions and Future Work

6.1 Summary and conclusions

Froth flotation is the most important technique to recover and separate fine and ultrafine minerals in mineral processing. When the particle size decreases to a certain limit (e.g., less than 20 μm for most minerals), however, the flotation process deteriorates rapidly in both value recovery efficiency and separation selectivity. Slow flotation kinetics of fine hydrophobic particles and high mechanical entrainment of fine gangue hydrophilic particles are two major problems in fine and ultrafine flotation. Current research and development effort mostly focuses on how to optimize the particle-bubble interaction of fine hydrophobic particles and promote their recovery. Much less attention has been paid to studying the behaviors of fine hydrophilic gangue particles to better manage their entrainment issues. In view of the two problems, this dissertation proposed the concept of a two-stage aggregation flotation strategy, aiming to improve the flotation efficiency and selectivity for fine and ultrafine minerals. Briefly, the strategy attempts to find appropriate methods and separately aggregate hydrophobic and hydrophilic particles, ideally forming both hydrophobic and hydrophilic aggregates in the slurry, then the typical flotation procedure can be used to separate them. Due to the substantial amount of study reported in the literature on aggregation of hydrophobic particles in flotation (e.g., shear flocculation, agglomeration flotation, carrier flotation, etc.), a significant effort in this dissertation was made to investigate the aggregation of ultrafine hydrophilic particles and their entrainment, in combination with hydrophobic flocculation.

In the present work, hematite and quartz of high purity were used as a model mineral system. Flotation tests were conducted using a Denver D-12 laboratory flotation machine as well as a custom-made flotation column. The reverse cationic flotation route that floats quartz from hematite and the direct flotation route that floats hematite from quartz were used, respectively.

Natural polymers including corn starch, corn dextrin, tannic acid (TAN) and synthetic polymer poly(ethylene oxide) (PEO) were selected as depressants, dispersant, and flocculant for the investigation. Centering on the concept of two-stage aggregation flotation process, a series of specific questions were explored, such as the influence of aggregation and dispersion states of hydrophilic particles on entrainment, flocculation process and floc properties of ultrafine hydrophilic quartz by the single and combined dual polymers, and effects of agitation intensity and foaming property on floc size distribution, entrainment degree and flotation kinetics/recovery when polymeric flocculation was used in flotation. The main conclusions drawn from this dissertation work were summarized as follows.

(1) It was possible to generate both hydrophobic and hydrophilic aggregates in the same slurry of fine and ultrafine mineral mixtures (quartz and hematite) and then separate them by flotation. Further, the dispersion of fine hydrophilic particles in slurry enhanced their entrainment whereas aggregation of fine hydrophilic particles can reduce their entrainment. The above conclusion was supported by the following observations.

- In-situ particle size analysis by focused beam reflectance measurement (FBRM) coupled with optical microscope imaging confirmed that fine hematite particles could be aggregated by corn starch and fine quartz could be aggregated by octadecylamine acetate (ODA). In contrast with corn starch, corn dextrin functioned as a dispersant and enabled fine hematite particles to disperse in slurry.
- In the reverse cationic flotation of quartz away from hematite using ODA as a collector, much less hematite was reported into froth using corn starch than using corn dextrin in the batch flotation of 1:1 fine hematite-quartz mixtures (-20 μm hematite and -15 μm quartz), while approximately equal Fe recovery in froth was observed in the flotation

mixtures of coarse hematite and fine quartz (-75+20 μm hematite and -15 μm quartz) using the two depressants.

- Micro-flotation and solvent extraction tests showed that surface hydrophilicity of hematite induced by the corn starch or corn dextrin was in an identical range in the presence of ODA, decoupling the effect of surface wettability and indicating that different separation result was solely caused by the different degrees of aggregation/dispersion of hematite particles by the two polymers.

(2) Using poly(ethylene oxide) (PEO, 8MDa) alone as a flocculant, the flocculation efficiency of ultrafine hydrophilic quartz decreased when suspension pHs increased from acid to alkaline. The prior addition of tannic acid (TAN) significantly improved the flocculation efficiency of quartz by PEO, especially in weakly alkaline solutions. Moreover, flocs formed by TAN-PEO dual polymers were larger, more shear resistant, and could be re-flocculated after the breakage in turbulence, depending on the TAN/PEO ratios and suspension pH.

(3) The beneficial effect of tannic acid in the PEO-quartz flocculation process was through the formation of a PEO-tannic acid associative complex, possibly through hydrogen bonding of the PEO's ether oxygen and tannic acid's vast number of hydroxyl groups. The associative PEO-tannic acid complex probably rendered the PEO molecular chain more rigid and more extended in the aqueous solution, both of which helped PEO's flocculation function.

(4) In column flotation, flocculating ultrafine quartz using the dual TAN-PEO polymer combination to form hydrophilic flocs was effective to reduce quartz entrainment. The reduced degree of quartz entrainment was related to floc size distribution, depending upon agitation intensity employed for slurry conditioning and foaming property of PEO. It was found that too large or too small hydrophilic flocs would not favor entrainment reduction. A linear correlation was established between mean floc size and the reduced entrainment degree when the average size of quartz flocs was less than 68 μm. In addition, dual TAN-PEO polymers enhanced both

flotation kinetics and recovery for hematite directly by n-octyl hydroxamic acid (OHA) as a collector in single hematite flotation, likely due to the synergistic effect between PEO and OHA bringing improved surface activity and frothing stability.

(5) Addition of TAN-PEO polymers benefited the separation efficiency of -20 μm hematite and -15 μm quartz in synthetic mineral mixture in column flotation. Tannic acid played dual roles in the column flotation of the quartz-hematite system: on one hand, TAN worked together with PEO to improve the flocculation of quartz and helped to obtain more shear-resistant flocs, on the other hand, TAN could weaken the surface activity and foaming stability of PEO, both of which will be beneficial in reducing the entrainment of ultrafine quartz.

6.2 Original contributions

(1) In this work the concept of two-stage aggregation flotation was proposed, i.e., to separately form hydrophobic aggregates and hydrophilic aggregates simultaneously or consecutively, then use froth flotation to separate the two types of aggregates. The feasibility of the concept has been confirmed using fine -20 μm hematite and -15 μm quartz as model minerals and may be extended to many other mineral systems. It provided a feasible option to deal with the low flotation rate of fine hydrophobic minerals but in the meantime, could lower the entrainment of fine hydrophilic minerals.

(2) The work of current research established for the first time the correlation between hydrodynamic agitation, hydrophilic floc size, and degree of entrainment when polymeric flocculation was used to reduce the entrainment of hydrophilic gangue particles. The correlation was established in the tannic acid – poly(ethylene oxide) – quartz flotation system, but the theoretical implication could be expanded into other mineral-polymer systems.

(3) This work investigated the combination of tannic acid and PEO for the first time in mineral flotation and revealed the dual functions of tannic acid in flotation system when PEO was used,

namely enhancing flocculation capability of PEO and at the same time weakening PEO’s foamability, both of which were desirable for PEO to be used in the proposed two-stage aggregation flotation strategy. The study also showed that the reason for the favorable dual function of tannic acid was due to the formation of tannic acid – PEO polymer associative complexes, possibly through hydrogen bonding of PEO’s ether oxygen and the vast number of hydroxyl groups of tannic acid. Such associative polymer complexes changed the configuration of PEO in aqueous solution and endowed the PEO-mineral flocs shear-resistance and re-flocculation capabilities after floc breakage (i.e., “healing” behavior), all of which are desirable properties when PEO is used as a flocculant in minerals industry.

6.3 Recommendations for future work

(1) This work uses mineral mixtures of quartz and hematite to verify the applicability of the two-stage aggregation/flocculation flotation concept. Since the separation of quartz and iron ore by reverse cationic flotation has been mature in industry, it would be necessary to investigate the findings with alternative minerals systems and flotation reagents.

(2) It is unclear whether the sequence of forming hydrophobic and hydrophilic aggregates would affect the mutual entrapment of mineral particles and the separation efficiency. Generally, several chemicals are added to promote aggregation in flotation slurry, in such a case, further investigation is needed to examine the effect of chemicals adding sequence.

(3) The flocculation mechanism using tannic acid and PEO has not been fully understood. Although the results indicated the complex bridging, the detailed adsorption process is still unknown. It would be helpful to study the adsorption process of the two polymers with mineral surfaces using characterization techniques that are more surface-sensitive, such as X-ray photoelectron spectroscopy.

(4) The observation that tannic acid and PEO polymers improved flotation kinetics and recovery of fine hematite by n-octyl hydroxamic acid is an interesting discovery, which inspires further studies of the synergism of polymer-surfactant combinations in improving fine minerals flotation.

(5) The foaming property in current dissertation was investigated in two phases containing only water and air, which is not the case for mineral flotation. In the presence of mineral solids, the foaming and frothing stability can vary substantially. Future work can be done to study the frothing properties of PEO or TAN-PEO polymers with particles of different solid contents or surface hydrophobicity.

Bibliography

A. Hassanzadeh, M. Safari, D.H. Hoang, H. Khoshdast, B. Albijanic, P.B. Kowalczuk, Technological assessments on recent developments in fine and coarse particle flotation systems, Minerals Engineering 180 (2022) 107509.

M.S. Lutandula, B. Maloba, Recovery of cobalt and copper through reprocessing of tailings from flotation of oxidised ores, Journal of Environmental Chemical Engineering 1 (2013) 1085-1090.

W. Trahar, A rational interpretation of the role of particle size in flotation, International Journal of Mineral Processing 8 (1981) 289-327.

G.J. Jameson, The effect of surface liberation and particle size on flotation rate constants, Minerals Engineering 36 (2012) 132-137.

T. Miettinen, J. Ralston, D. Fornasiero, The limits of fine particle flotation, Minerals Engineering 23 (2010) 420-437.

L. Wang, Y. Peng, K. Runge, D. Bradshaw, A review of entrainment: Mechanisms, contributing factors and modelling in flotation, Minerals Engineering 70 (2015) 77-91.

S. Farrokhpay, L. Filippov, D. Fornasiero, Flotation of fine particles: A review, Mineral Processing and Extractive Metallurgy Review 42 (2021) 473-483.

M. Sajjad, A. Otsuki, Correlation between Flotation and Rheology of Fine Particle Suspensions, Metals 12 (2022) 270.

E. Forbes, Shear, selective and temperature responsive flocculation: A comparison of fine particle flotation techniques, International Journal of Mineral Processing 99 (2011) 1-10.

Z. Zhou, Z. Xu, J. Finch, J. Masliyah, R. Chow, On the role of cavitation in particle collection in flotation–A critical review. II, Minerals Engineering 22 (2009) 419-433.

J.Z. Zhou, H. Li, R.S. Chow, Q. Liu, Z. Xu, J. Masliyah, Role of mineral flotation technology in improving bitumen extraction from mined Athabasca oil sands — II. Flotation hydrodynamics of water - based oil sand extraction, The Canadian Journal of Chemical Engineering 98 (2020) 330-352.

M. Mankosa, J. Kohmuench, L. Christodoulou, E. Yan, Improving fine particle flotation using the StackCell™(raising the tail of the elephant curve), Minerals Engineering 121 (2018) 83-89.

V. Samygin, V. Panin, L. Filippov, N.Y. Stenin, Development of a reactor-separator flotation machine designed by the Moscow Institute of Steel and Alloys, Metallurgist 54 (2010) 394-400.

Y. Yu, L. Ma, M. Cao, Q. Liu, Slime coatings in froth flotation: A review, Minerals Engineering 114 (2017) 26-36.

Q. Liu, D. Wannas, Y. Peng, Exploiting the dual functions of polymer depressants in fine particle flotation, International journal of mineral processing 80 (2006) 244-254.

B.A. Wills, J.A. Finch, Froth flotation, Wills' Mineral Processing Technology 7 (2016).

H. Schubert, On the optimization of hydrodynamics in fine particle flotation, Minerals Engineering 21 (2008) 930-936.

B. Gorain, J. Franzidis, E. Manlapig, Flotation cell design: application of fundamental principles, Julius Kruttschnitt Mineral Research Centre. Indooroopilly. Queensland. Australia (2000).

A. Haxhiaj, B. Haxhiaj, The Management of Lead Concentrate Acquisition in "Trepca", TMS Annual Meeting & Exhibition, Springer, 2018, pp. 185-198.

B. Derjaguin, S. Dukhin, Theory of flotation of small and medium-size particles, Progress in Surface Science 43 (1993) 241-266.

A. Nguyen, H.J. Schulze, Colloidal science of flotation, CRC Press2003.

A. Nguyen, H. Schulze, J. Ralston, Elementary steps in particle—bubble attachment, International Journal of Mineral Processing 51 (1997) 183-195.

D. Tao, A. Sobhy, Nanobubble effects on hydrodynamic interactions between particles and bubbles, Powder technology 346 (2019) 385-395.

J. Duan, D. Fornasiero, J. Ralston, Calculation of the flotation rate constant of chalcopyrite particles in an ore, International Journal of Mineral Processing 72 (2003) 227-237.

C.M. Phan, A.V. Nguyen, J.D. Miller, G.M. Evans, G.J. Jameson, Investigations of bubble–particle interactions, International Journal of Mineral Processing 72 (2003) 239-254.

P. Smith, L. Warren, Entrainment of particles into flotation froths, Mineral Procesing and Extractive Metallurgy Review 5 (1989) 123-145.

I. Achaye, Effect of particle properties on froth stability, (2017).

T. Leistner, U.A. Peuker, M. Rudolph, How gangue particle size can affect the recovery of ultrafine and fine particles during froth flotation, Minerals Engineering 109 (2017) 1-9.

M. Cao, Q. Liu, Reexamining the functions of zinc sulfate as a selective depressant in differential sulfide flotation—The role of coagulation, Journal of colloid and interface science 301 (2006) 523-531.

J. Gong, Y. Peng, A. Bouajila, M. Ourriban, A. Yeung, Q. Liu, Reducing quartz gangue entrainment in sulphide ore flotation by high molecular weight polyethylene oxide, International Journal of Mineral Processing 97 (2010) 44-51.

D. Liu, Y. Peng, Reducing the entrainment of clay minerals in flotation using tap and saline water, Powder Technology 253 (2014) 216-222.

Q. Liu, Selective aggregation of hydrophilic gangue minerals in froth flotation, MRS Online Proceedings Library (OPL) 1380 (2012).

X. Zheng, N. Johnson, J.-P. Franzidis, Modelling of entrainment in industrial flotation cells: Water recovery and degree of entrainment, Minerals Engineering 19 (2006) 1191-1203.

Z. Konopacka, J. Drzymala, Types of particles recovery—water recovery entrainment plots useful in flotation research, Adsorption 16 (2010) 313-320.

S. Neethling, J. Cilliers, The entrainment of gangue into a flotation froth, International Journal of Mineral Processing 64 (2002) 123-134.

L.J. Warren, Determination of the contributions of true flotation and entrainment in batch flotation tests, International Journal of Mineral Processing 14 (1985) 33-44.

T. Subrahmanyam, E. Forssberg, Froth stability, particle entrainment and drainage in flotation—a review, International Journal of Mineral Processing 23 (1988) 33-53.

D. Mesa, A.J. Morrison, P.R. Brito-Parada, The effect of impeller-stator design on bubble size: Implications for froth stability and flotation performance, Minerals Engineering 157 (2020) 106533.

A.J. Morrison, Tank design modifications for the improved performance of froth flotation equipment, Imperial College London, 2017.

E. Tabosa, K. Runge, P. Holtham, The effect of cell hydrodynamics on flotation performance, International Journal of Mineral Processing 156 (2016) 99-107.

H. Schubert, On the turbulence-controlled microprocesses in flotation machines, International journal of mineral processing 56 (1999) 257-276.

G. Cutting, Effect of froth structure and mobility on plant performance, Mineral Procesing and Extractive Metallurgy Review 5 (1989) 169-201.

L. Wang, Y. Xing, J. Wang, Mechanism of the combined effects of air rate and froth depth on entrainment factor in copper flotation, Physicochemical Problems of Mineral Processing 56 (2020).

F. Shi, X. Zheng, The rheology of flotation froths, International Journal of Mineral Processing 69 (2003) 115-128.

S. Farrokhpay, The significance of froth stability in mineral flotation—A review, Advances in colloid and interface science 166 (2011) 1-7.

T. Subrahmanyam, K.E. Forssberg, Fine particles processing: shear-flocculation and carrier flotation—a review, International Journal of Mineral Processing 30 (1990) 265-286.

J.S. Laskowski, J. Ralston, Colloid chemistry in mineral processing, Elsevier2015.

L.J. Warren, Shear-flocculation of ultrafine scheelite in sodium oleate solutions, Journal of Colloid and Interface Science 50 (1975) 307-318.

S. Lu, Y. Ding, J. Guo, Kinetics of fine particle aggregation in turbulence, Advances in Colloid and Interface Science 78 (1998) 197-235.

P. Koh, J.R. Andrews, P. Uhlherr, Flocculation in stired tanks, Chemical engineering science 39 (1984) 975-985.

L. Valderrama, J. Rubio, High intensity conditioning and the carrier flotation of gold fine particles, International Journal of Mineral Processing 52 (1998) 273-285.

P. Jarvis, B. Jefferson, J. Gregory, S.A. Parsons, A review of floc strength and breakage, Water research 39 (2005) 3121-3137.

D. Thomas, S. Judd, N. Fawcett, Flocculation modelling: a review, Water research 33 (1999) 1579-1592.

Q. Liu, J.S. Laskowski, Polysaccharide application in mineral processing, Encyclopaedia of surface and colloid science. Marcel & Dekker, New York (2006) 5035-5055.

D. Wang, F. Jiao, W. Qin, X. Wang, Effect of surface oxidation on the flotation separation of chalcopyrite and galena using sodium humate as depressant, Separation Science and Technology 53 (2018) 961-972.

J. Rutledge, C.G. Anderson, Tannins in mineral processing and extractive metallurgy, Metals 5 (2015) 1520-1542.

P. Huang, M. Cao, Q. Liu, Using chitosan as a selective depressant in the differential flotation of Cu–Pb sulfides, International Journal of Mineral Processing 106 (2012) 8-15.

P. Huang, L. Wang, Q. Liu, Depressant function of high molecular weight polyacrylamide in the xanthate flotation of chalcopyrite and galena, International Journal of Mineral Processing 128 (2014) 6-15.

S. Li, L. Gao, J. Wang, H. Zhou, Y. Liao, Y. Xing, X. Gui, Y. Cao, Polyethylene oxide assisted separation of molybdenite from quartz by flotation, Minerals Engineering 162 (2021) 106765.

M. Lapointe, B. Barbeau, Dual starch–polyacrylamide polymer system for improved flocculation, Water research 124 (2017) 202-209.

J. Gregory, S. Barany, Adsorption and flocculation by polymers and polymer mixtures, Advances in colloid and interface science 169 (2011) 1-12.

K. Ding, J. Laskowski, Effect of conditioning on selective flocculation with polyacrylamide in the coal reverse flotation, Mineral Processing and Extractive Metallurgy 116 (2007) 108-114.

C. Wang, C. Sun, Q. Liu, Formation, breakage, and re-growth of quartz flocs generated by non-ionic high molecular weight polyacrylamide, Minerals Engineering 157 (2020) 106546.

W. Yu, G. Li, Y. Xu, X. Yang, Breakage and re-growth of flocs formed by alum and PACl, Powder Technology 189 (2009) 439-443.

W. Yu, J. Gregory, L.C. Campos, Breakage and re-growth of flocs formed by charge neutralization using alum and polyDADMAC, Water research 44 (2010) 3959-3965.

Q. Liu, J. Laskowski, The role of metal hydroxides at mineral surfaces in dextrin adsorption, II. Chalcopyrite-galena separations in the presence of dextrin, International Journal of Mineral Processing 27 (1989) 147-155.

J. Laskowski, Q. Liu, N. Bolin, Polysaccharides in flotation of sulphides. Part I. Adsorption of polysaccharides onto mineral surfaces, International journal of mineral processing 33 (1991) 223-234.

Q. Liu, J. Laskowski, The role of metal hydroxides at mineral surfaces in dextrin adsorption, I. Studies on modified quartz samples, International Journal of Mineral Processing 26 (1989) 297-316.

Q. Liu, Y. Zhang, J. Laskowski, The adsorption of polysaccharides onto mineral surfaces: an acid/base interaction, International Journal of Mineral Processing 60 (2000) 229-245.

H. Hao, L. Li, P. Somasundaran, Z. Yuan, Adsorption of pregelatinized starch for selective flocculation and flotation of fine siderite, Langmuir 35 (2019) 6878-6887.

K. Shrimali, V. Atluri, Y. Wang, S. Bacchuwar, X. Wang, J.D. Miller, The nature of hematite depression with corn starch in the reverse flotation of iron ore, Journal of Colloid and Interface Science 524 (2018) 337-349.

E. Manev, R. Pugh, Frother/collector interactions in thin froth films and flotation, Colloids and Surfaces A: Physicochemical and Engineering Aspects 70 (1993) 289-295.

R. Pugh, Non-ionic polyethylene oxide frothers in graphite flotation, Minerals Engineering 13 (2000) 151-162.

J. Rubio, J. Kitchener, The mechanism of adsorption of poly (ethylene oxide) flocculant on silica, Journal of Colloid and Interface Science 57 (1976) 132-142.

S. Mathur, B.M. Moudgil, Adsorption mechanism (s) of poly (ethylene oxide) on oxide surfaces, Journal of colloid and interface science 196 (1997) 92-98.

E. Koksal, R. Ramachandran, P. Somasundaran, C. Maltesh, Flocculation of oxides using polyethylene oxide, Powder technology 62 (1990) 253-259.

T.G. van de Ven, Association-induced polymer bridging by poly (ethylene oxide)–cofactor flocculation systems, Advances in colloid and interface science 114 (2005) 147-157.

T. Lindström, G. Glad-Nordmark, Flocculation of latex and cellulose dispersions by means of transient polymer networks, Colloids and surfaces 8 (1984) 337-351.

M.R. Wu, J. Paris, T.G. van de Ven, Flocculation of papermaking fines by poly (ethylene oxide) and various cofactors: Effects of PEO entanglement, salt and fines properties, Colloids and Surfaces A: Physicochemical and Engineering Aspects 303 (2007) 211-218.

M. Cadotte, M.E. Tellier, A. Blanco, E. Fuente, T.G. Van De Ven, J. Paris, Flocculation, retention and drainage in papermaking: a comparative study of polymeric additives, The Canadian Journal of Chemical Engineering 85 (2007) 240-248.

S. Ata, Phenomena in the froth phase of flotation—A review, International Journal of Mineral Processing 102 (2012) 1-12.

J. Drzymala, Characterization of materials by Hallimond tube flotation. Part 1: maximum size of entrained particles, International Journal of Mineral Processing 42 (1994) 139-152.

S. Neethling, J. Cilliers, The entrainment factor in froth flotation: Model for particle size and other operating parameter effects, International Journal of Mineral Processing 93 (2009) 141-148.

X. Zheng, J.-P. Franzidis, N. Johnson, E. Manlapig, Modelling of entrainment in industrial flotation cells: the effect of solids suspension, Minerals Engineering 18 (2005) 51-58.

E. Cilek, B. Yılmazer, Effects of hydrodynamic parameters on entrainment and flotation performance, Minerals Engineering 16 (2003) 745-756.

E.C. Cilek, The effect of hydrodynamic conditions on true flotation and entrainment in flotation of a complex sulphide ore, International Journal of Mineral Processing 90 (2009) 35-44.

V. Kirjavainen, Review and analysis of factors controlling the mechanical flotation of gangue minerals, International journal of mineral processing 46 (1996) 21-34.

O.Y. Gulsoy, A simple model for the calculation of entrainment in flotation, Korean Journal of Chemical Engineering 22 (2005) 628-634.

N. Mhonde, J. Wiese, B. McFadzean, Comparison of collector performance for a South African and a Brazilian iron ore considering mineralogical characteristics, Minerals Engineering 113 (2017) 55-67.

M. Gao, M. Young, P. Allum, IsaMill fine grinding technology and its industrial applications at Mount Isa Mines, 34th Annual Meeting Of The Canadian Mineral Processors, 2002.

V.F.D. De, Cationic froth flotation of iron ore, Google Patents, 1949.

A.F. Colombo, Effect of tapioca flour on the anionic flotation of gangue from iron ores, US Department of Interior, Bureau of Mines1972.

S. Cooke, N. Schulz, E. Lindroos, The effect of certain starches on quartz and hematite suspensions, TRANSACTIONS OF THE AMERICAN INSTITUTE OF MINING AND METALLURGICAL ENGINEERS 193 (1952) 697-698.

D.W. Frommer, A.F. Colombo, Process for improved flotation treatment of iron ores by selective flocculation, Google Patents, 1966.

A. Colombo, Beneficiation of fine-grained iron-bearing materials, Beneficiation of Mineral Fines-Problems and Research Needs. AIME, USA (1979) 237-252.

D. HORTON, Pyrolysis of starch. in Starch, Chemistry and Technology (1965) 428-429.

C. Chang, S. Cooke, R. Huch, Starches and starch products as depressants in amine flotation of iron ore, Trans. AIME 196 (1953) 1282-1286.

J.M. Wie, D. Fuerstenau, The effect of dextrin on surface properties and the flotation of molybdenite, International journal of mineral processing 1 (1974) 17-32.

J. Miller, C. Lin, S. Chang, Coadsorption phenomena in the separation of pyrite from coal by reserve flotation, Coal Perparation 1 (1984) 21-38.

J. Schnarr, Brunswick mining and smelting corporation, Milling Practice in Canada, CIM Special Volume, Brunswick Mining and Smelting Corporation1978, pp. 158-161.

G. Nyamekye, The differential flotation of INCO matte with the use of polysaccharides, Copper 91(Cobre 91) (1991).

K. Kydros, G. Gallios, K. Matis, Modification of pyrite and sphalerite flotation by dextrin, Separation science and technology 29 (1994) 2263-2275.

A.L. Valdivieso, T.C. Cervantes, S. Song, A.R. Cabrera, J. Laskowski, Dextrin as a non-toxic depressant for pyrite in flotation with xanthates as collector, Minerals engineering 17 (2004) 1001-1006.

G.F. Moreira, E.R. Peçanha, M.B. Monte, L.S. Leal Filho, F. Stavale, XPS study on the mechanism of starch-hematite surface chemical complexation, Minerals Engineering 110 (2017) 96-103.

S. Pavlovic, P.R.G. Brandão, Adsorption of starch, amylose, amylopectin and glucose monomer and their effect on the flotation of hematite and quartz, Minerals Engineering 16 (2003) 1117-1122.

P. Weisseborn, L. Warren, J. Dunn, Selective flocculation of ultrafine iron ore. 1. Mechanism of adsorption of starch onto hematite, Colloids and Surfaces A: Physicochemical and Engineering Aspects 99 (1995) 11-27.

B. Siwek, M. Zembala, A. Pomianowski, A method for determination of fine-particle flotability, International Journal of Mineral Processing 8 (1981) 85-88.

J. Laskowski, Oil assisted fine particle processing, Developments in mineral processing, Elsevier1992, pp. 361-394.

J.S. Laskowski, Z. Yu, Oil agglomeration and its effect on beneficiation and filtration of low-rank/oxidized coals, International Journal of Mineral Processing 58 (2000) 237-252.

A. Ozkan, S. Aydogan, M. Yekeler, Critical solution surface tension for oil agglomeration, International Journal of Mineral Processing 76 (2005) 83-91.

D. Gómez-Díaz, J.M. Navaza, L. Quintáns-Riveiro, Intrinsic viscosity and flow behaviour of Arabic gum aqueous solutions, International Journal of Food Properties 11 (2008) 773-780.

A. Senaputra, F. Jones, P.D. Fawell, P.G. Smith, Focused beam reflectance measurement for monitoring the extent and efficiency of flocculation in mineral systems, AIChE Journal 60 (2014) 251-265.

R.G. Sparks, C.L. Dobbs, The use of laser backscatter instrumentation for the on‐line measurement of the particle size distribution of emulsions, Particle & particle systems characterization 10 (1993) 279-289.

Y. Kyoda, A. Costine, P. Fawell, J. Bellwood, G. Das, Using focused beam reflectance measurement (FBRM) to monitor aggregate structures formed in flocculated clay suspensions, Minerals Engineering 138 (2019) 148-160.

N.P. Lima, G.E. Valadão, A.E. Peres, Effect of amine and starch dosages on the reverse cationic flotation of an iron ore, Minerals Engineering 45 (2013) 180-184.

G. Caesar, N. Gruenhut, M. Cushing, Molecular weight and intrinsic viscosity of nitric triesters of corn starches and dextrins, Journal of the American Chemical Society 69 (1947) 617-621.

G.B. Raju, A. Holmgren, W. Forsling, Adsorption of dextrin at mineral/water interface, Journal of colloid and interface science 193 (1997) 215-222.

J.W. Chew, P.S. Chow, R.B. Tan, Automated in-line technique using FBRM to achieve consistent product quality in cooling crystallization, Crystal growth & design 7 (2007) 1416-1422.

X. Sun, L. Ma, X. Tan, K. Wang, Q. Liu, Effect of particle size on the flocculation of sub-micron titanium dioxide by polyacrylic acid, Minerals Engineering 149 (2020) 106253.

H. Li, M. Liu, Q. Liu, The effect of non-polar oil on fine hematite flocculation and flotation using sodium oleate or hydroxamic acids as a collector, Minerals Engineering 119 (2018) 105-115.

R. Pascoe, B. Wills, Selective aggregation of ultrafine hematite and quartz under high shear conditions with conventional flotation collectors, Minerals Engineering 7 (1994) 647-656.

D. Wang, Q. Liu, Hydrodynamics of froth flotation and its effects on fine and ultrafine mineral particle flotation: A literature review, Minerals Engineering 173 (2021) 107220.

D. Wang, Q. Liu, Influence of aggregation/dispersion state of hydrophilic particles on their entrainment in fine mineral particle flotation, Minerals Engineering 166 (2021) 106835.

J. Addai-Mensah, Enhanced flocculation and dewatering of clay mineral dispersions, Powder Technology 179(1-2) (2007) 73-78.

H. Shi, P. Fatehi, H. Xiao, Y. Ni, Optimizing the polyethylene oxide flocculation process for isolating lignin of prehydrolysis liquor of a kraft-based dissolving pulp production process, Industrial & engineering chemistry research 51(14) (2012) 5330-5335.

A. Alvarez, L. Gutierrez, J.S. Laskowski, Use of polyethylene oxide to improve flotation of fine molybdenite, Minerals Engineering 127 (2018) 232-237.

A.M. Bodratti, B. Sarkar, P. Alexandridis, Adsorption of poly (ethylene oxide)-containing amphiphilic polymers on solid-liquid interfaces: Fundamentals and applications, Advances in colloid and interface science 244 (2017) 132-163.

J. Rubio, The flocculation properties of poly (ethylene oxide), Colloids and surfaces 3(1) (1981) 79-95.

E. Koksal, R. Ramachandran, P. Somasundaran, C. Maltesh, Flocculation of oxides using polyethylene oxide, Powder technology 62(3) (1990) 253-259.

C. Negro, E. Fuente, A. Blanco, J. Tijero, Flocculation mechanism induced by phenolic resin/PEO and floc properties, AIChE journal 51(3) (2005) 1022-1031.

K.R. Stack, L.A. Dunn, N.K. Roberts, Study of the interaction between poly (ethylene oxide) and phenol-formaldehyde resin, Colloids and surfaces 61 (1991) 205-218.

A.E. Imel, A.K. Naskar, M.D. Dadmun, Understanding the impact of poly (ethylene oxide) on the assembly of lignin in solution toward improved carbon fiber production, ACS applied materials & interfaces 8(5) (2016) 3200-3207.

C. Lu, R. Pelton, Flocculation with poly (ethylene oxide)/tyrosine-rich polypeptide complexes, Langmuir 21(9) (2005) 3765-3772.

C. Maltesh, P. Somasundaran, R. Kulkarni, S. Gundiah, Polymer-polymer complexation in dilute aqueous solutions: poly (acrylic acid)-poly (ethylene oxide) and poly (acrylic acid)-poly (vinylpyrrolidone), Langmuir 7(10) (1991) 2108-2111.

K. Khoultchaev, P. Pang, R. Kerekes, P. Englezos, Enhancement of the retention performance of the poly (ethylene oxide)—tannic acid system by poly (diallyldimethyl ammonium chloride), The Canadian Journal of Chemical Engineering 76(2) (1998) 261-266.

R. Gaudreault, T.G. van de Ven, M. Whitehead, Salt necessary for PEO-cofactor association: The role of molecular modelling in PEO flocculation mechanisms, Proc. First Applied Pulp and Paper Molecular modelling symposium, 2005.

S. Mathur, B.M. Moudgil, Adsorption mechanism (s) of poly (ethylene oxide) on oxide surfaces, Journal of colloid and interface science 196(1) (1997) 92-98.

E. Antunes, F.A. Garcia, P. Ferreira, A. Blanco, C. Negro, M.G. Rasteiro, Effect of water cationic content on flocculation, flocs resistance and reflocculation capacity of PCC induced by polyelectrolytes, Industrial & engineering chemistry research 47(16) (2008) 6006-6013.

C. Negro, A. Blanco, I. San Pío, J. Tijero, Methodology for flocculant selection in fibre–cement manufacture, Cement and Concrete Composites 28(1) (2006) 90-96.

J.D. Hem, Complexes of ferrous iron with tannic acid, US Government Printing Office1960.

A. Tohry, R. Dehghan, L. de Salles Leal Filho, S.C. Chelgani, Tannin: An eco-friendly depressant for the green flotation separation of hematite from quartz, Minerals Engineering 168 (2021) 106917.

S. Cowen, H.A. Al-Abadleh, DRIFTS studies on the photodegradation of tannic acid as a model for HULIS in atmospheric aerosols, Physical Chemistry Chemical Physics 11(36) (2009) 7838-7847.

A. Ricci, K.J. Olejar, G.P. Parpinello, P.A. Kilmartin, A. Versari, Application of Fourier transform infrared (FTIR) spectroscopy in the characterization of tannins, Applied Spectroscopy Reviews 50(5) (2015) 407-442.

I. Pucić, T. Jurkin, FTIR assessment of poly (ethylene oxide) irradiated in solid state, melt and aqeuous solution, Radiation Physics and Chemistry 81(9) (2012) 1426-1429.

A. Blanco, E. Fuente, C. Negro, J. Tijero, Flocculation monitoring: focused beam reflectance measurement as a measurement tool, The Canadian Journal of Chemical Engineering 80(4) (2002) 1-7.

A. Blanco, C. Negro, A. Hooimeijer, J. Tijero, Polymer optimization in paper mills by means of a particle size analyser: an alternative to zeta potential measurements, Appita journal 49(2) (1996) 113-116.

J.S. Pérez, E.R. Porcel, J.C. López, J.F. Sevilla, Y. Chisti, Shear rate in stirred tank and bubble column bioreactors, Chemical Engineering Journal 124(1-3) (2006) 1-5.

J. Nan, M. Yao, T. Chen, S. Li, Z. Wang, G. Feng, Breakage and regrowth of flocs formed by sweep coagulation using additional coagulant of poly aluminium chloride and non-ionic polyacrylamide, Environmental Science and Pollution Research 23(16) (2016) 16336-16348.

W.-z. Yu, J. Gregory, L. Campos, G. Li, The role of mixing conditions on floc growth, breakage and re-growth, Chemical Engineering Journal 171(2) (2011) 425-430.

P. Jarvis, B. Jefferson, S.A. Parsons, Breakage, regrowth, and fractal nature of natural organic matter flocs, Environmental science & technology 39(7) (2005) 2307-2314.

P.T. Spicer, S.E. Pratsinis, J. Raper, R. Amal, G. Bushell, G. Meesters, Effect of shear schedule on particle size, density, and structure during flocculation in stirred tanks, Powder Technology 97(1) (1998) 26-34.

V. Chaignon, B. Lartiges, A. El Samrani, C. Mustin, Evolution of size distribution and transfer of mineral particles between flocs in activated sludges: an insight into floc exchange dynamics, Water Research 36(3) (2002) 676-684.

A. Horn, E. Merrill, Midpoint scission of macromolecules in dilute solution in turbulent flow, Nature 312(5990) (1984) 140-141.

A. Faghihnejad, K.E. Feldman, J. Yu, M.V. Tirrell, J.N. Israelachvili, C.J. Hawker, E.J. Kramer, H. Zeng, Adhesion and surface interactions of a self-healing polymer with multiple hydrogen-bonding groups, Advanced Functional Materials 24(16) (2014) 2322-2333.

I. Gadwal, A brief overview on preparation of self-healing polymers and coatings via hydrogen bonding interactions, Macromol 1(1) (2020) 18-36.

V.K. Thakur, M.R. Kessler, Self-healing polymer nanocomposite materials: A review, Polymer 69 (2015) 369-383.

Y. Du, W.Z. Qiu, Z.L. Wu, P.F. Ren, Q. Zheng, Z.K. Xu, Water-Triggered Self-Healing Coatings of Hydrogen-Bonded Complexes for High Binding Affinity and Antioxidative Property, Advanced Materials Interfaces 3(15) (2016) 1600167.

C. Wang, P. Wang, X. Tan, G. Huang, J. Kou, C. Sun, Q. Liu, Selective aggregation of fine quartz by polyaluminum chloride to mitigate its entrainment during fine and ultrafine mineral flotation, Separation and Purification Technology 279 (2021) 119606.

R. Loerke, X. Tan, Q. Liu, Dewatering of oil sands mature fine tailings by dual polymer flocculation and pressure plate filtration, Energy & Fuels 31(7) (2017) 6986-6995.

B. Salopek, D. Krasic, S. Filipovic, Measurement and application of zeta-potential, Rudarsko-geolosko-naftni zbornik 4(1) (1992) 147.

T. Shutava, M. Prouty, D. Kommireddy, Y. Lvov, pH responsive decomposable layer-by-layer nanofilms and capsules on the basis of tannic acid, Macromolecules 38(7) (2005) 2850-2858.

V. Kozlovskaya, E. Kharlampieva, I. Drachuk, D. Cheng, V.V. Tsukruk, Responsive microcapsule reactors based on hydrogen-bonded tannic acid layer-by-layer assemblies, Soft Matter 6(15) (2010) 3596-3608.

R. Osawa, T.P. Walsh, Effects of acidic and alkaline treatments on tannic acid and its binding property to protein, Journal of Agricultural and Food Chemistry 41(5) (1993) 704-707.

F. Weber, E. Sagstuen, Q.-Z. Zhong, T. Zheng, H. Tiainen, Tannic acid radicals in the presence of alkali metal salts and their impact on the formation of silicate-phenolic networks, ACS applied materials & interfaces 12(47) (2020) 52457-52466.

H. Zhang, X. Hu, Y. Zhang, S. Wang, F. Xin, X. Chen, D. Yu, 3D-crosslinked tannic acid/poly (ethylene oxide) complex as a three-in-one multifunctional binder for high-sulfur-loading and high-stability cathodes in lithium-sulfur batteries, Energy Storage Materials 17 (2019) 293-299.

A.M. Grande, R. Martin, I. Odriozola, S. Van Der Zwaag, S.J. Garcia, Effect of the polymer structure on the viscoelastic and interfacial healing behaviour of poly (urea-urethane) networks containing aromatic disulphides, European Polymer Journal 97 (2017) 120-128.

J. Gong, The role of high molecular weight polyethylene oxide in reducing quartz gangue entrainment in chalcopyrite flotation by xanthate collectors, PhD Thesis, University of Alberta, Edmonton, Alberta, Canada (2011).

S. Liao, L. Ou, Flocs Properties and Flotation Performance of Fine Diaspore with Energy Input Pretreatment Induced Using Sodium Oleate, Minerals 9 (2019) 433.

Y. Hu, G. Qiu, J. Miller, Hydrodynamic interactions between particles in aggregation and flotation, International journal of mineral processing 70 (2003) 157-170.

B. Oyegbile, P. Ay, S. Narra, Flocculation kinetics and hydrodynamic interactions in natural and engineered flow systems: A review, Environmental Engineering Research 21 (2016) 1-14.

S.-x. Song, A. Lopez-Valdivieso, J. Reyes-Bahena, C. Lara-Valenzuela, Floc flotation of galena and sphalerite fines, Minerals Engineering 14 (2001) 87-98.

W. Chen, Q. Feng, G. Zhang, L. Li, S. Jin, Effect of energy input on flocculation process and flotation performance of fine scheelite using sodium oleate, Minerals Engineering 112 (2017) 27-35.

S. Zou, X. Ma, S. Wang, H. Zhong, W. Qin, Flotation of rhodochrosite fines induced by octyl hydroxamic acid as hydrophobic agglomerates, Powder Technology 392 (2021) 108-115.

D. Bache, Floc rupture and turbulence: a framework for analysis, Chemical Engineering Science 59 (2004) 2521-2534.

L. Liang, J. Tan, B. Li, G. Xie, Reducing quartz entrainment in fine coal flotation by polyaluminum chloride, Fuel 235 (2019) 150-157.

A. Cervantes-Martínez, A. Maldonado, Foaming behaviour of polymer–surfactant solutions, Journal of Physics: Condensed Matter 19 (2007) 246101.

R. Petkova, S. Tcholakova, N. Denkov, Foaming and foam stability for mixed polymer–surfactant solutions: effects of surfactant type and polymer charge, Langmuir 28 (2012) 4996-5009.

L. Filippov, V. Severov, I. Filippova, An overview of the beneficiation of iron ores via reverse cationic flotation, International journal of mineral processing 127 (2014) 62-69.

X. Zhang, X. Gu, Y. Han, N. Parra-Álvarez, V. Claremboux, S. Kawatra, Flotation of iron ores: A review, Mineral processing and extractive metallurgy review 42 (2021) 184-212.

S. Assis, L. Montenegro, A. Peres, Utilisation of hydroxamates in minerals froth flotation, Minerals engineering 9 (1996) 103-114.

M. Liu, H. Li, T. Jiang, Q. Liu, Flotation of coarse and fine pyrochlore using octyl hydroxamic acid and sodium oleate, Minerals Engineering 132 (2019) 191-201.

M. Fuerstenau, R. Harper, J. Miller, Hydroxamate vs fatty-acid flotation of iron oxide, TRANS SOC MINING ENG AIME 247 (1970) 69-73.

H. Li, M. Liu, Q. Liu, Oil-assisted flotation of fine hematite using sodium oleate or hydroxamic acids as a collector, Physicochemical Problems of Mineral Processing 54 (2018).

J. Gong, The role of high molecular weight polyethylene oxide in reducing quartz gangue entrainment in chalcopyrite flotation by xanthate collectors, (2011).

D. Liu, Y. Peng, Foaming and aggregation behaviours of polyethylene oxide and polyacrylamide in inhibiting mechanical entrainment of kaolinite in flotation using saline water, Journal of Molecular Liquids 359 (2022) 119299.

J. Israelachvili, The different faces of poly (ethylene glycol), Proceedings of the National Academy of Sciences 94 (1997) 8378-8379.

M.C. Pirrung, J.H.-L. Chau, A convenient procedure for the preparation of amino acid hydroxamates from esters, The Journal of Organic Chemistry 60 (1995) 8084-8085.

X. Ni, Q. Liu, The adsorption and configuration of octyl hydroxamic acid on pyrochlore and calcite, Colloids and Surfaces A: Physicochemical and Engineering Aspects 411 (2012) 80-86.

C. Marion, A. Jordens, R. Li, M. Rudolph, K.E. Waters, An evaluation of hydroxamate collectors for malachite flotation, Separation and Purification Technology 183 (2017) 258-269.

F. Li, X. Zhou, G. Zhao, R. Lin, A novel decyl-salicyl hydroxamic acid flotation collector: Its synthesis and flotation separation of malachite against quartz, Powder Technology 374 (2020) 522-526.

S. Farrokhpay, I. Ametov, S. Grano, Improving the recovery of low grade coarse composite particles in porphyry copper ores, Advanced Powder Technology 22 (2011) 464-470.

D. Xu, I. Ametov, S. Grano, Detachment of coarse particles from oscillating bubbles—The effect of particle contact angle, shape and medium viscosity, International Journal of Mineral Processing 101 (2011) 50-57.

S. Bilgen, B. Wills, Shear flocculation—A review, Minerals Engineering 4 (1991) 483-487.

M. WonáKim, Molecular weight dependence of the surface tension of aqueous poly (ethylene oxide) solutions, Faraday Discussions 98 (1994) 245-252.

F.K.G. Santos, E.L.B. Neto, M.C.P. Moura, T.N.C. Dantas, A.A.D. Neto, Molecular behavior of ionic and nonionic surfactants in saline medium, Colloids and Surfaces A: Physicochemical and Engineering Aspects 333 (2009) 156-162.

I. Solomentseva, S. Bárány, J. Gregory, The effect of mixing on stability and break-up of aggregates formed from aluminum sulfate hydrolysis products, Colloids and Surfaces A: Physicochemical and Engineering Aspects 298 (2007) 34-41.

Appendices

Figure A1 shows the cumulative recovery of water and quartz in column flotation using PEO of different molecular weights and dosages. As can be seen, when the high molecular weight (8 MDa) PEO was replaced by a lower molecular weight (1MDa) PEO, under the same flotation conditions it failed to reduce the entrainment of quartz. The reason was likely that the combination of tannic acid and 1MDa PEO could not effectively flocculate quartz. As reported in the literature that PEO MW was a particularly interesting variable in cofactor/PEO-induced flocculation and 1 MDa PEO was only on the marginal to cause effective flocculation [1].

On the other hand, it was found that when PEO was used alone with OHA, it did not decrease the entrainment recovery of quartz, conversely, both water recovery and quartz entrainment increased above 40% despite a small concentration of 40 g/t PEO. The discovery contradicted the results of previous research [2]. Here the possible reasons were given for the inconsistent flotation results.

(1) Despite a similar pH (about 9) range in slurry, previous work used lime (CaO) to adjust pH in the grinding mill and flotation cell [2, 3] as compared with sodium hydroxide (NaOH) used for the current study. The release of Ca^{2+} along with the addition of lime can bring complicated affection for quartz flotation [4]. It can reduce the negative surface charge of quartz and may help the flocculation of quartz by PEO, or the hydrophilic $Ca(OH)^+$ species may precipitate on the quartz surface to further hinder the entrainment recovery of quartz. Whereas in the present study, the aggregation study indicated that the flocculation of quartz by PEO was not efficient in alkaline solutions.

(2) Previous work [2] was carried out in a mechanical flotation cell and the current investigation was performed in a column. Hydrodynamic environments differed a lot from the two flotation devices. Within the column, the bubble size was much smaller (μm-range)

than that in the flotation cell (mm-range), as well as having a higher gas holdup. Given so, the surface-active of PEO would be more pronounced in promoting fine bubbles generation and frothing stability. It has been revealed that applying small bubbles in fine minerals flotation can usually contribute to increasing particle and water recoveries but deteriorating selectivity due to severe entrainment [5-9].

(3) In the flotation system of previous research, PEO was used together with sodium isopropyl xanthate, a typical collector for sulfide minerals. In contrast, the OHA was used as colletor in the present study. Although both collectors cannot interact with quartz surfaces, the OHA tended to possess stronger frothing capability than sodium isopropyl xanthate. Especially when OHA was used together with PEO, the possible synergetic effect between them can bring a very different frothing property in quartz flotation.

Regardless of the reasons, the current investigation demonstrated that using individual PEO to flocculate quartz may not work well in the flotation column to reduce entrainment. However, the pre-addition of tannic acid before PEO could benefit to realize the purpose in the flotation column. Results in Figure A1 also indicated that increasing the concentrations of tannic acid and PEO by five times, namely 400 g/t tannic acid and 200 g/t PEO, can still be effective in reducing quartz entrainment, which was different from previous research that using PEO alone [2, 10]. Results in Figure A1 verified the dual functions of tannic acids when it was used with PEO for entrainment reduction.

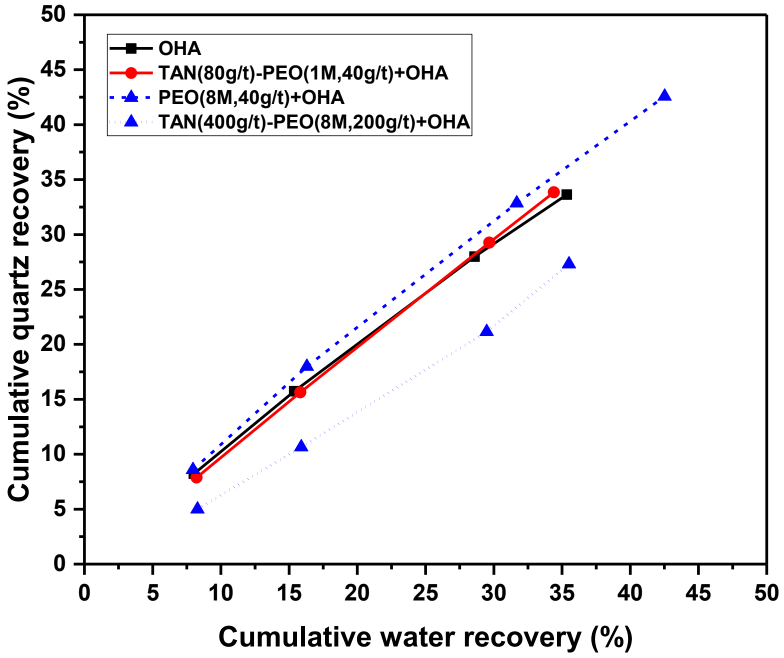

Figure A1 Effect of PEO molecular weight and dosage on cumulative recovery of water and quartz in column with and without tannic acid under an agitation intensity of 600 rpm.

References

[1] C. Lu, R. Pelton, Flocculation with poly (ethylene oxide)/tyrosine-rich polypeptide complexes, Langmuir 21 (2005) 3765-3772.

[2] J. Gong, The role of high molecular weight polyethylene oxide in reducing quartz gangue entrainment in chalcopyrite flotation by xanthate collectors, (2011).

[3] J. Gong, Y. Peng, A. Bouajila, M. Ourriban, A. Yeung, Q. Liu, Reducing quartz gangue entrainment in sulphide ore flotation by high molecular weight polyethylene oxide, International Journal of Mineral Processing 97 (2010) 44-51.

[4] M. Zanin, H. Lambert, C. Du Plessis, Lime use and functionality in sulphide mineral flotation: A review, Minerals Engineering 143 (2019) 105922.

[5] D. Wang, Q. Liu, Hydrodynamics of froth flotation and its effects on fine and ultrafine mineral particle flotation: A literature review, Minerals Engineering 173 (2021) 107220.

[6] V. Chipakwe, R. Jolstera, S.C. Chelgani, Nanobubble-assisted flotation of apatite tailings: Insights on beneficiation options, ACS omega 6 (2021) 13888-13894.

[7] S. Schwarz, S. Grano, Effect of particle hydrophobicity on particle and water transport across a flotation froth, Colloids and Surfaces A: Physicochemical and Engineering Aspects 256 (2005) 157-164.

[8] W. Trahar, L. Warren, The flotability of very fine particles—A review, International Journal of Mineral Processing 3 (1976) 103-131.

[9] T. Miettinen, J. Ralston, D. Fornasiero, The limits of fine particle flotation, Minerals Engineering 23 (2010) 420-437.

[10] D. Liu, Y. Peng, Reducing the entrainment of clay minerals in flotation using tap and saline water, Powder Technology 253 (2014) 216-222.